The relationship between litho-stratigraphy and geomechanical properties of Arab-D Reservoir outcrop analogue- Central Saudi Arabia

BY

Ammar Juma Abdlmutalib

A Thesis Presented to the
DEANSHIP OF GRADUATE STUDIES

KING FAHD UNIVERSITY OF PETROLEUM & MINERALS

DHAHRAN, SAUDI ARABIA

In Partial Fulfillment of the
Requirements for the Degree of

MASTER OF SCIENCE

In

Geology

April 2015

KING FAHD UNIVERSITY OF PETROLEUM & MINERALS

DHAHRAN- 31261, SAUDI ARABIA

DEANSHIP OF GRADUATE STUDIES

This thesis, written by **Ammar Juma Abdlmutalib** under the direction his thesis advisor and approved by his thesis committee, has been presented and accepted by the Dean of Graduate Studies, in partial fulfillment of the requirements for the degree of **Master of Sciences in Geology**

Dr. Osman Abdullatif
(Advisor)

Dr. Abdulaziz Al-Shaibani
Department Chairman

Prof. Gabor Korvin
(Member)

Dr. Salam A. Zummo
Dean of Graduate Studies

Dr. Abdulazeez Abdulraheem
(Member)

18/6/15

Date

To my father, mother, brother, and sisters who motivated me to accomplish this achievement…

To my teachers from school stage up to university who gave me the key of the success..

To my friends and colleagues who shared me the pain and getting tired..

Thanks for Allah for providing me with fitness and strength to fulfill this research ….

Thanks for King Fahd University of Petroleum and Minerals for granting scholarship to complete MSc.

Thanks for Earth Sciences Department and the chairman Dr. Abdulaziz Al-Shaibani for providing me with all needs and facilities

Thanks are also for other faculty members for their guidance and assistance during courses and research periods.

Thanks for Research Institute – Center for Engineering Research for their contributions in the measurements parts..

I am very grateful for my thesis committee which was chaired by Dr.Osman Abdullatif, Prof. Gabor Korvin, and Dr. Abdulazeez Abdulraheem for their critical and effective revision.

Contents

LIST OF FIGURES

List of tables:

LIST OF ABBREVIATIONS

NFR Naturally Fractured Reservoirs

CAGS Central Arabian Graben System

RMR Rock Mass Ratting

Q Quality index

LiDar Light and Detection Ranging

DEM Digital Elevation Modeling

R_N Schmidt Hammer Rebound Number

IS (50) Point Load index (calibrated for 50 mm sample size)

Ø Porosity (%)

K Permeability (md)

V_p P-wave velocity ms^{-1}

V_s S-wave velocity ms^{-1}

E_d Dynamic Young's Modulus

V_d Dynamic Poisson's Ratio

ABSTRACT

Full Name : Ammar Juma Abdlmutalib

Thesis Title : THE RELATIONSHIP BETWEEN STRATIGRAPHY AND GEOMECHANICAL PROPERTIES OF ARAB-D OUTCROP ANALOGUE – CENTRAL SAUDI ARABIA

Major Field : Geology

Date of Degree : [April 2015]

In this study, integrated field and laboratory investigations were carried out to characterize fractures of the late Jurassic Arab-D member and underlying Upper Jubaila Formation and to measure their geomechanical properties. Sedimentological and fractures analysis (orientation, length, spacing, aperture, and displacement) were carried out. A total of sixty samples were collected for petrographic analysis, porosity and permeability measurements, and geomechanical properties such as Schmidt Hammer, Point Load index, P and S-wave velocities and dynamic elastic moduli. The results revealed several lithofacies deposited in lower to upper slope and ramp crest (upper Jubaila), and deep to shallow lagoonal settings (Arab-D). Fracture analysis shows three sets intersecting Upper Jubaila Formation and five sets affecting on Arab-D member. Obvious impact of lithofacies change on fractures development was observed. Fractures intensity and other properties are controlled by several factors including changes in lithofacies and their geomechanical properties, bed thicknesses, and burial depth. Various types of cross-cutting relationships were found, this enables to identify the relative age of each set with respect to the others. Three geomechanical units were established; Unit-1 is characterized by large variability from low to high strength index, porosity, wave velocity and dynamic moduli, this is due to strong stratigraphic cyclicity. Unit-2 is characterized by relatively low strength index, Young's modulus, and velocity and high porosity and Poisson's ratio, this unit is more consistent and equivalent to

upper part of Upper Jubaila Formation. Unit-3 has relatively higher strength index, Young's modulus and velocity and low porosity and Poisson's ratio. These units proved depositional, stratigraphic, and diagenetic impact on properties. Various correlations were established between several geomechanical properties and porosities and permeabilities, this implies that geomechanical can be predicted using core based porosity\ permeability values effectively. The results of this study might assist to understand fractures and geomechanical behaviors of tight carbonate reservoirs in the subsurface.

ملخص الرسالة

الاسم الكامل:عمار جمعة عبدالمطلب محمد

عنوان الرسالة: العلاقة بين الخصائص الطبقية والجيوميكانيكية للنظير السطحي لخزان العرب-د- وسط المملكة العربية السعودية

التخصص: جيولوجيا

تاريخ الدرجة العلمية: أبريل 2015

في هذه الدراسة أجريت التحقيقات الميدانية والمخبرية المتكاملة لتمييز الشقوق المؤثرة في عضو العرب-د ومكون الجبيلة العليا وقياس خصائصها الجيوكيكانيكية .أجريت تحاليل الشقوق) التوجه؛ الطول؛ التباعد؛ الفتحة؛ الازاحة(؛ تم جمع ما مجموعه ستون عينة لاجراء الاختبارات المسامية؛ النفاذية؛ والتحاليل الصخرية المجهرية؛ والخصائص الجيوميكانيكية مثل :معامل مطرقة شميدت؛ مؤشر حمل النقطة؛ سرعات موجات القص والموجات الانضغاطية؛ والمعاملات الديناميكية المرنة.

كشفت النتائج وجود عدة سحنات صخرية تشمل رسوبيات المنحدر الأعلى والأدنى وقمة المنحدر) الجبيلة العليا(؛ ورسوبيات النظام البحيري البحري الضحل) العرب-د .(تظهر نتائج تحليل الشقوق وجود ثلاث أنظمة كسورتؤثر على على عضو العرب-د .يظهر تأثير تغير السحنات الصخرية المختلفة على أنماط وتطور الكسور خلالها .هذه الكسور تفتقر في معظمها الى الازاحة فيماعدا تلك التي تأخذ اتجاه شمال غرب -جنوب شرق .فسرت هذه النتائج على أنها تكونت نتيجة لنظام وسط الجزيرة العربية الأخدودي .تم انشاء ثلاث وحدات جيوميكانيكية تتميز الوحدة الأولى بتقلب واضح من مؤشر قوة عالي الى منخفض؛ وكذلك المسامية ومعاملات المرونة؛ ويرجع ذلك الى دوروية الطبقية العالية .الوحدة الثانية تتميز بمؤشر قوة منخفض نسبيا ومسامية عالية؛ هذه الوحدة أكثر اتساقا؛ وتعادل الجزء الأعلى من مكون الجبيلة العليا وعضو العرب-د .الوحدة الثالثة تتميز بمؤشر قوة عالي نسبيا) يمثل الأكثر عمقا (ومسامية منخفضة ومعامل بويسون منخفض .هذه الوحدات أوضحت تأثيرات مشتركة لكل من العوامل الرسوبية والطبقية على الخصائص الجيوميكانيكية ,كماظهرت عدة علاقات بين الخصائص الجيوميكانيكية وكل من المسامية والنفاذية المحيوبة من العينات الأسطوانية ,هذه النتائج يمكن أن تساعد على فهم السلوك الجيوميكانيكي وسلوك الكسور لصخور الكربونات ضيقة المسامات تحت السطح.

CHAPTER ONE
INTRODUCTION

1.1.Introduction:

Carbonate reservoirs are considered as an important proportion of hydrocarbon bearing reservoirs, it has been reported that they represent 60% of the hydrocarbon reservoirs and 85% of them are Naturally Fractured Reservoirs (NFR) (Larsen et al. 2010, Lucia 1999, Ahr 2008).

Both natural fractures and geomechanical properties are inter-related. The hydromechanical properties of these kinds of reservoirs depend on their fractures patterns and matrix. In particular their ability to contain fluids and to transport them (i.e. porosity and permeability) (Longeran et al. 2007). These properties are important during production and reservoir development stages.

Many factors control the propagation of natural fractures network through rock media, such as lithofacies types, layering, geomechanical properties and stress regimes (Gale et al. 2004). So many previous researches have proved relationships between lithological properties such as grain size and fracturing behaviors of carbonate rocks. However; the geomechanical properties of carbonate rocks vary with time. For example, carbonate rocks with different mechanical properties that deposited at certain time usually are subjected to extensive digenetic processes such as compaction and cementation. All these parameters together cause difficulties for such investigations.

Three dimensional views for fracture patterns and network can be obtained from outcrop easier than the subsurface, continuous measurements can be carried out within outcrops

due to their accessibility and lateral variability can be followed through outcrops. Therefore, they can be used to integrate the subsurface data and to predict those (Bertotti et al. 2009).

This study provides high-resolution geological data from outcrop analog stratigraphically equivalent to the Late Jurassic Arab-D reservoir, one of the important oil reservoirs in the Saudi Arabia (Lindsay and Hughes 2010; Lindsay et al. 2006; Hughes 2004). The geological and geomechanical data and rock heterogeneity at high-resolution scale (meter to centimeters) that is unavailable from subsurface data, that is, by integrating both field and laboratory data from outcrop stratigraphically equivalent to the Arab-D reservoir in the subsurface and unavailable from elsewhere. The needs of high-resolution geological data for reservoir are always important including geomechanical data. Such information

is of significance and has implications in assessing, understanding, and predicting reservoir quality and architecture. The data will also help to fill the gap for high-resolution geological data in the subsurface, and this will contribute to refining reservoir characterization models based on subsurface data. Also, it can provide guides and leads to reservoir exploration,

development, recovery, production, and management

The study area is located in Wadi Nisah graben nearly 90 kilometers south Riyadh. The width of the graben is 2 to 3.7 kilometers and it extends to 90 kilometers (Weijermars, 1998). These outcrops exist in the flanks of the graben were Arab-D member is overlain by Arab-C member. The contact between those two members is covered by Hith evaporitic dissolution collapse (Meyer et al.,1996). The exposure represents the surface

equivalent of the Arab-D reservoir (Okla, 1987). In addition to upper Jubaila, the outcrop consists of Arab-C member overlying Arab-D member. The contact between those two components is covered by fallen rocks derived from dissolution of Arab-D evaporite (Figure 1.1).

1.2. Objectives and methodologies

1.2.1. Objectives

The main objectives of the study are to identify the fracture patterns and geomechanical properties of Arab-D member and underlying Upper Jubaila Formation at outcrop scale and establish relations between these characteristics and lithofacies properties.

The specific objectives of this study are:

1- To characterize the geomechanical properties of the Arab-D and Jubaila Formation at outcrop scale.
2- To identify and characterize the fractures types and their origin.
3- To describe and characterize the lithofacies and stratigraphy.
4- To investigate the relationship between sedimentology and geomechanical properties of Arab-D and Upper Jubaila Formation.

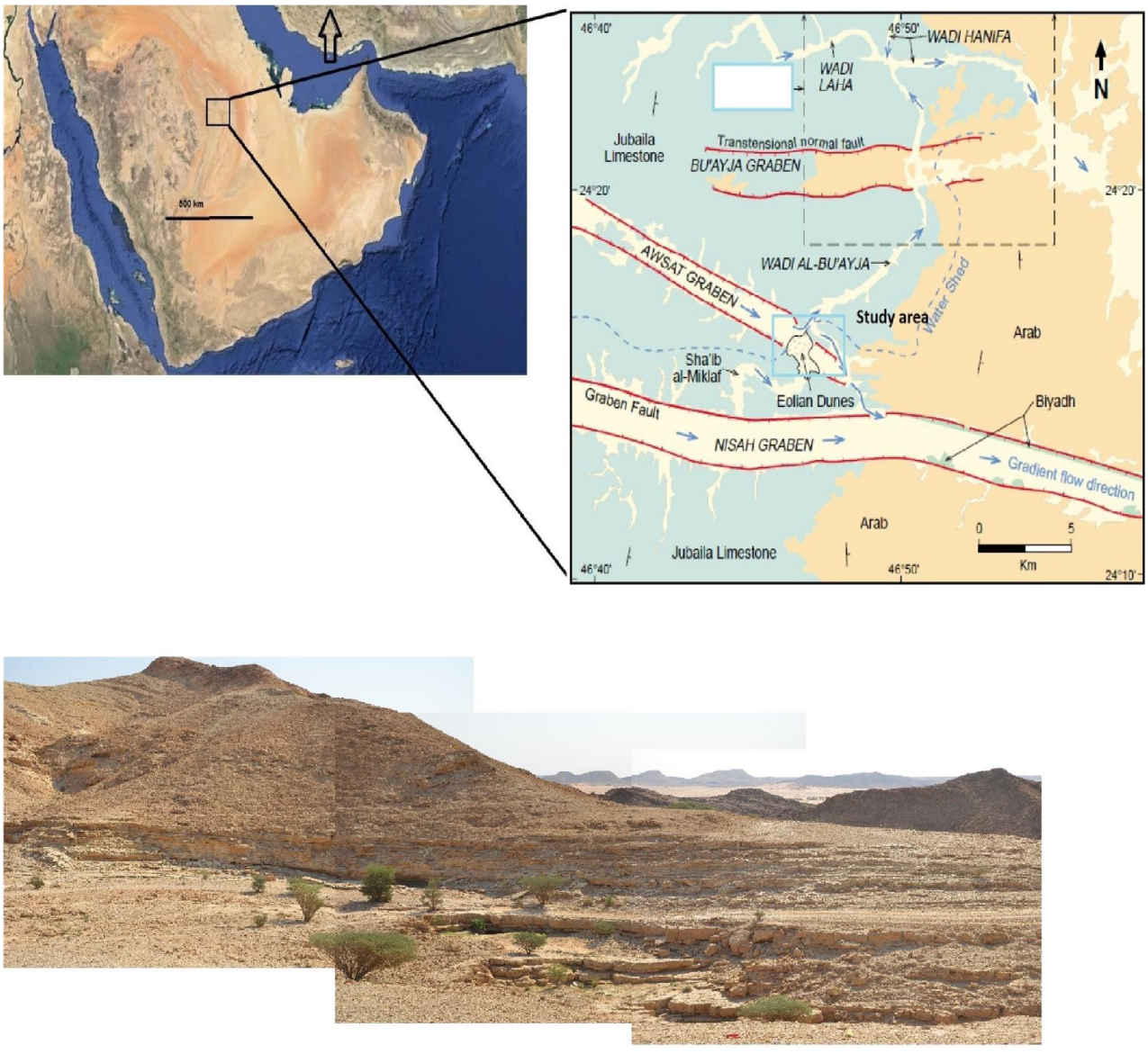

Figure 1.1 Google map of Saudi Arabia and location of study area (right), geological and structural map of the study area (left)

1.2.2. Methodologies

In this study, integrated field and laboratory investigations were carried out. In the field, several lithofacies associations were identified and fracture patterns were analyzed through orientation (strike and dip), scale, spacing, intensity, and opening measurements. Representative rock samples were collected for lithofacis and geomechanical analysis.

In the laboratory, thin sections were described using Dunham classification to recognize different lithofacies. geomechanical, lithofacies, porosity, and permeability observations were performed. Geomecahnical properties that were measured are Schmidt Hammer Rebound Number (R_N), Point Load Index (IS_{50}), P-wave and S-wave velocities, Grain density, dynamic Poisson's ratio, and Young's modulus.

The results of fractures analysis were presented on histograms and scatter plots. Orientation data were presented on rose diagrams and stereoplots using ROCK WARE software. Simple regression models were applied on the resulting values of geomechanical measurements to specify the nature of the relationship with each other, and with porosity and permeability (linear, polynomial, exponential, or power correlation) each case the goodness of fit R^2 was estimated.

1.3. Previous works

Arab-D reservoir is defined as reservoir unit comprised of Arab-D member of Arab Formation overlain by Upper Jubaila Formation (Figure 1.2) and dated as Upper Jurassic (Kimmeridgian) based on the presence of ammonites bio-components (Steinike et al. 1958; Powers et al. 1966, Powers 1968; Meyer et al. 1996; Hughes 1996; Cantrell and Hagerty 1999; Cantrell and Swart 2004; Hughes 2004; Lindsay et al. 2006; Cantrel et al. 2007).

Depositional environments, stratigraphy, and paleogeography studies were carried out by Ziegler (2001). Arab-D reservoir outcrop exposure was studied for the first time by Okla (1987) in Wadi Nisah area 90 Km south of Riyadh.

Morad et al. (2010) studied Arab-D and C members in UAE focusing on their microporosity and digenesis. Those two aspects were studied in stratigraphic framework in Wadi Nisah by Eltom et al. (2013). Porosity and permeability distribution were investigated by Cantrell and Hagerty (2009) and Meyer et al. (1996).

Lithofacies, biofacis, stratigraphic, geochemical analysis and geostatistical modeling were performed by Eltom et al. (2014).

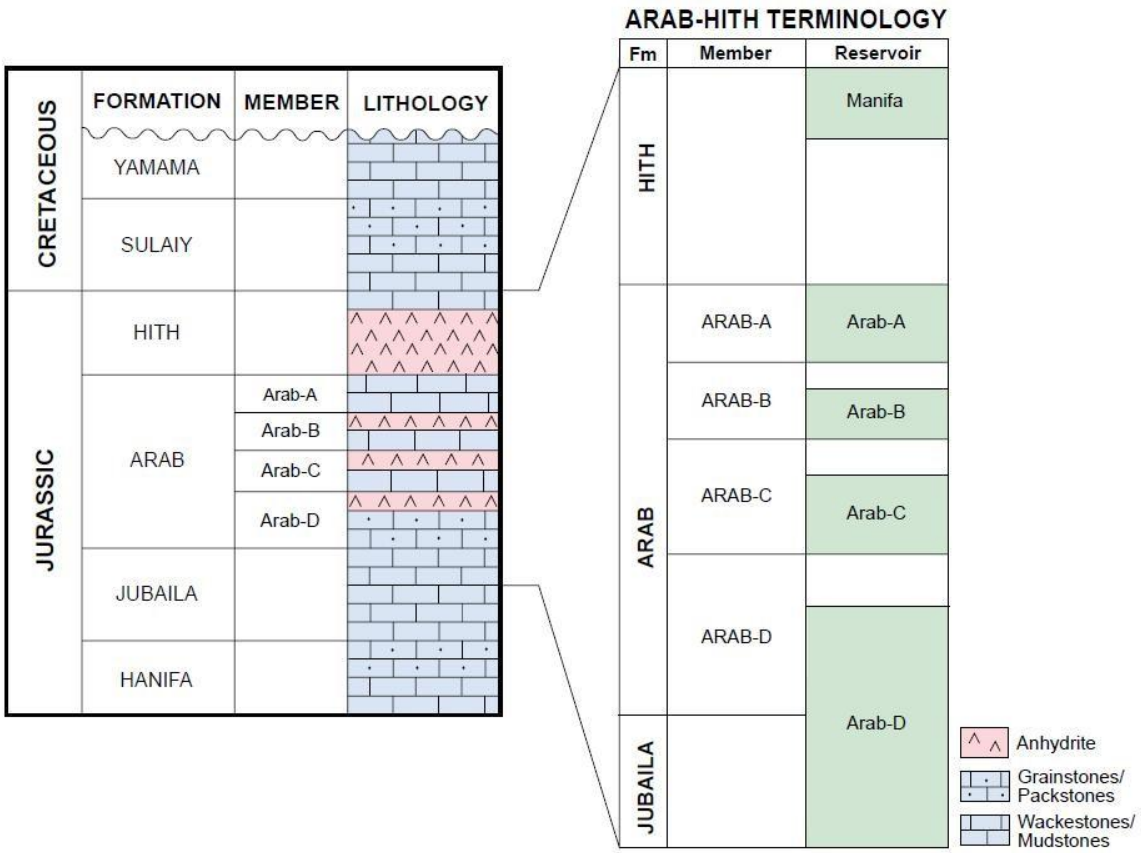

Figure 1.2 Generalized Jurassic and Cretaceous terminologies for reservoir and stratigraphic units (Cantrell & Hagerty, 1999).

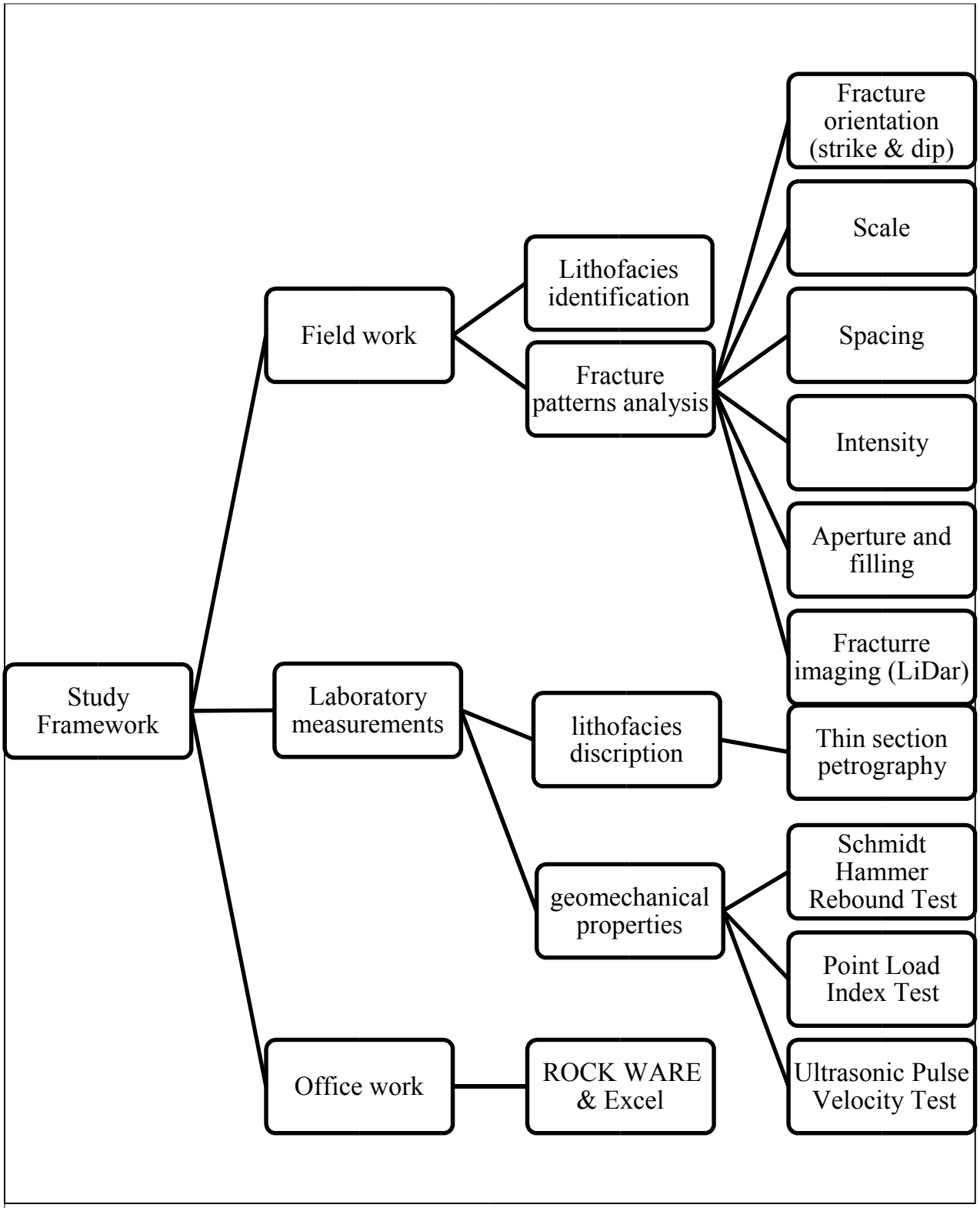

Figure 1.3 Study framework showing the followed methods and objectives

CHAPTER TWO

LITERATURE REVIEW

2.1. Geological setting

2.1.1. Paleo-environment

According to Ziegler (2001); Kimmeridgian time (149 Ma) witnessed the Arab and overlying Hith Formations deposition in Saudi Arabia and Gotnia in Kuwait and Iraq. The late stage of this time is equivalent to Upper Jurassic unconformity.

During this time, shallow marine carbonate was deposited and interbedded carbonate and evaporites (rhythmites) of arid intra-tidal to supra-tidal conditions built shoaling upward cycles. Four members (Arab-A to Arab-D) in addition to capping evaporitic Hith Formation were deposited due to progressive see level rise (Figure 2.1). This corresponds to (MFS J70 to K10 and the base of AP8).

Sea floor spreading of Afro-Arabian and Indian plates lead to development of new passive margins south-east of Oman during this time.

2.1.2. Tectonic setting

Wadi Nisah is a graben oriented in the east west direction, it is connected to the east with Wadi Sahba, and they together make up hundreds of Kilometers long lineament with east west striking trend, the graben is bounded with normal fault with dip slip ranging between 100 and 500 meters

According to Weijermars (1998); geological and structural mapping revealed the presence of graben system in Central Saudi Arabia, which is obviously formed in south of Riyadh.

This graben system is called Central Arabian Graben Sestem (CAGS). It is comprised of a group of lineaments and grabens and forms a large arc of 500 Kilometers length.

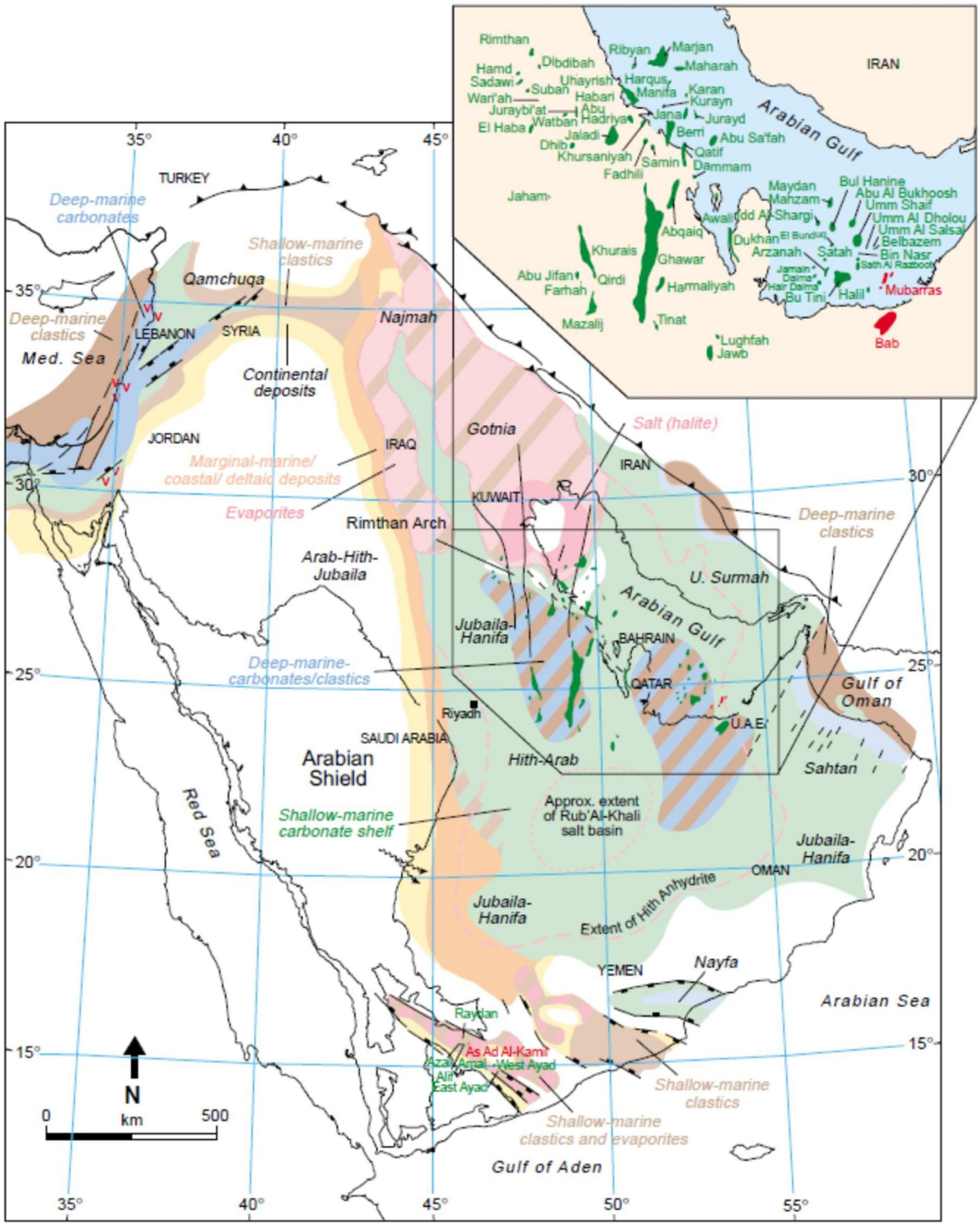

Figure 2.1 Paleo-environment map of Arabian plate illustrating the depesitional settings during Kimmerdgian or upper Jurassic time (Zeigler 2001).

Convexing toward west, these grabens are shown in (Figure 2.2).

This graben system surrounds East Arabian block which hosts most oil fields in Saudi Arabia. The East Arabaian block is bounded by strike slip fault that transfers the motion into transtensional motion in CAGC.

2.2. Fractures in Carbonate rocks:

Handin (1963) reported greater fracture intensity associated with quartzite, dolostones, sandstones, and finally limestones. They found a link between intensity and the ability of rocks to be ductile with depth of burial. Das Gupta (1978) noticed direct proportion between degree of dolomitization and fracture intensity with considering burial depth.

Larsen et al. (2009) studied orientations, spacing, and apertures of fractures systems in Gargano peninsula in Italy. Their study concluded that laminated mudstones are characterized by small spacing fractures and peritidal cycles are characterized by large spacing fractures. Frost and Kerans (2009) discussed the patterns and factors that control syndepositional fractures. They found that depositional and stratigraphic positions and bed thicknesses play an essential role in fracture development.

Ortega et al. (2010) analyzed fractures along 1D scanlines targeting the relationships between fracture intensity and several sedimentological characteristics such as lithofacies change, stratigraphy, bed thickness, dolomitization and mud content. They concluded that the major controlling factor is dolomite content followed by depositional and stratigraphic controls.

Larsen et al. (2010) discussed fracture penetration\offset in the Pizzicoli quarry in Italy.

They found that existence of laminated mudstone lithofacies of microbial origin is major factor that control the fracture linkage. They proposed three mechanisms for arrest\ offset and\or deflection:

I. Elastic Young's modulus mismatch.

II. Stress barriers formation as a result of principal stress rotation along bed boundaries.

III. Tensile stress which is induced along bed boundaries.

Lamarche et al. (2012) studied the patterns of fractures in 9 outcrops of tight carbonates from south-east basin in France. They suggested that fractures (especially stylolites) patterns are less dependent on lithofacies or bed thickness than on their physical and mechanical properties such as P-wave velocity and porosity. Lavenu et al. (2013) studied lithofacies together with fracture patterns within the flanks of Nerthe anticline (southeastern France) to find out their origin. They recognized that these fractures are of non-tectonic origin based on their diagenetic and geodynamic history.

Hariri (2013) studied systems and sets of fractures that are intersecting Dammam Dome. He identified three fracture sets based on their scales and orientations; these are major, minor, and localized.

Al-Fahmi et al. (2014) studied Cenozoic carbonate outcrops of Dammam Dome in integration with near surface seismic data to characterize, interpret, and understand fractures patterns within the dome. They identified three sets based on their scales and trends. They proposed a relationship between these sets and the doming process.

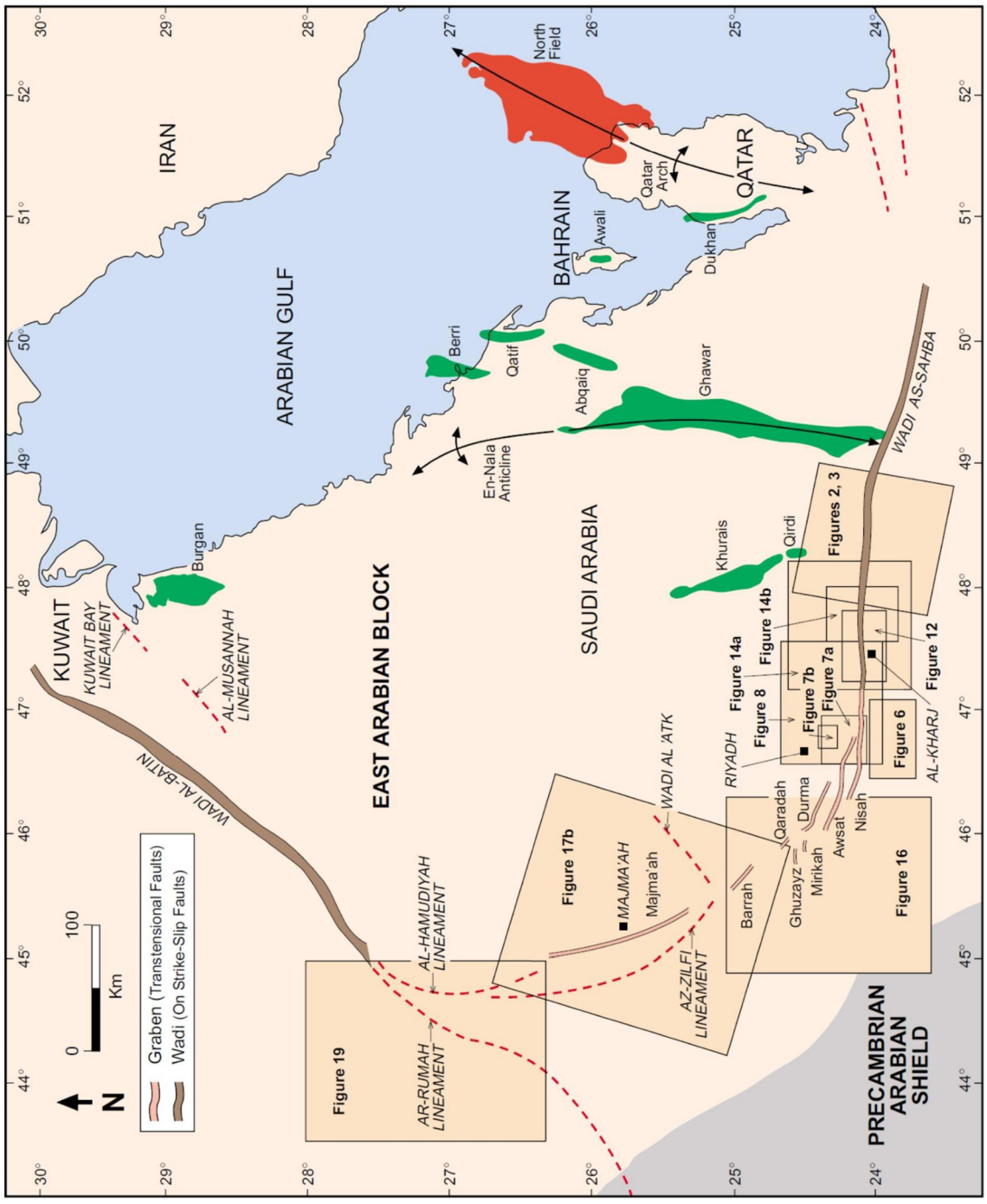

Figure 2.2 Collections of lineaments and grabens that form Central Arabian Graben System (Weijermars, 1998)

2.3. Geomechanical properties of carbonate rocks

Many other authors investigated geomechanical properties of carbonate rocks such as

Turgel and Zarif (2000) studied the effects of weathering on the geological and geomechanical properties of Devonian limestone rocks in eastern Istanbul, Turkey. They concluded that porosity and chemical features are good indicators for weathering, many micro-structural and textural changes during transition time are observed, these changes cause strength changes. Grain to micrite ratio affects strength, the unit weight decreases and porosity increases with strength.

Eberli et al. (2003) discussed factors that govern the elastic properties of carbonate rocks. They found that porosity values generally are inversely related to velocity but some deviations are caused by pore types (inter-crystalline, inter-particles, or moldic).

Shalabi et al. (2007) studied the relationship between rock hardness and many rock properties such as uniaxial compressive strength and Poisson's ratio for dolomite, dolomitic limestone, and limestone. They concluded that unconfined compressive strength is related linearly to Schmidt hammer hardness. They also concluded that Poisson's ratio decreases with increase in rock hardness and strength.

Kahraman and Yeken (2008) found good correlation between all physical parameters and P-wave velocity, linear correlation has been identified, they compared it with relations in the literature, they concluded also that these relations should be validated because they are applied under specific conditions and for certain rock types.

Abdullatif (2009) investigated geomechanical parameters in lower and middle Rus formation in Dammam dome, rock mass rating (RMR), and rock mass quality (Q). He

found the relationship between these parameters and correlated between two rating systems. He concluded that the rock quality and rating in lower Rus is lower than in middle Rus.

Ameen et al. (2009) analyzed representative samples from oil wells in Ghawar oil field and integrated core and log data for Arab-D reservoir. They re-divided Arab-D reservoir into units based on their mechanical properties. They also proved the role of texture and mineral content on mechanical properties.

Arman et al. (2012) collected many samples from various locations in the rock units belonging to the lower Oligocene Asmari formation. The study concluded that the fractional amount of dolomite increases the strength while the calcite "chalk" fraction decreases it.

Many authors have reported empirical equations through which unconfined compressive strength can be predicted from point load index and Schmidt hammer number particularly for carbonate rocks (Read et al. 1980, Katz et al. 2000, Yasar and Erdogan 2004).

CHAPTER THREE
FRACTURE ANALYSIS

3.1. Introduction

In this study, I conducted two field trips. During the first trip I studied 120 fractures along two detailed high resolution scan-lines or sample-lines (Figure 3.1), and during the second trip, a general overview were carried out to identify fractures sets which intersect both Arab-D member and the underlying Upper Jubaila Formation.

During the field investigations, several fractures patterns were observed and measured and the parameters are as follows:

- Fractures Parameters Several fracture parameters were observed and measured. These parameters are:

I. Fracture trend (strike and dip). The results are represented in rose diagram and stereo-net.

II. Fracture scale or length

III. Fracture intensity:

It is defined as the number of fractures per length unit (Ortega et al. 2006) along scan-line or sample line. It is considered as the most significant aspect for predicting the flow patterns in tight rocks. However, it is difficult to estimate it in the subsurface due to sampling problems (Ortega et al. 2010).

Nelson et al. (2001) recognized four factors that control fracture intensity. These are texture, bed thickness, composition, and tectonics.

IV. Fracture spacing:

It is the distance between fracture surfaces along the sample line. According to

Priest (1993), spacing is the opposite to frequency or intensity. V.

Fracture aperture:

It is the distance perpendicular to the two parallel (usually irregular or non-smooth) surfaces of the fractures, the word opening is used instead of aperture by some authors (Bai and Pollard 2001). Kinematic aperture represents the whole fracture opening including both filled and open parts. In this study, I used aperture as a kinematic aperture.

VI. Fracture arrest\ deflection:

According to Gudmundsson et al. (2010), usually fractures develop for short distances before being terminated or arrested. This termination takes place along interface, contact or discontinuity. Interface is contact between similar (or dissimilar rock media according to Priest (1993), discontinuity is a fracture or contact with negligible tensile strength. When a fracture meets one of the abovementioned surfaces, either it stops its development (arrested), penetrate, or deflected (in one or two directions) (Figure 3.2).

 Terrestial Laser Scanning (Lidar) for fracture imaging :

Terrestial Laser Scanning (Lidar) is a recently innovated approach designed for the purpose of spatial data collection in which the exposed outcrop can be modeled digitally with high resolution. This tool gives a good opportunity to establish a three dimensional photorealistic model to be visualized and interpreted.

To gain acceptable results from lidar scanning, a well- planned work flow is required (Figure 3.3). This work flow is described in details by Buckly et al. (2008) starting from acquisition to interpretation.

The basic principle of lidar is that the instrument emits a laser pulse which returns back. The time is measured and converted to range value. The instrument is attached with digital for data with true colors. The instrument and site are chosen based on the purpose of the study.

The data is collected in the form of (x,y,z) co-ordinates and the returning laser intensity. These data are called point cloud.

The first step in processing is data registration, it records the absolute or relative positioning of scan data (point cloud) and external picture image using GPS. The decision of either absolute or relative positioning is user defined.

The raw data is calibrated with digital camera image then the color is assigned to each point of the point cloud. This registered point cloud is then processed based on the user's wish by drawing polygons around points of interest.

The next step is to establish triangulated mesh or to find the best fitting surface to create the virtual outcrop model. This triangulated mesh is called Digital Elevation Model (DEM).

The last step is the integration between digital cameras with triangulated mesh to produce virtual outcrop model. The output of this stage is then interpreted using several software applications.

In this study, polywork software was used for processing and VRGS was used for interpretation.

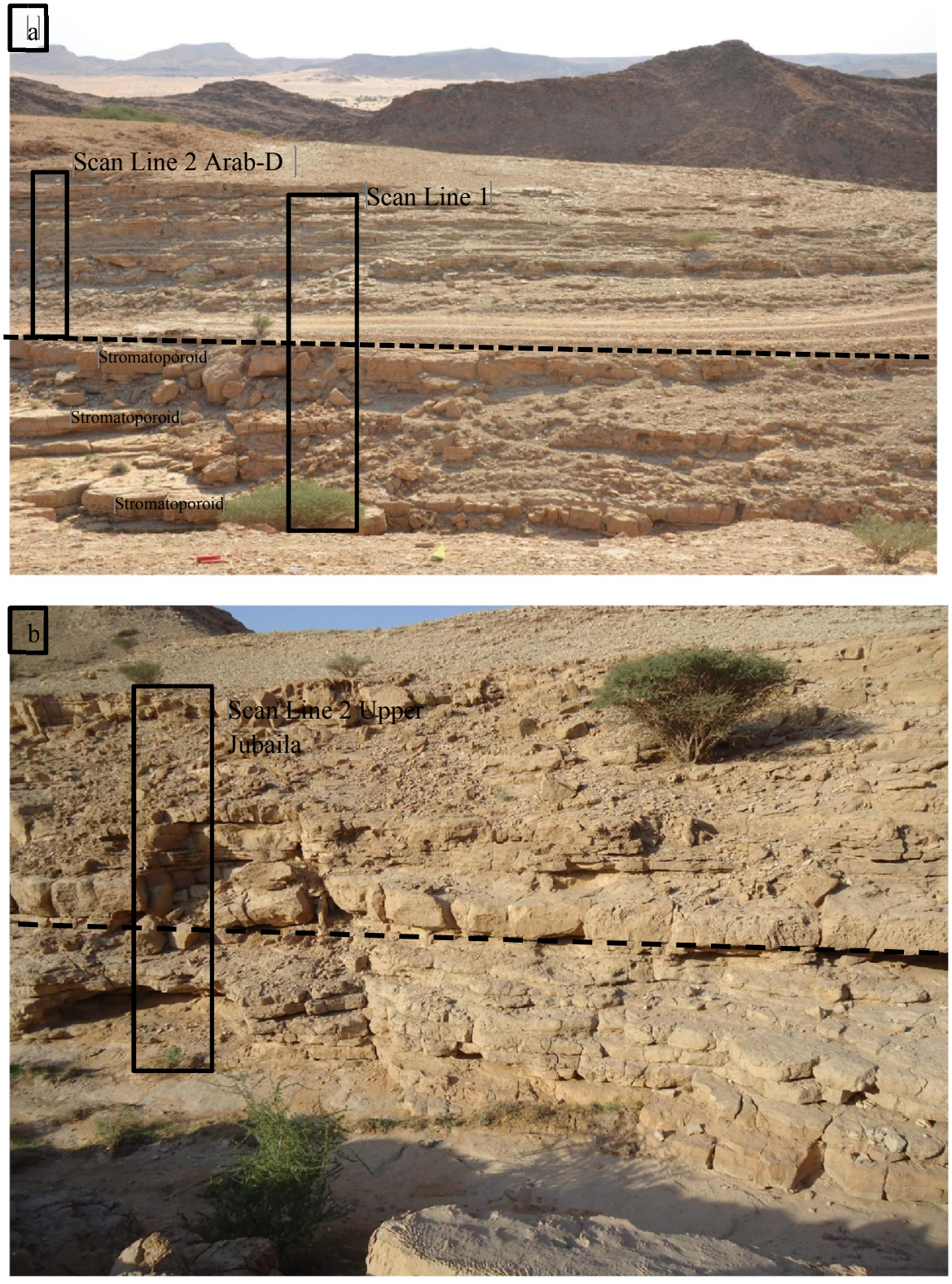

Figure 3.1 Positions of scan-lines in Wadi Nisah outcrop of Arab-D member and Upper Jubaila Formation: (a) Northern side and (b) Southern side

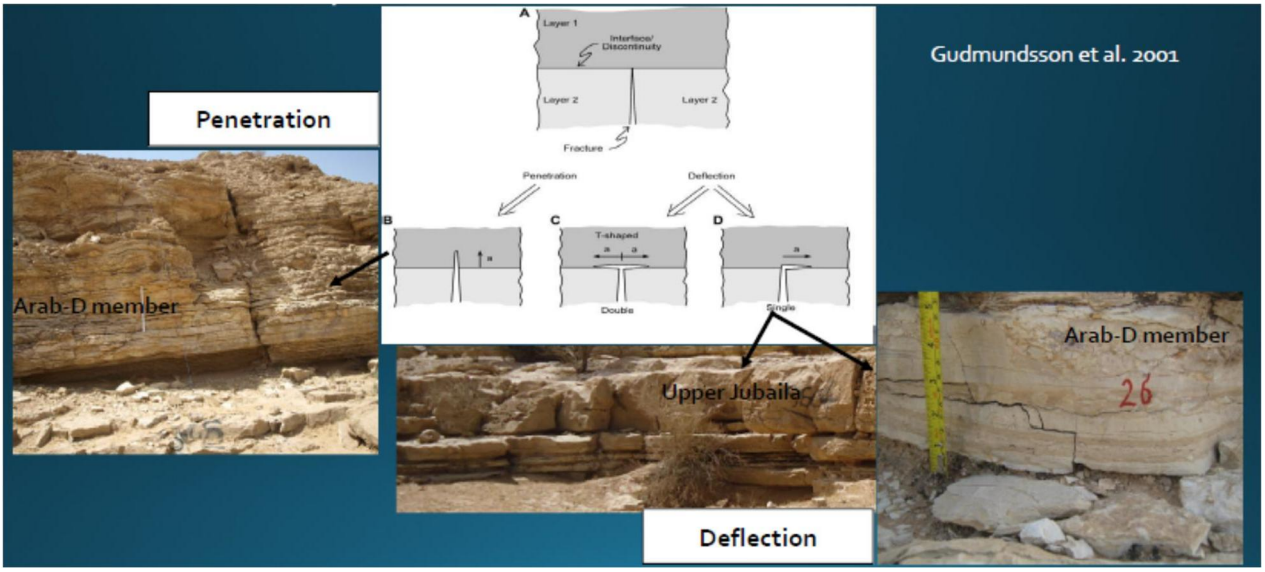

Figure 3.2 Fractures development along several rock units either penetrating or deflected (modified after Gudmundsson et al. 2010).

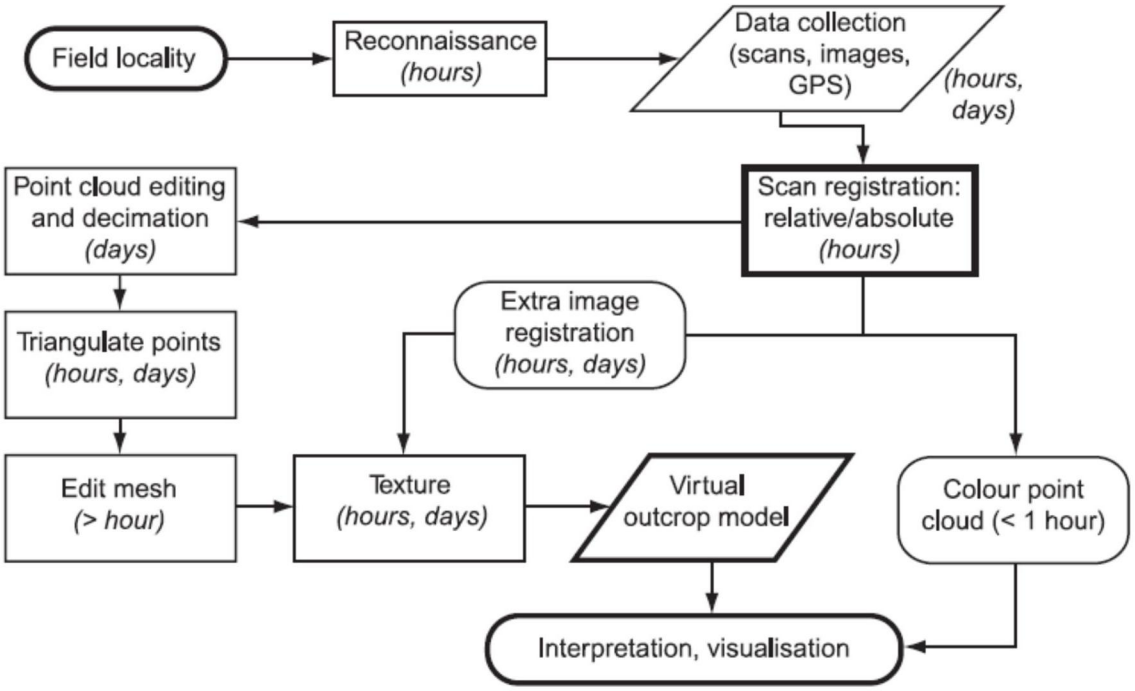

Figure 3.3 Work flow of Lidar data acquisition, processing and interpretation (Buckly et al., 2008)

3.2. Results and discussions

Fracture intensity was found inversely correlated with bed thickness (Figure 3.4) and fracture spacing (Figure 3.5). Bed thickness is directly related to spacing (Figure 3.6).

Fracture intensity and pattern is influenced by several factors including lithofacies change, bed thickness, geomechanical properties, and burial depth (Figure 3.7). These factors are jointly affecting the fractures' patterns and development.

3.2.1. Fracture patterns within Upper Jubaila Formation

Upper Jubaila is intersected by three sets of fractures; these are oriented N40° E, N20° E, and NW. The most common set is NW oriented or striking set. These sets are dipping towards SW, SE, NW, E, and S, with dominance of fractures striking NW (Figure 3.8) and dipping SW and SE (figure 3.9).

Most of these fractures are near horizontal and near vertical (Figure 3.10). Based on fracture intensity, upper Jubaila is subdivided into two units; the upper unit is characterized by higher fracture intensity and smaller spacing, the lower part is with lower fracture intensity and larger spacing. The most significant factors controlling fracture intensity (and spacing) are bed thickness and burial depth. Higher bed thickness is related with lower intensity and higher spacing, and lower bed thickness is related with higher intensity and smaller spacing (figure 3.11).

Ductility tends to increase downward. Therefore, more resistance to brittle deformation takes place. Rock type and lithofacies play a secondary role in propagation of fractures

within the joint effect of bed thickness and burial depth. In general, the stromatoporoid packstones lithofacies are more fractured than dolomitic mudstone lithofacies. This indicates a lithofacies and textural influence on fracture patterns.

- N 20̊ E fracture set

Part of it dips in SE direction and other part dips in NW direction They have regular shape, open aperture (several centimeters), they are considered as medium scale fractures (1 meter) relative to other sets. They are arrested within Stromatoporoid lithofacies and changing their pattern along. They lack any vertical displacement and are characterized by small intensity. They are generally widely spaced (figure 3.12).

- N 40̊ E fractures set

These fractures are crosscutting the previous set which leads to collapse of rock blocks. Most of these fractures dip along the NW direction and minor fractures dip along SE direction. They have regular shape and small parts of them have irregular shape. They are medium scale fractures and arrested within one bed of stromatoporoid lithofacies. They lack also any vertical displacement and most of them have closed aperture and they are more intensive than the previous sets and more closely spaced (Figure 3.13).

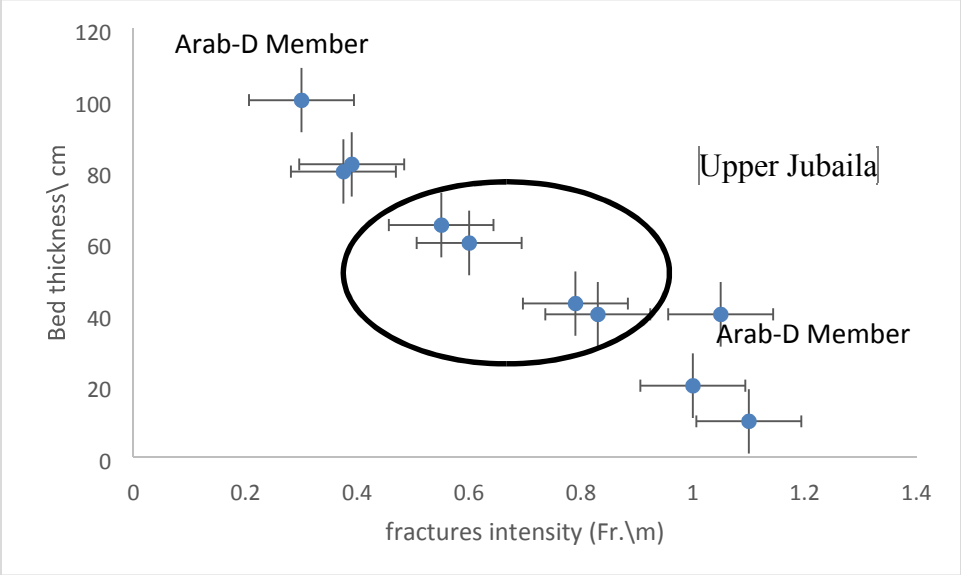

Figure 3.4 Bed thickness versus fracture intensity for Arab-D Member and Upper Jubaila Formation

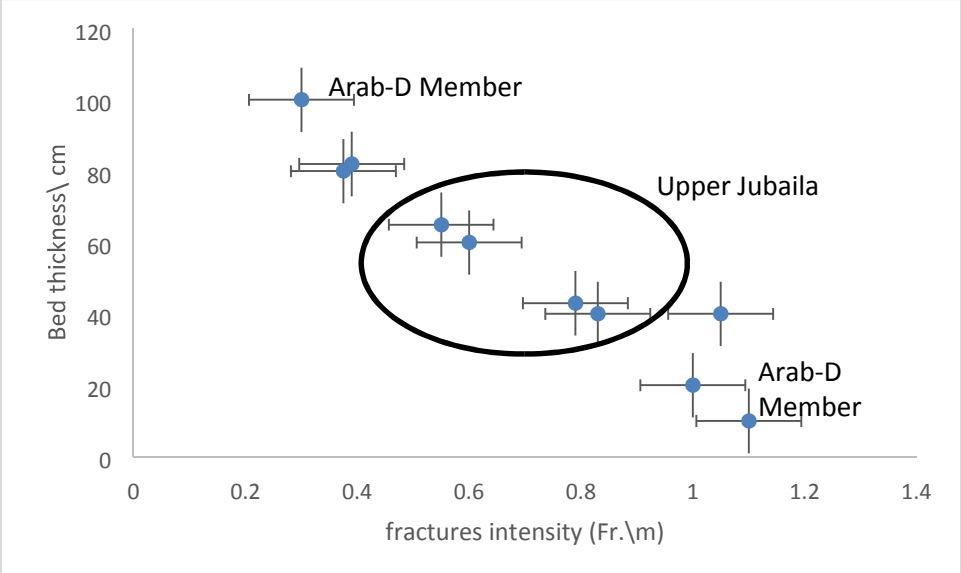

Figure 3.5 Bed thickness versus fracture spacing for Arab-D Member and Upper Jubaila Formation

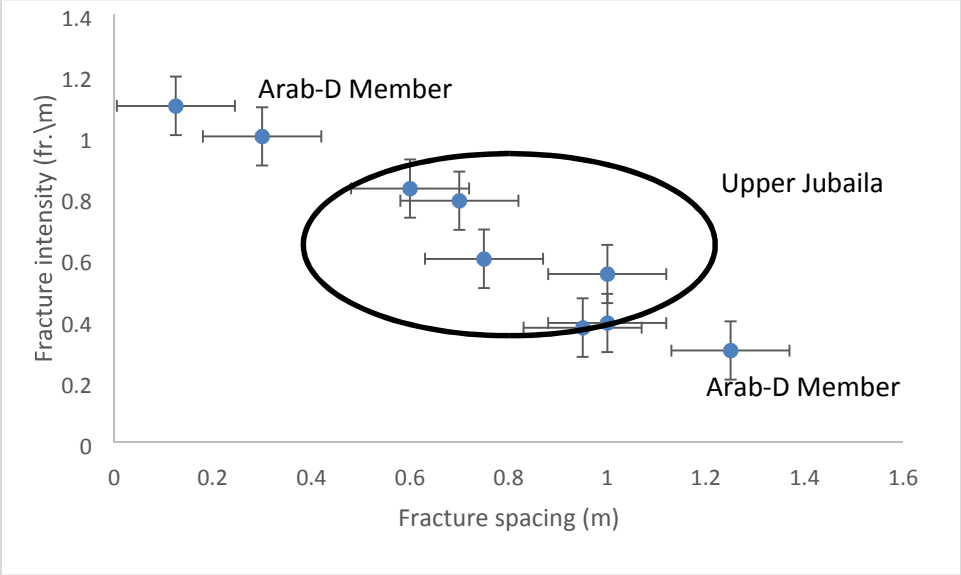

Figure 3.6 Fracture intensity versus fracture spacing for Arab-D Member and Upper Jubaila Formation

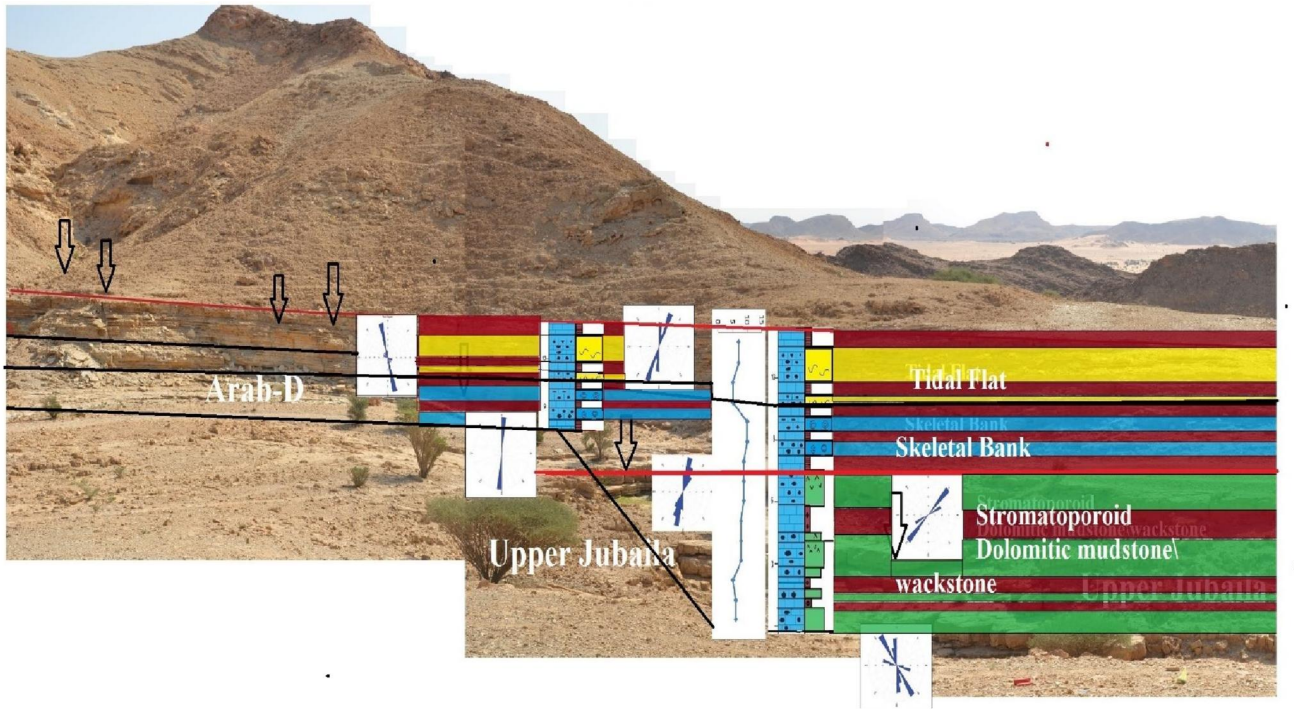

Figure 3.7 Photomosaic including lateral change of lithofacies associations with various fractures and intensity profile.

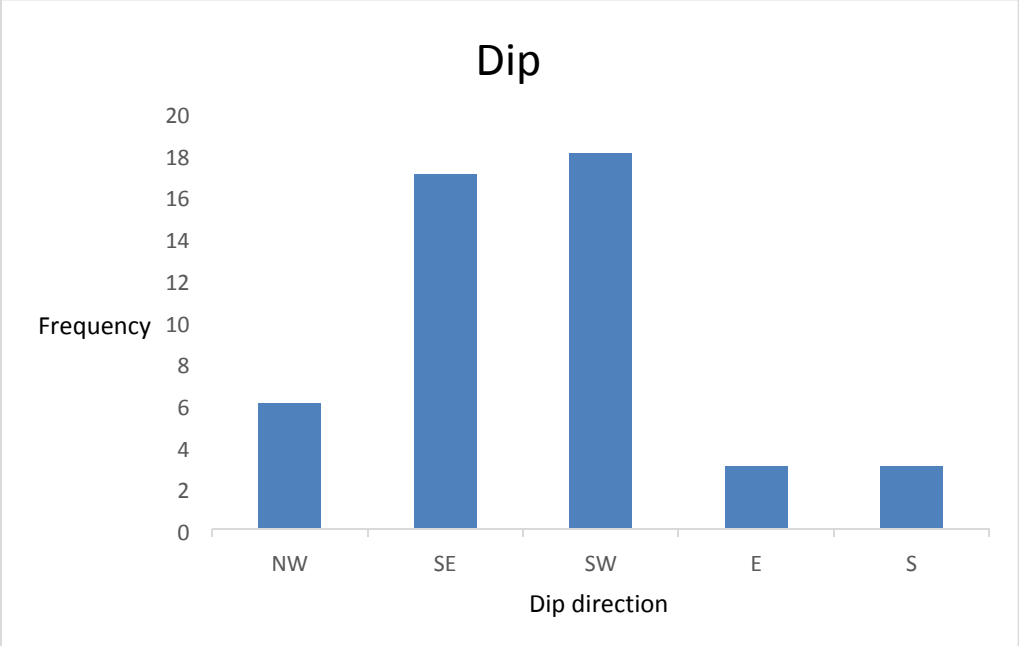

Figure 3.8 Histogram of dip directions in Upper Jubaila Formation

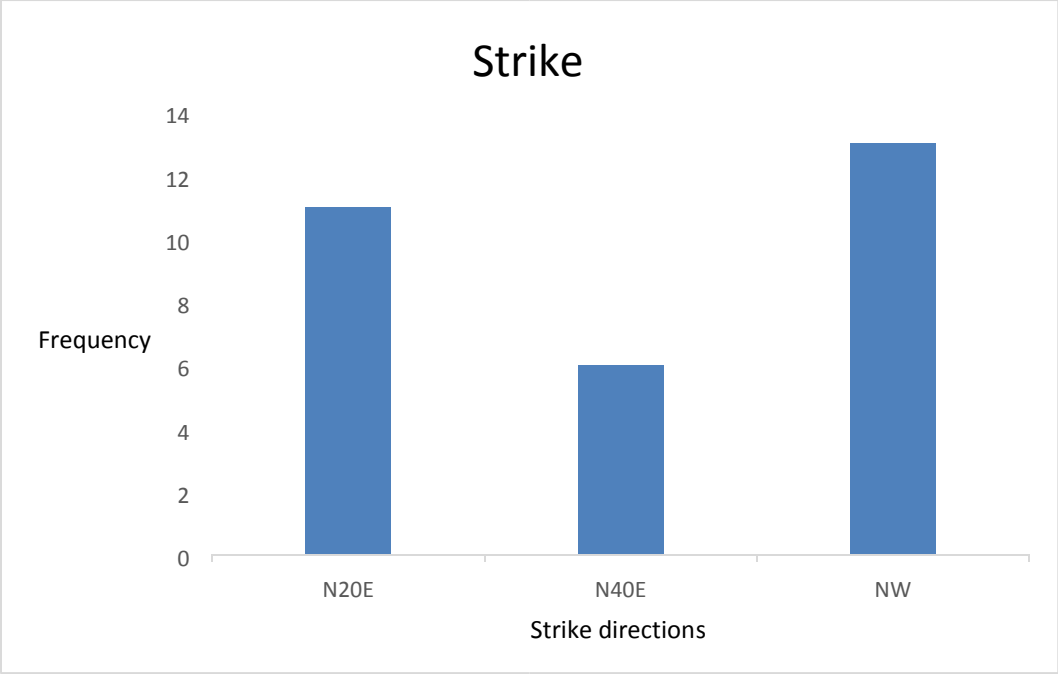

Figure 3.9 Histograms of strike and dip directions within Upper Jubaila Formation

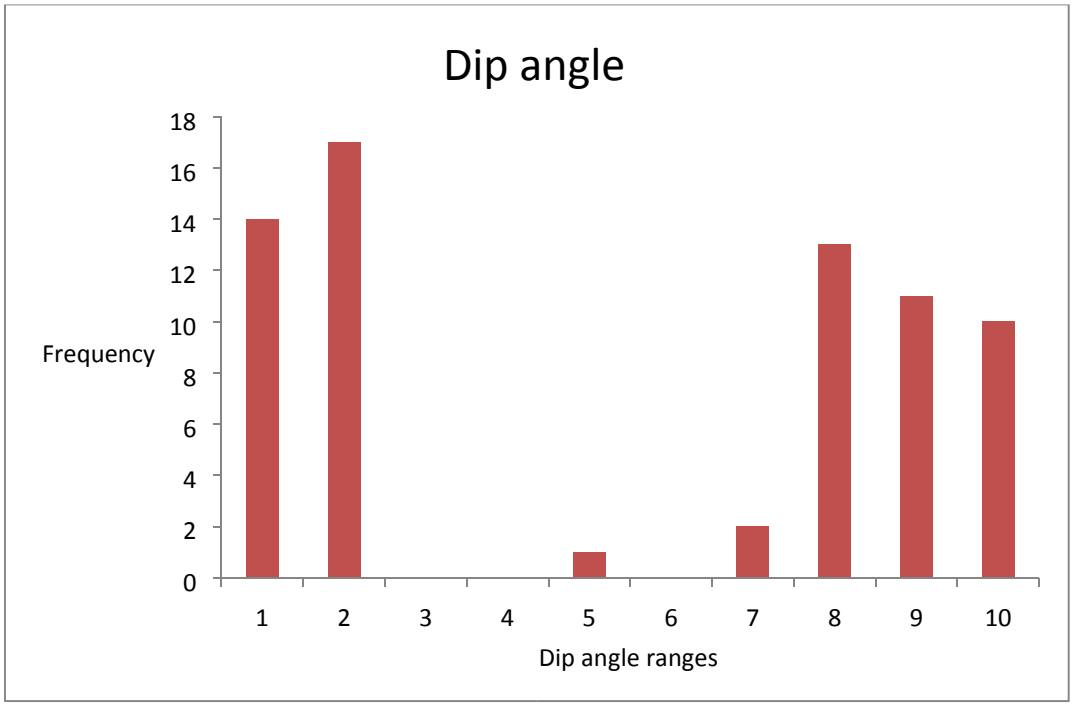

Figure 3.10 Histogram for dip angles of fractures within Upper Jubaila Formation

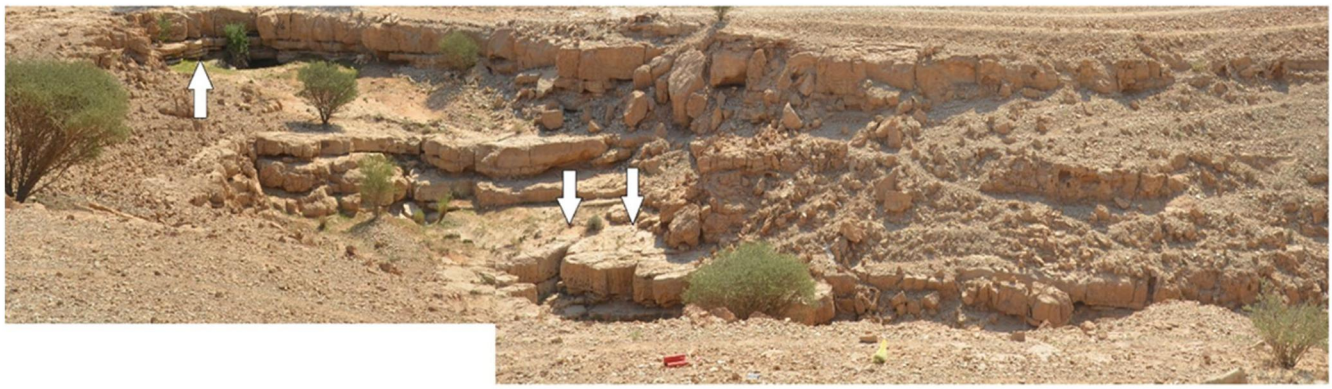

Figure 3.11 Fractures sets within Upper Jubaila Formation

- NW set

Some fractures within this set dip toward NE and small fractures dip toward SW (Figure 3.14). They are characterized by regular shapes. They are also large scale fractures and cut through several beds (stromatoporoid and dolomitic lithofacies). They are characterized by some extensional vertical displacement and small apertures filled with diagenetic materials (Figure 3.15), they are penetrating through two or several beds, and are relatively largely spaced, less intensive within each bed.

- Horizontal fractures

These fractures are aligned along bed boundaries and some of them are contained within the beds (Figure 3.16). Most of these fractures are striking in or around EW direction (along the escarpment strike). These horizontally dipping fractures are widely opened and some of them are filled with some materials.

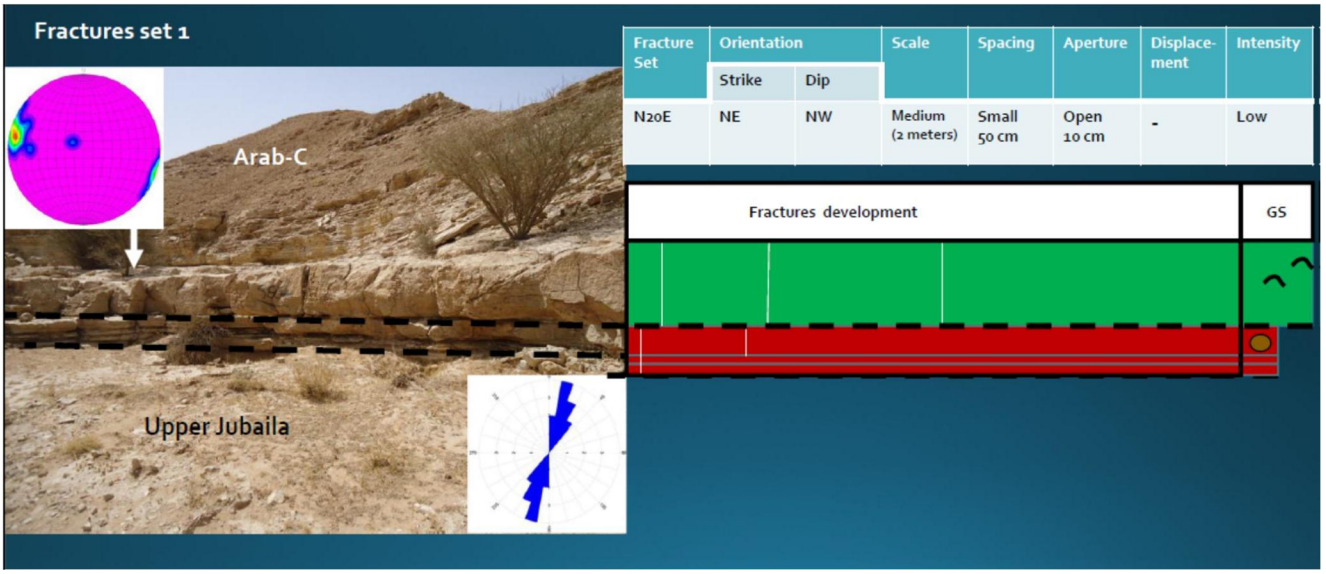

Figure 3.12 North 20 East fracture set within Upper Jubaila with stereonet and rose diagram

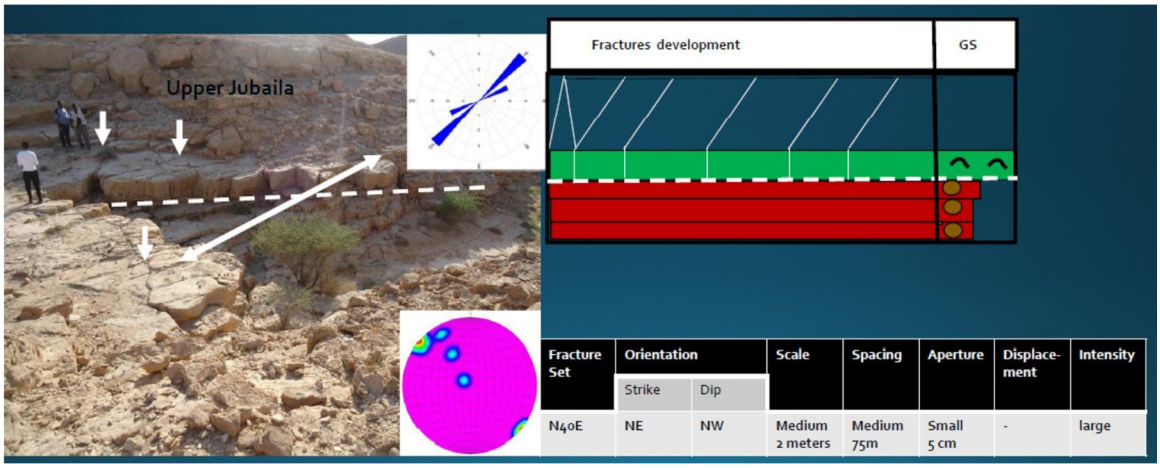

Fracture Set	Orientation		Scale	Spacing	Aperture	Displace-ment	Intensity
	Strike	Dip					
N40E	NE	NW	Medium 2 meters	Medium 75m	Small 5 cm	-	large

Figure 3.13 North 40 East set within Upper Jubaila Formation with rose diagram and stereonet

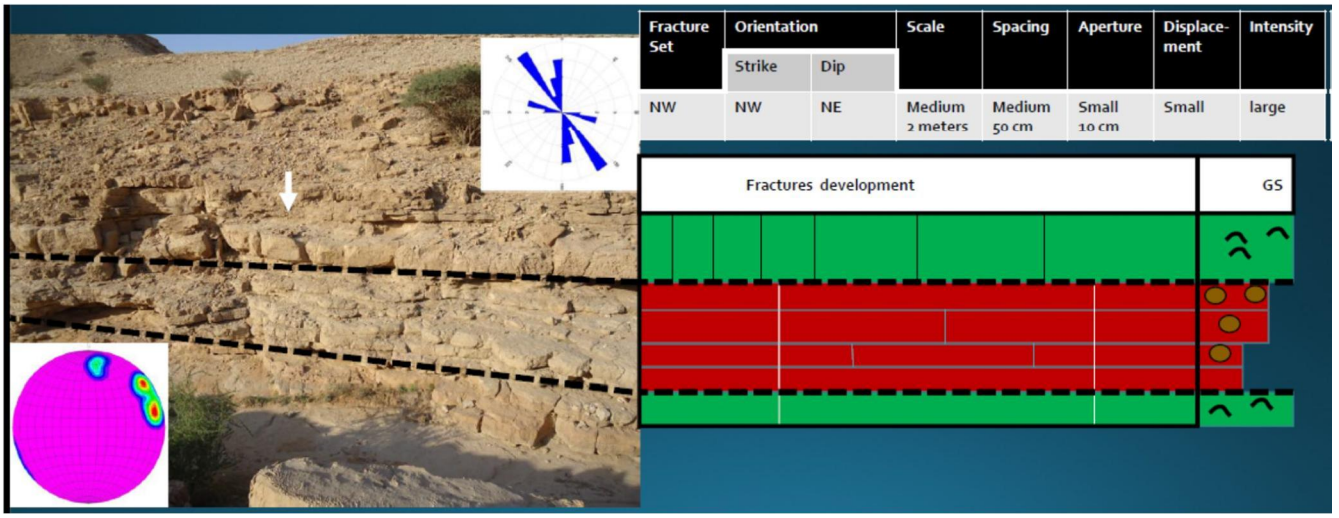

Figure 3.14 North west fractures set within Upper Jubaila Formation with rose diagram and steronet

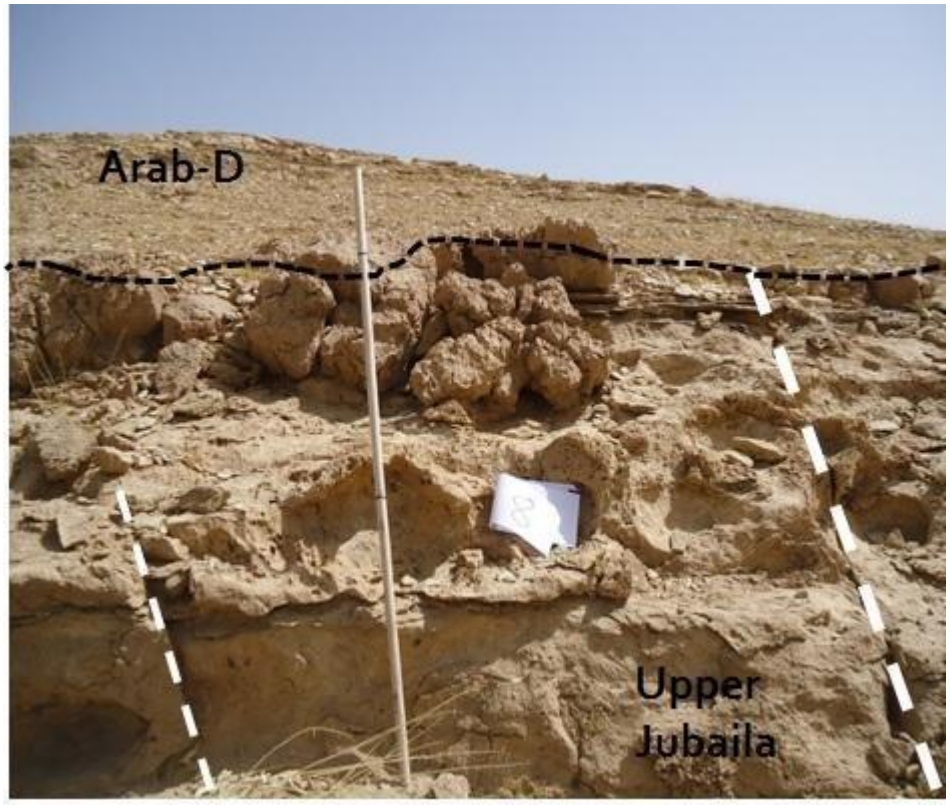

Figure 3.15 Large scale fractures NW striking fractures penetrating through several beds

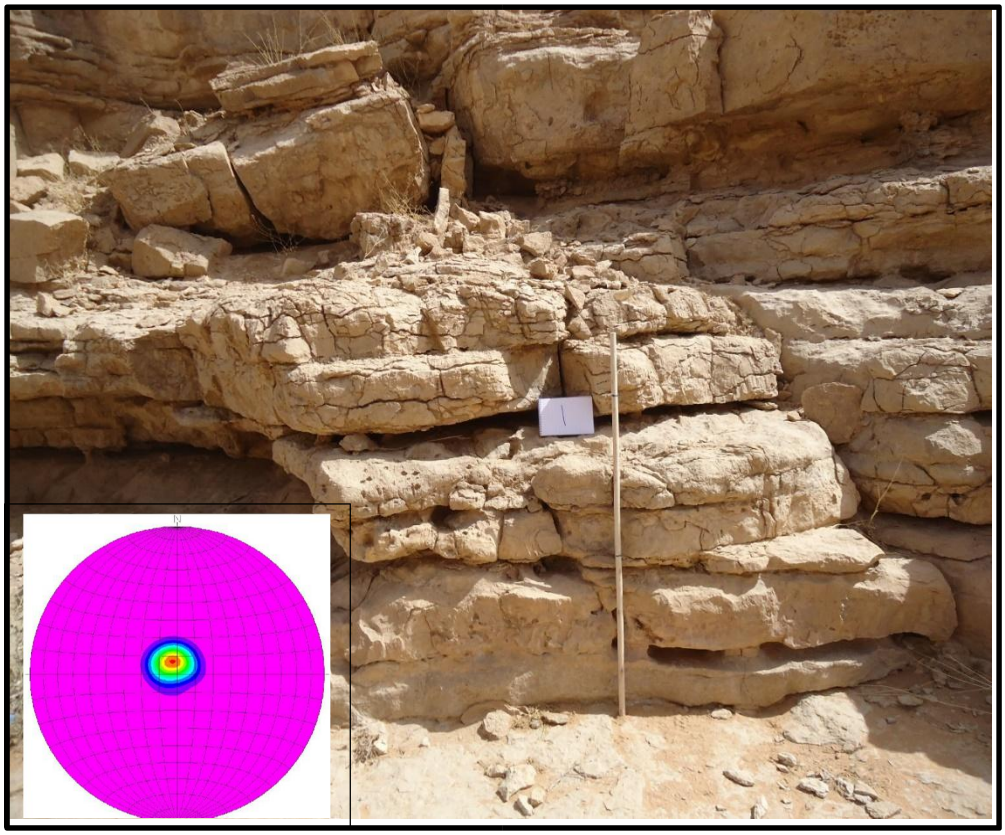

Figure 3.16 Stereonet and picture for horizontal fractures in the upper Jubaila Formation

3.2.2. Fractures patterns within Arab-D Member

Fractures within Arab-D member are striking NW, EW, NE, and NS directions with dominance of NW striking. Most of these fractures are dipping NE (Figure 3.17) and are either near horizontal or near vertical (Figure 3.18).

Bed thickness and lithofacies association changes have an impact on the fractures' development and patterns. Small bed thickness are characterized by high intensity and narrow spacing. Thickly bedded strata are affected by fractures of small intensity and wide spacing (Figure 3.19).

Fractures are arrested and change their patterns along stratigraphic boundaries (figure 3.20). Based on these factors the Arab-D member is divided into two units. The upper unit is comprised of the upper part of tidal flat lithofacies association, this unit is characterized by small intensity. The lower unit is comprised of the lower unit of tidal flat and skeletal bank association and characterized by higher intensity and smaller spacing.

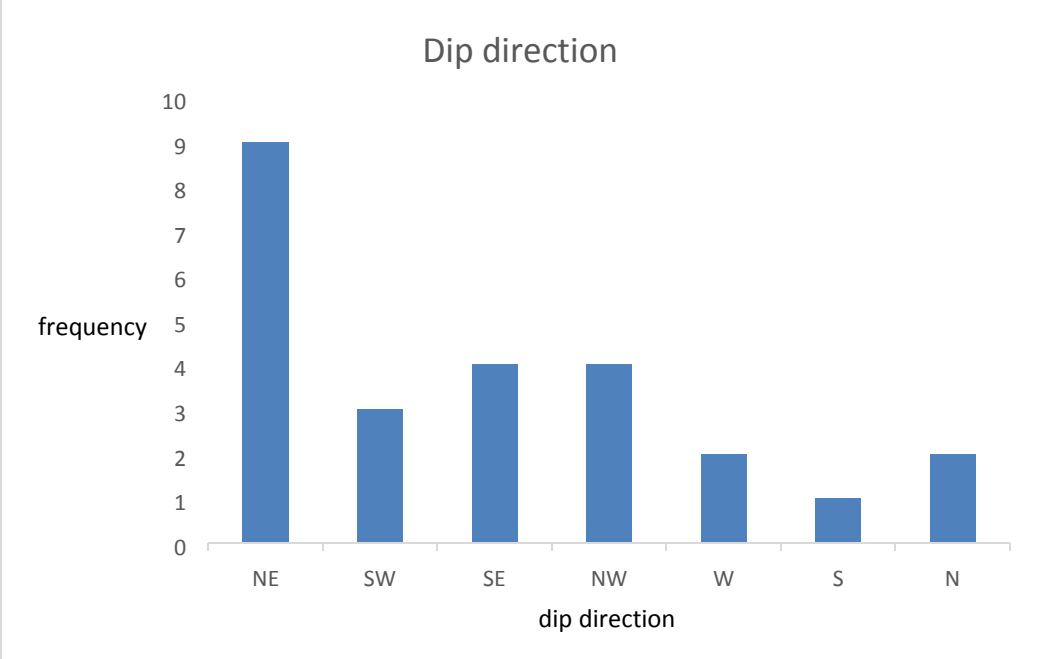

Figure 3.17 Histogram of strike and dip of several fractures sets within Arab-D member

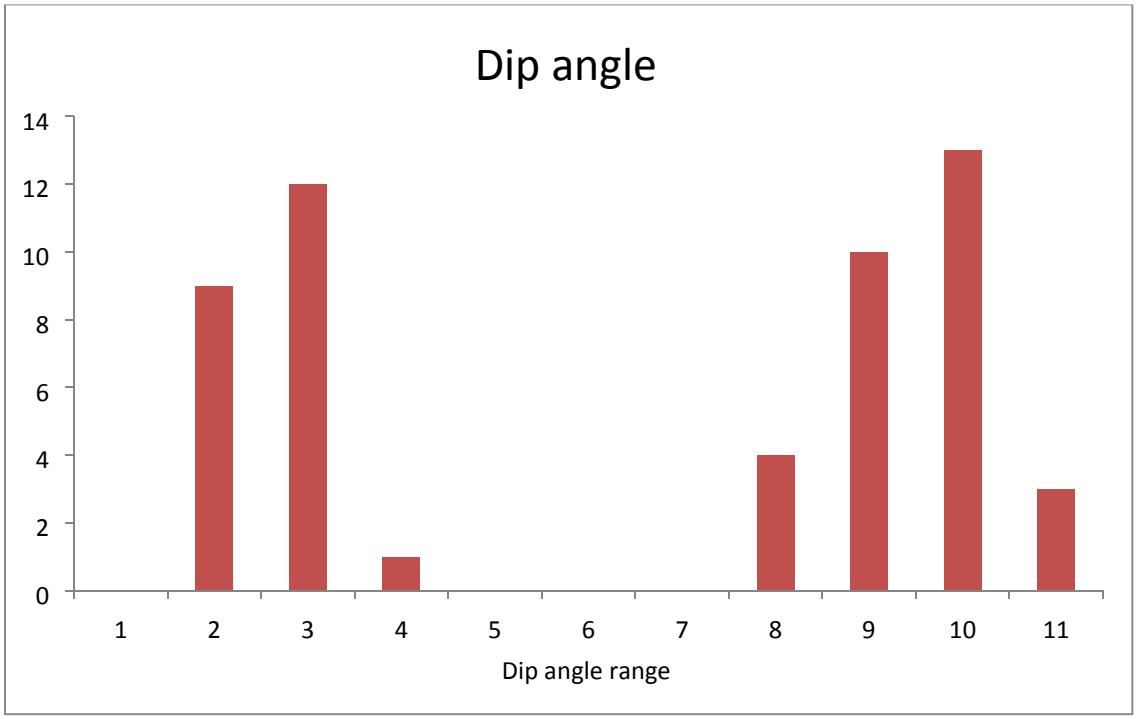

Figure 3.18 Histogram of dip values ranges for various fractures sets within Arab-D member

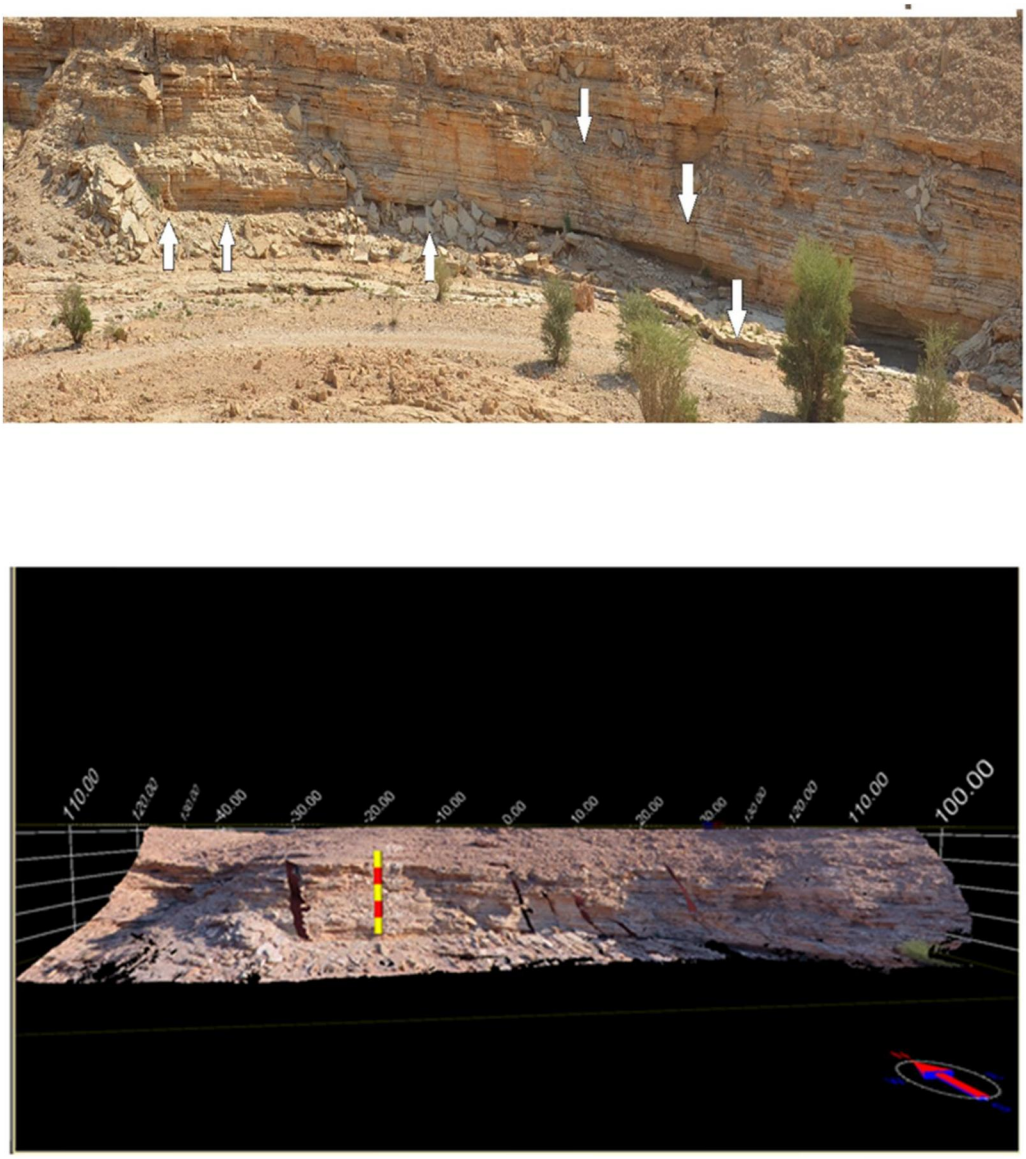

Figure 3.19 Mosaic showing fractures sets within Arab-D member (up), Lidar image (down) illustrating various frctures sets within Arab-D Member

- NW fractures set

Fractures within this set are dipping toward NE and few of them are dipping toward SW. Also most of them are dipping near vertically and near horizontally (Figure 3.20). They are closely to moderately spaced and tight to closed apertures, vertical displacement is noticed within this set's fractures (Figure 3.21)

- N-S fractures set

Fractures within this set are vertically dipping (Figure 3.22) and small scale (cutting through thin beds). They are constricted within peloidal fossiliferous grainstone lithofacies and borrowed wackstone lithofacies within skeletal bank lithofacies association. They reveal closed apertures and small spacing.

- N 20˚E

Most ~~of~~ fractures within this set dip toward NW direction and few of them are oriented toward SE (Figure 3.23). Most of them are near vertically dipping. These fractures are large scale fractures cutting through several beds. They are widely spaced with widely opened apertures, no materials filling their apertures.

- E-W fractures set

Fractures within this set are oriented along the escarpment strike and are seen on the top of resistive peloidal fossiliferous grainstone lithofacies (Figure 3.24). All these fractures are restricted to small scale fractures that are cutting through one bed. They are vertically and near vertically dipping (around 80°). Most of them dip toward N and NW and the rest S and SW. Fractures within this set are relatively widely opened and filled with some plant

residuals and crosscutting NW oriented fractures which indicates that they are relatively older. They are regular in shape and closely spaced.

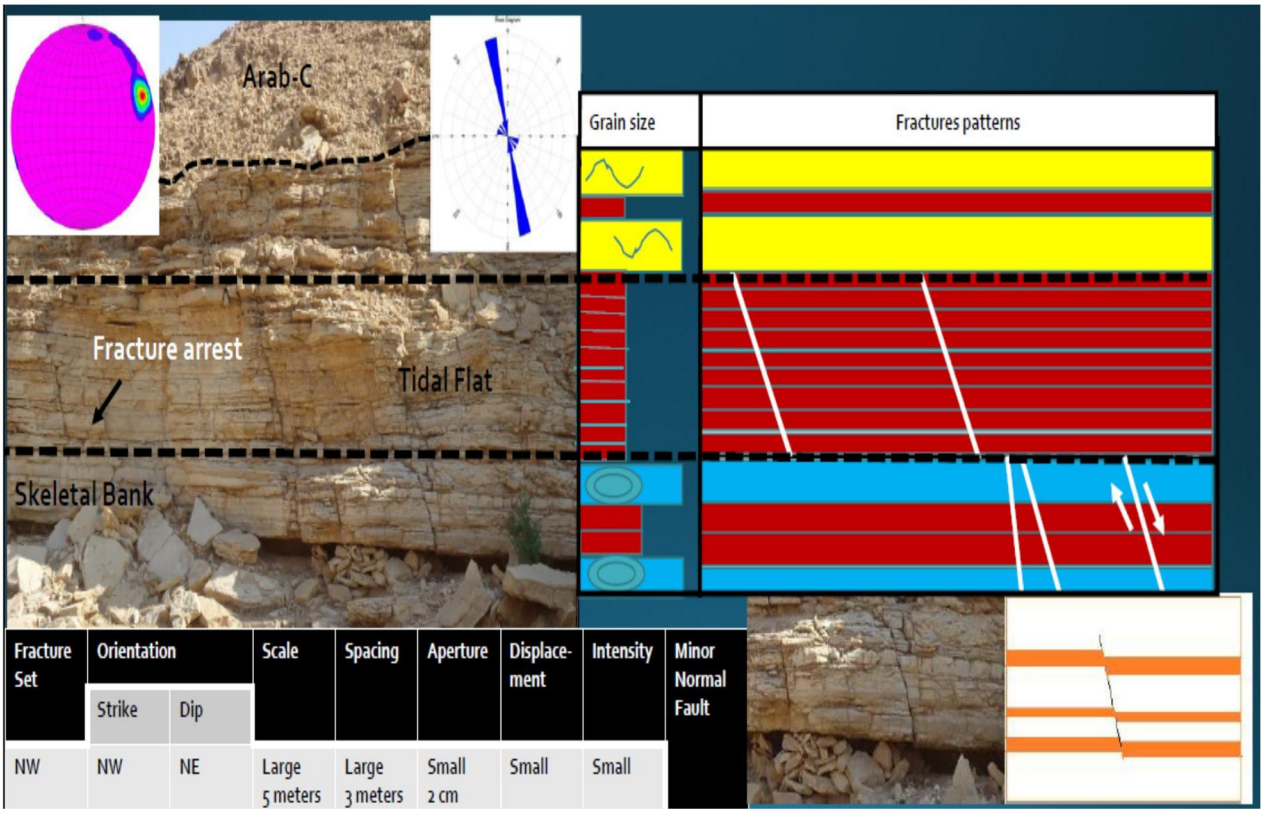

Fracture Set	Orientation		Scale	Spacing	Aperture	Displace-ment	Intensity	Minor Normal Fault
	Strike	Dip						
NW	NW	NE	Large 5 meters	Large 3 meters	Small 2 cm	Small	Small	

Figure 3.20 NW fractures set within Arab-D member with rose diagram and stereonet

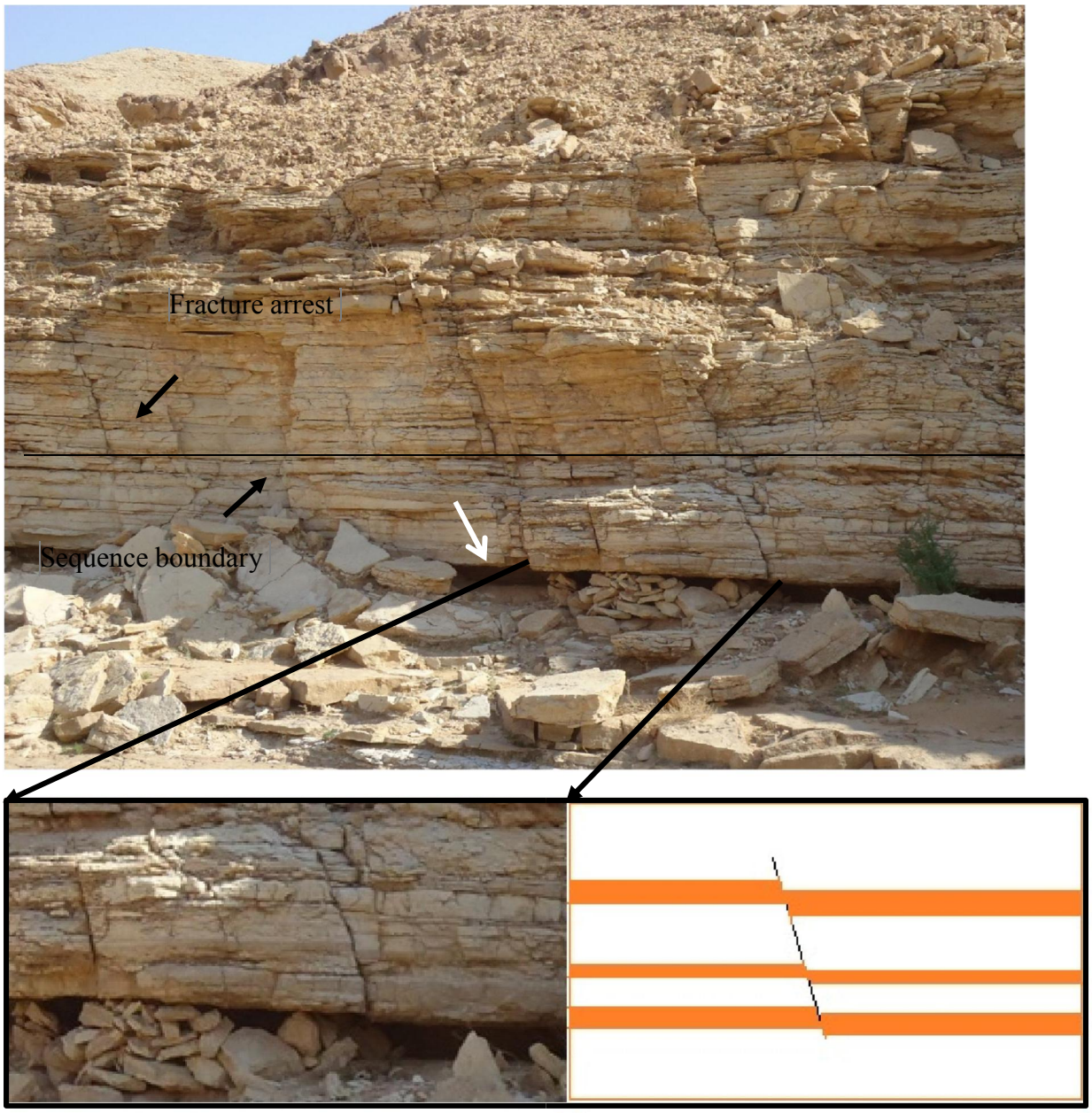

Figure 3.21 Displacement characterizing NW striking fractures in Arab-D member

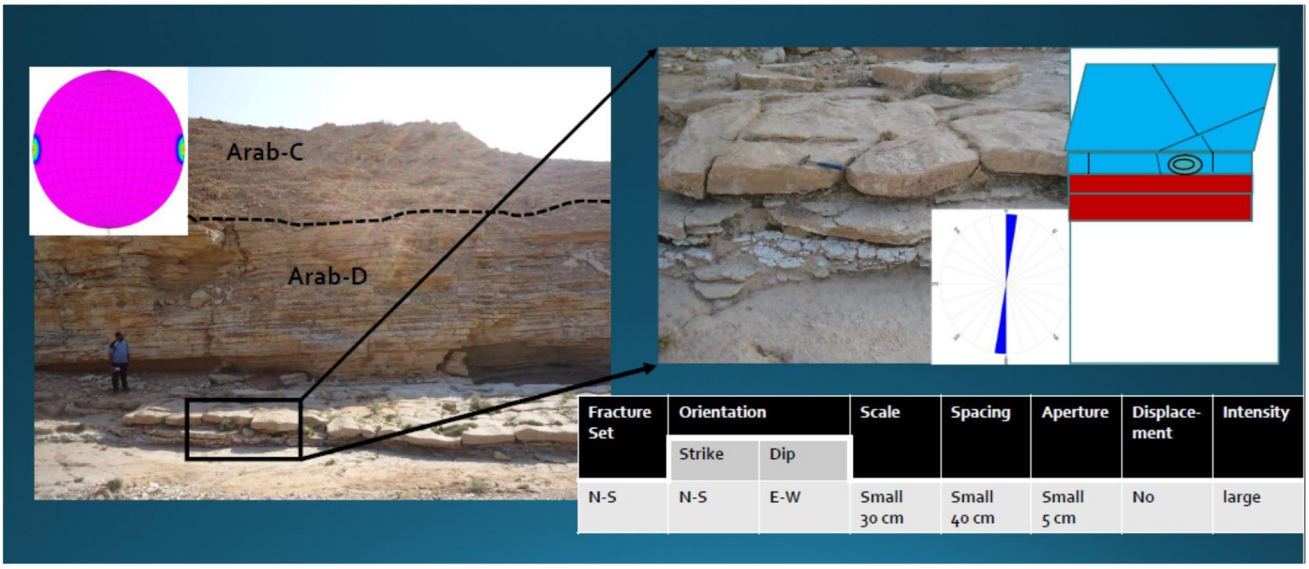

Fracture Set	Orientation		Scale	Spacing	Aperture	Displace-ment	Intensity
	Strike	Dip					
N-S	N-S	E-W	Small 30 cm	Small 40 cm	Small 5 cm	No	large

Figure 3.22 N-S oriented fractures rose diagram, stereonet

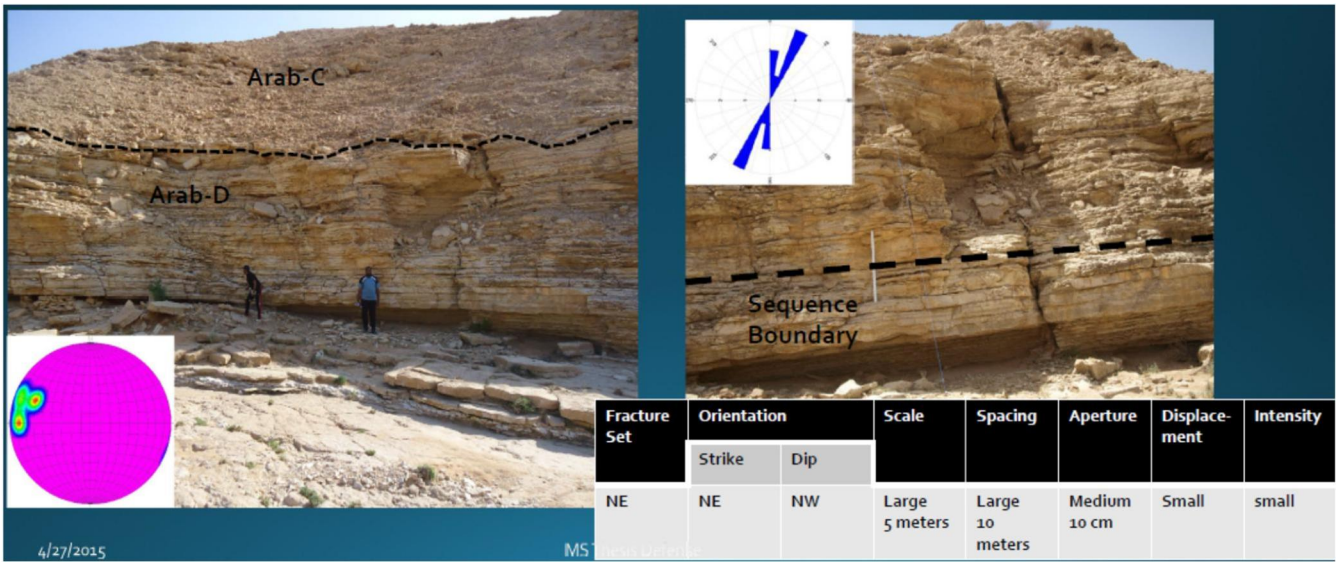

Fracture Set	Orientation		Scale	Spacing	Aperture	Displace-ment	Intensity
	Strike	Dip					
NE	NE	NW	Large 5 meters	Large 10 meters	Medium 10 cm	Small	small

Figure 3.23 North East oriented fracture set in Arab-D member

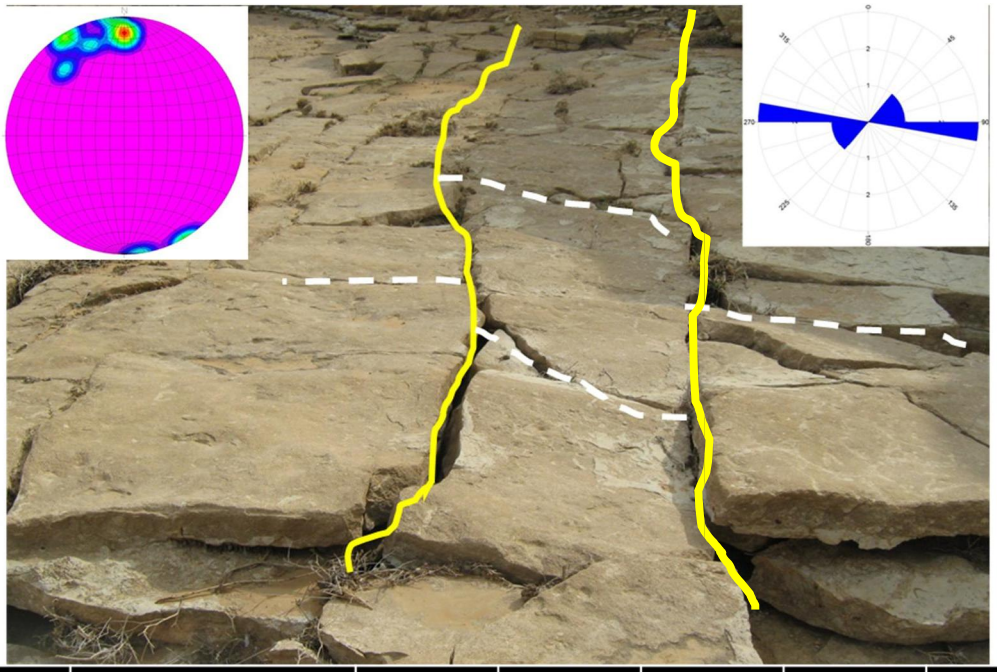

Fracture Set	Orientation		Scale	Spacing	Aperture	Displace-ment	Intensity
	Strike	dip					
EW	EW	N-S	Small	Small	Small	No	Large

Figure 3.24 Fracture set oriented along E-W direction in Arab-D member

3.3. Localized (small scale) fractures

These fractures are lacking any preferred orientations or trends. They are characterized by small length and small opening and sometimes they are closed (Figure 3.25). Their openings are usually filled.

Hariri (2013) interpreted these types of fractures, he proposed that these types are formed as a result of change in the rock properties, in this study; fractures within this scale characterize certain lithofacies. Most random fractures were found in laminated mudstone lithofacies and found to be filled with chemical materials. The least random sets were found within peloidal lithofacies, they change their trends along specific zones, and those lithofacies represents the weakest lithofacies according to the results of strength index tests which is consistent with the findings of Hariri (2013).

3.4. Cross-cutting Relationships

Plan views provide opportunity to find out the relative age relationships between different sets. In Arab-D member, the plan view on top of resistive peloidal bed reveals that the E-W oriented set represents the youngest set intersecting Arab-D member, proceeded by N-S, and the oldest one is N20E. NW set is not seen in the plan view.

In upper Jubaila Formation, NW oriented fractures are cross-cut by NE set which indicates that the NE oriented fracture represents the youngest set intersecting Upper Jubaila Formation.

Fractures sets were also recognized in and around my study area using Google map. There are number of drainage systems which are influenced by fractures systems, they are oriented along E-W and NW-SE. the density of these fractures increases with the

vicinity of Wadi Nisah (Figure 3.26). These sets are intersected by large number of wades and drainage systems and some displacement can be noticed. According to Weijermars (1998), the floor of the graben is filled with recent alluvial sediments.

Most fractures within Upper Jubaila Formation are striking NW-SE, NE-SW, this implies that these fractures sets were produced as a result of maximum stress normal to these directions. i.e.: NE-SW, NW-SE. Arab-D member is clearly affected CAGS in which large scale fractures are extending laterally more than several meters (Figure 3.27). These sets are oriented E-S and interpreted to be as a result of CAGS. Most of the fractures are without vertical displacement which implies shear stress. Slight extensional stress is obvious in Upper Jubaila and it is increasing upward in Arab-D member.

Figure 3.25 Localized small scale fractures within Arab-D member (up), cross-cutting fractures on the top of Upper Jubaila Formation

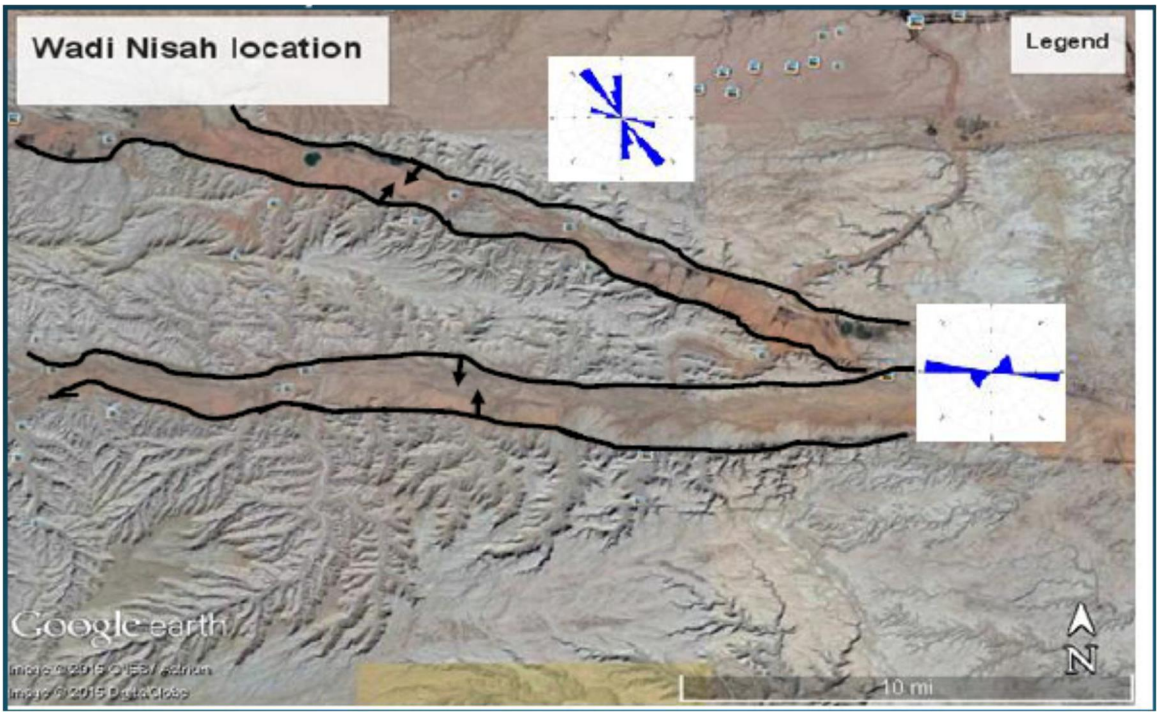

Figure 3.26 Google map showing fracture controlled drainage system in Wadi Nisah

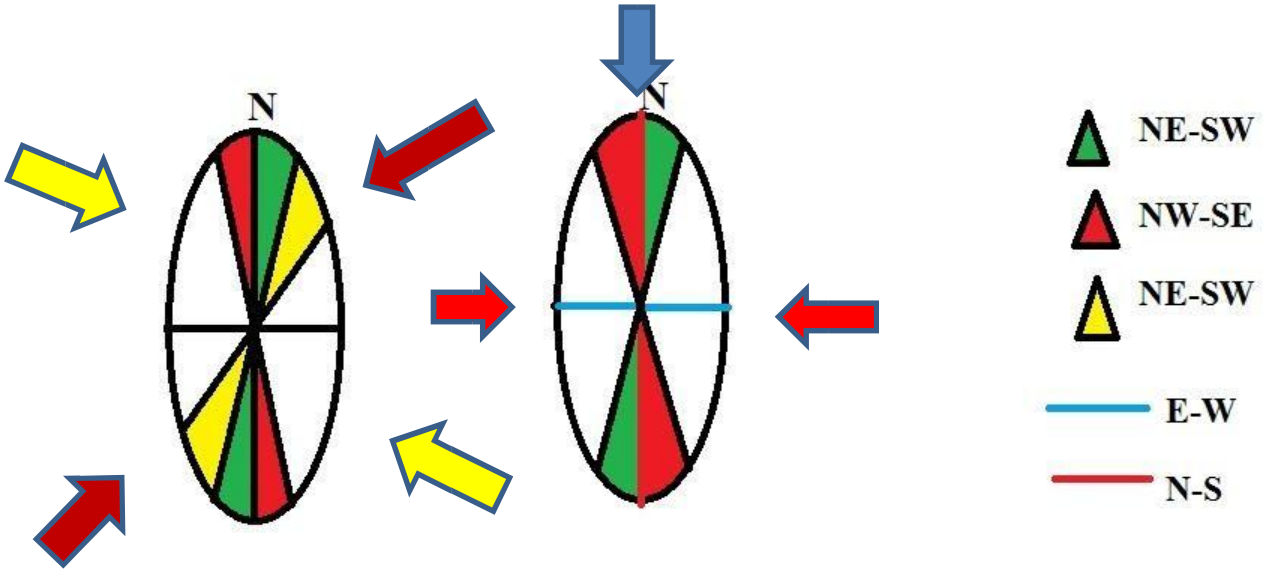

Figure 3.27 Maximum stress direction influencing Upper Jubaila (right), and Arab-D member (left)

Table 3.1 Parameters (strike, dip, fracture intensity, spacing, aperture filling, and displacement) of fractures sets affecting Arab-D member and Upper Jubaila Formation

	Strike	Dip	Scale	Intensity	Spacing	Aperture filling	Displacement
Upper Jubaila	N20E	NW>SE	Medium to large	Low	Large	Opened	Horizontal
	N40E	NW>SE	Medium	Medium	Small	Closed	Horizontal
	NW	NE	Medium to large	High	Small	Opened Filled	Horizontal to vertical
Arab-D	NW	NE>SW	Large	Low	Large	Closed	Vertical
	N20E	NW>SE	Large	Low	Large	Opened	Horizontal
	N-S	-	Small	High	Small	Narrow opening	Horizontal
	E-W	-	Small	High	Small	Narrow opening	Horizontal

CHAPTER FOUR

GEOMECHANICAL PROPERTIES OF TIGHT CARBONATE

4.1. Introduction

This chapter presents laboratory experiments which were carried out, and results of these experiments were analysed statistically and correlated with each other and with porosity and permeability. Correlation of Co-efficient "R^2" were determined. Intact rock classification designed by Deere and Miller were constructed for both Arab-D Member and Upper Jubaila Formation. Most importantly, geomechanical units were reconstructed based on similarity (or differences) on several geomechanical properties.

A group of samples were collected to investigate lithofacies through preparing thin sections and petrographic analysis and description.Porosity and permeability were measured in core plugs. Regular cubes or rock pieces were prepared from rock specimens.

The measurements which were carried out are the following:

4.1.1. Schmidt Hammer Rebound test:

Schmidt hammer has been used in rock mechanical practice since the sixties as nondistructive index test for a quick characterization of rock strength and hardness (Miller, 1965). The Schmidt hammer is characterized by its rapidity, portability, and simplicity. It is mostly used during the initial stages of design (Figure 4.1).

The results' reliability are affected by many factors such as rebound value, normalization, type of hammer, smoothness of the surface, specimen dimension, moisture content, weathering, gathering, and reduction of data (Aydin and Basu, 2005).

The Schmidt hammers is perpendicularly pressed to the surface. The piston is released toward the surface, and part of the piston's impact energy is absorbed and other part is transformed (to sound and heat). The remaining part depends on is the degree to which the surface resists the penetration or the surface hardness. This energy causes the rebound of the piston. The harder the surface the shorter the depth of penetration, the greater the rebound. The ratio between the traveled distances by piston after the rebound to the original extension is the rebound value.

There are two types of hammer, L and N types. They differ in their impact energy (0.735 and 2.207 Nm). ISRM (1978a) preferred using L hammer for testing rocks but ASTM (2001) did not specify the preferred type.

Ayday and Gotkan (1992) suggested correlations between index readings of the two hammer types. Sabatakakis et al. (1993) suggested linear correlation for limestone between dry unit and rebound value. Aydin and Basu (2005) proved the same linear relation in granitic rocks. Many authors have proved correlations between unconfined compressive strength, Young's modulus and Schmidt hammer for different lithologies.

4.1.2. Ultrasonic wave (pulse) tests:

According to ISRM, (1978), cylindrical specimen is prepared by trimming the ends. Before test, sample length is measured. An ultrasonic instrument consists of digital indicator, generator of pulse, transmitter, and receiver transducer (Figure 4.2). Both transmitter and receiver are placed at the ends of the sample. The travel time of wave pulse is measured. Finally, the velocity is measured through dividing the sample length by the time

Figure 4.1. Schmidt Hammer Rebound Test equipment

Figure 4.2 Ultrasonic pulse velocity test (Pundit equipment)

According to ISRM (1978 a), the ultrasonic wave velocity through any solid materials depends upon the material's elastic properties and density. Thus, the ultrasonic wave test can indicate the quality of the material.

Wave velocities can be used to calculate a number of elastic constants, including Young's modulus, shear modulus, and Poisson's ratio, all of which help define strength parameters of the rock. Young's modulus relates the resultant strain to a given stress, and shear modulus is the ratio of shear stress to shear strain. Poisson's ratio is the ratio of transverse contraction strain to longitudinal extension strain in the direction of stretching force (Burger, 1992). The equations are as follows:

Equation 1 Dynamic elastic moduli estimation from Vp and Vs

$$E = \frac{\left[\rho \times V_s^2 \times \left(3 \times V_p^2 - 4 \times V_s^2\right)\right]}{\left(V_p^2 - V_s^2\right)}$$

$$G = \rho \times V_s^2$$

$$\nu = \frac{\left(V_p^2 - 2 \times V_s^2\right)}{\left[2 \times \left(V_p^2 - V_s^2\right)\right]}$$

$$\lambda = \rho \times \left(V_p^2 - 2 \times V_s^2\right)$$

$$K = \frac{\rho \times \left(3 \times V_p^2 - 4 \times V_s^2\right)}{3}$$

E= Young's modulus (GPa); Vs = Shear (secondary) wave velocity (ms^{-1}).

V_p =Compressional (primary) wave velocity (ms^{-1}). ρ= density ($gm\backslash cm^3$).

4.1.3. Point Load Index

Point load index test IS (50) has been developed by Broch and Franklin, (1972). Many authors suggested linear regression between UCS and point load and part of them proposed power relations (Kahraman et al, 2005). According to Broch & Franklin (1972) in point

load test, the sample is loaded until failure state through applying a concentrated load through a pair of conical (Figure 4.3), spherically truncated platens, the machine also contains a manual control handle, and dial gauges, and the failure is achieved within 10-60 seconds using a manual handle.

The corrected size index value is measured at D= 50 mm, the PLS index can be represented as:

$$IS_{(50)} = F\ P \backslash De^2$$

where: IS= corrected PLS index. F= the size correction factor, P= the peak load,

De= Diameter of sample,

IS (50) can be used for several shapes (irregular lumps, cylindrical, circular specimens)

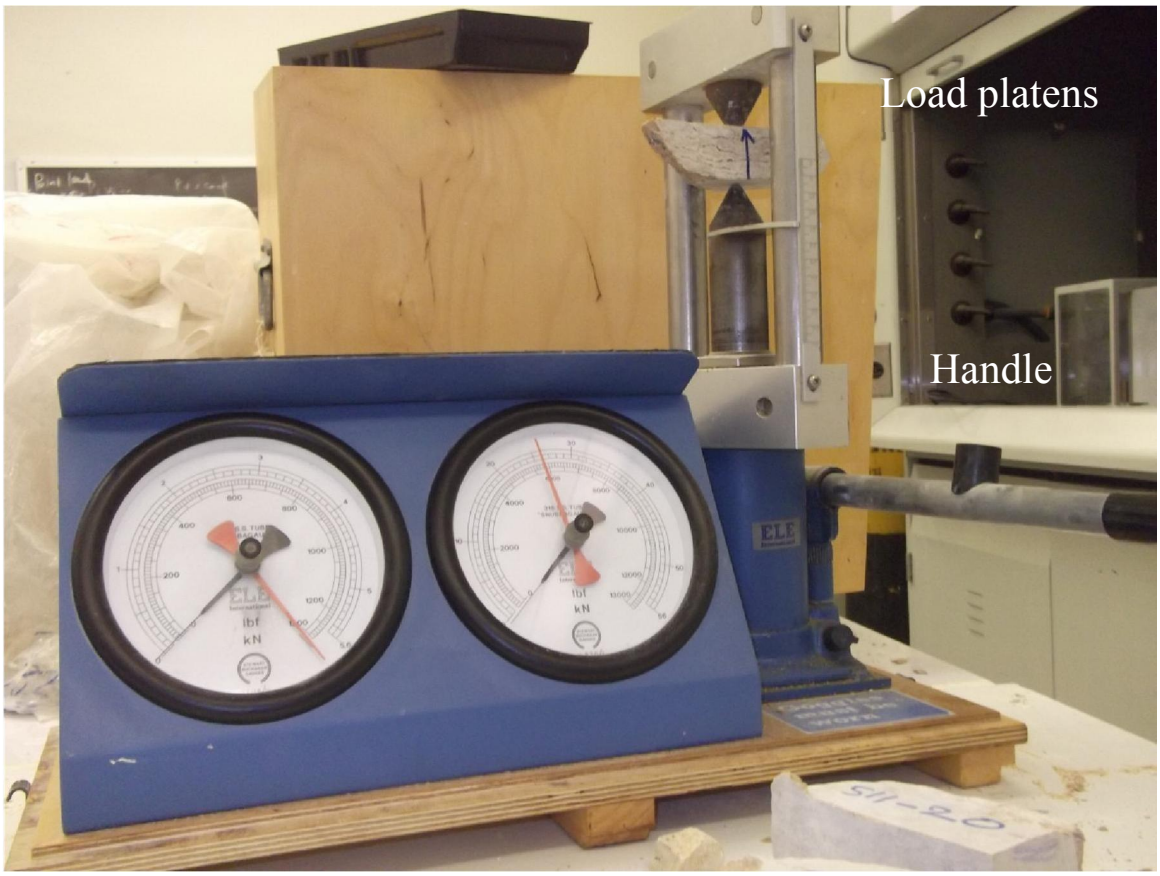

Figure 4.3 Point Load index test instrument

4.2. Results and Discussions:

4.2.1. Lithofacies Analysis:

This study reveals several lithofacies deposited in Upper Jubaila Formation and Arab-D member. Upper Jubaila Formation is comprised of stromatoporoid wackstone\ packstone and dolomitic mudstone\ wackstone. These lithofacies were deposited in l ower to upper slope and ramp crest setting.

In Arab-D member; borrowed wackstone and peloidal fossiliferous grainstone were deposited (skeletal bank lithofacies association), also laminated mudstone and wavy rippled sandy grainstone lithofacies were deposited (tidal flat lithofacies association). Arab-D member represents deposition under deep to shallow lagoonal depositional settings. Breccia or rip-up clasts were also deposited in Arab-D member (Figure 4.4).

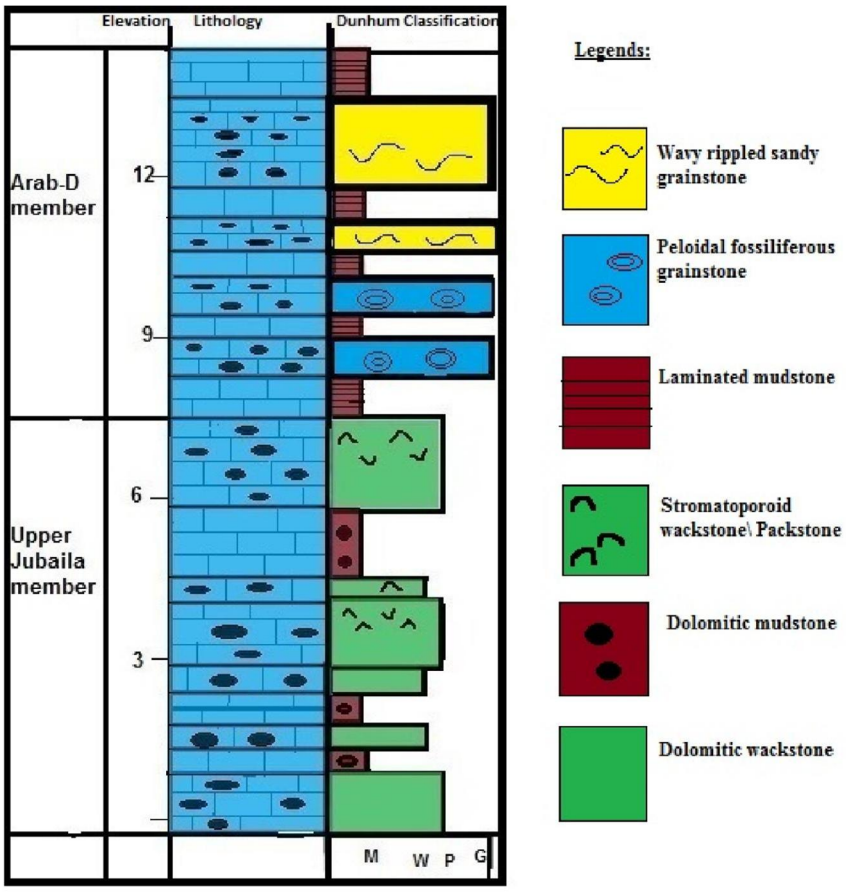

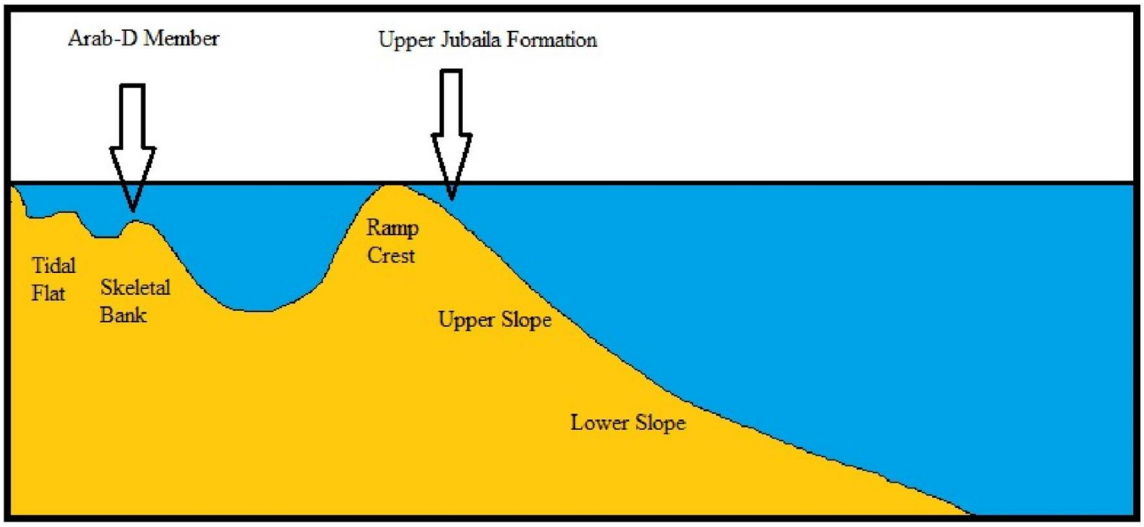

Figure 4.4 Measured composite section in Arsb-D and Upper Jubaila (up), Depositional model (down).

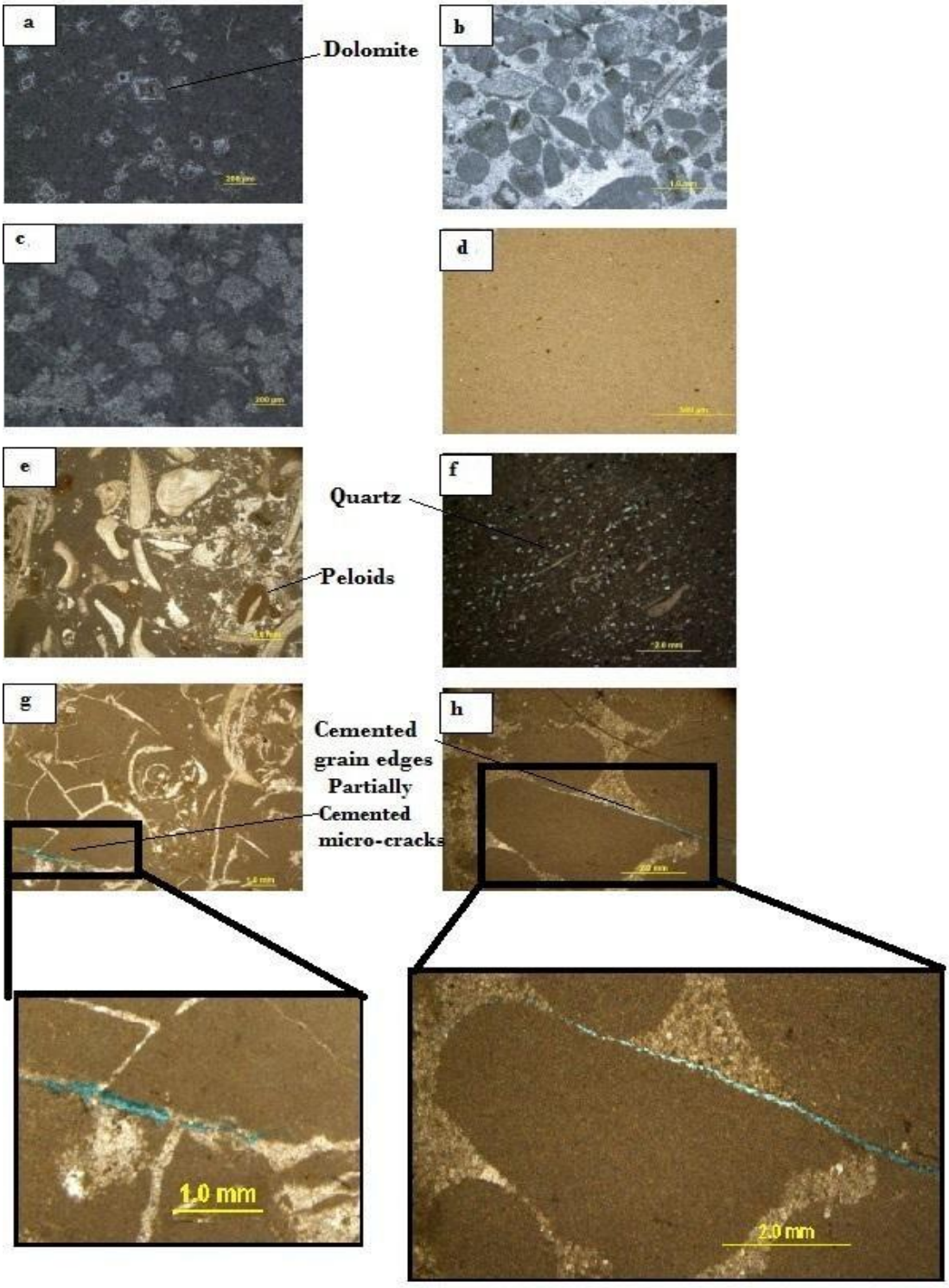

Figure 4.5 Thin sections microphotographs for Upper Jubaila lithofacies: a) Dolomitic mudstone b) Stromatoporoid packstone c) Dolomitic wackstone. Arab-D member lithofacies: d) laminated mudstone e) Peloidal fossiliferous grainstone f) wavy rippled sandy grainstone (rich in quartz) g) partially filled and non-filled micro-fractures within laminated mudstone facies (known as channelized pores) h) breccias and mud clasts (microfractures along clasts edges)

4.2.2. Geomechanical units

The studied outcrop section is composed of upper Jubaila that is overlain by Arab-D member, and the Arab-D member is overlain by Arab-C member at the top.

The upper Jubaila is horizontally stratified, moderately to thickly bedded and its rock material is strong. Therefore, it is more resistant to disintegration and weathering, while the Arab-D member is dominated by thinly to moderately bedded, horizontally stratified carbonate; most of its lithofacies are characterized by low strength and are less resistant to weathering and disintegration. The strata in both upper Jubaila and Arab-D member show meter-scale cyclicity laterally continuously for more than 100 m in the outcrop.

All these features have clear impact on the geomechanical properties. The strength values including both point Load index (IS (50)) and Schmidt Hammer Rebound Number (RN) are higher in upper Jubaila than in the Arab-D member; strength is inversely correlated to porosity. The boundary between Upper Jubaila and Arab-D member is characterized by curve shifting toward higher Schmidt Hammer Number and Unconfined Compressive Strength. This is because of the increased amount of quartz grains in peloidal facies compared to laminated mudstone lithofacies. A further, smaller textural effect is indicated by the fact that muddy to wacky Upper Jubaila is characterized by high strength index relative to muddy to grainy Arab-D member. This was observed by Ameen et al. (2009).

The Upper Jubaila consists of stromatoporoid wackstone- packstone and dolomitic mudstone-wackstone lithofacies deposited in lower to upper slope (Figure 4.5), while, the lithofacies of Arab-D member include skeletal bank lithofacies association made of peloidal wackstone and peloidal fossiliferous grainstone. Also, there is a tidal flat

association represented by breccias, laminated mudstone, and wavy rippled sandy grainstone (Eltom et al. 2014).

Some micro-fractured zones are seen in thin sections that might have decreased the strength in some lithofacies. These zones are represented by small scale fractures which formed as a result of dissolution of cementing materials along the edges of intraclasts during diagenesis, partially filled and non-filled fractures within laminated mudstone in Arab-D member. Other lithofacies in Arab-D lack any post-depositional fractures in thin sections, core plugs, or at outcrop scale. Weakness zones along these micro-fractures are induced when applying point load were traced. Cemented micro-cracks in Stromatoporoid lithofacies are one of these weakness zones (Figure 4.5). When samples are subjected to point load, isolated microcracks are connected which leads to enhanced permeability (Figure 4.7).

Three geomechanical units (Figure 4.6) were defined based on the relationship between geomechanical properties and lithofacies characteristics:

1- Unit-1:

This unit is comprised of tidal flat lithofacies association (wavy rippled sandy grainstone and laminated mudstone). It is characterized by low to high, highly variable R_N due to strong variability.

This zone is characterized by low to high velocity. The higher value is corresponding to wavy rippled sandy grainstone lithofacies, and the lower to laminated mudstone (Figure 4.8).

Wavy rippled sandy grainstone is characterized by low porosity while laminated mudstone has high porosity.

2- Unit-2:

This zone is comprised of the lower part of Arab-D member and the upper part of the exposed Jubaila Formation. It is characterized by low RN, relatively high porosity, and low to moderate velocity. This unit consists of skeletal bank lithofacies association and part of Stromatoporid association (Figure 4.9), it is characterized by lower dolomite content and higher grain supported textures.

3- Unit-3:

The third unit represents the lower part of Upper Jubaila Formation of high RN , it has relatively low porosity and moderate consistent wave velocity, based on these units, depth plays an essential role in the correlation between textural and geomechanical properties. This zone is characterized by large dolomite content and clear mud supported textures (Figure 4.10).

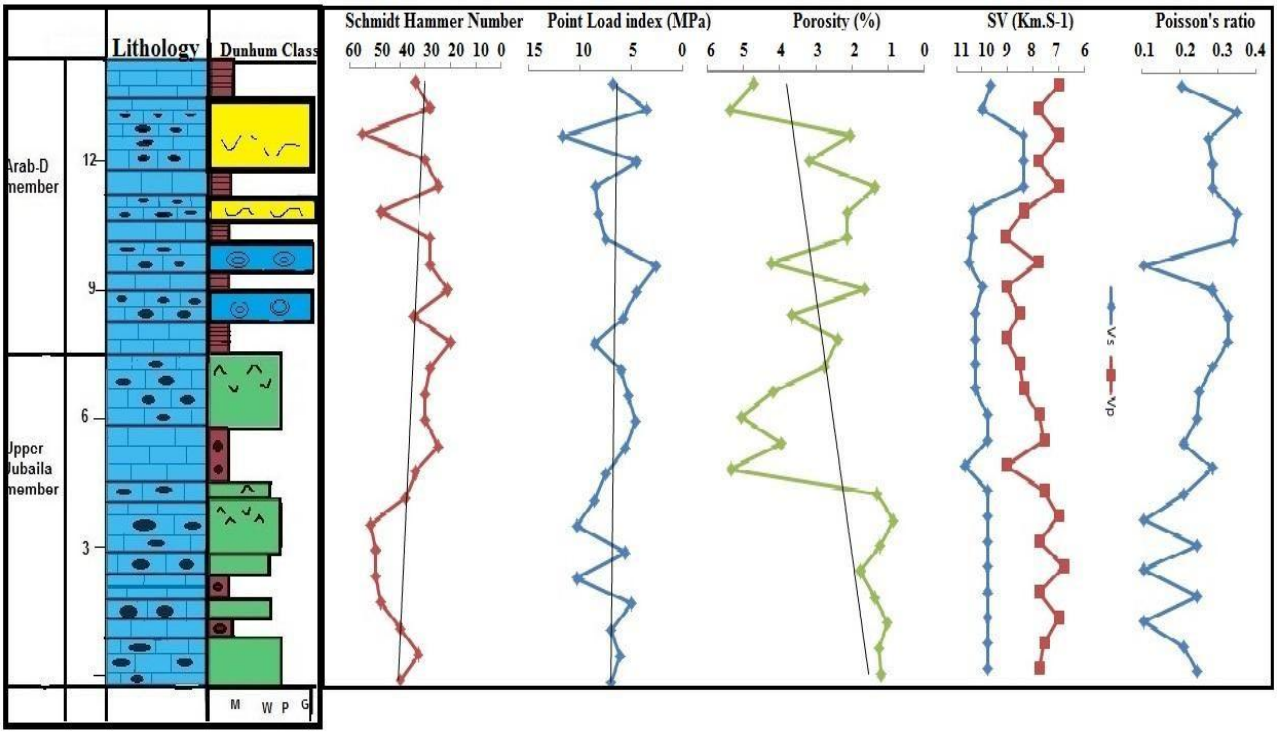

Figure 4.6 Vertical profiles for several geomechanical properties within Upper Jubaila and Arab-D member

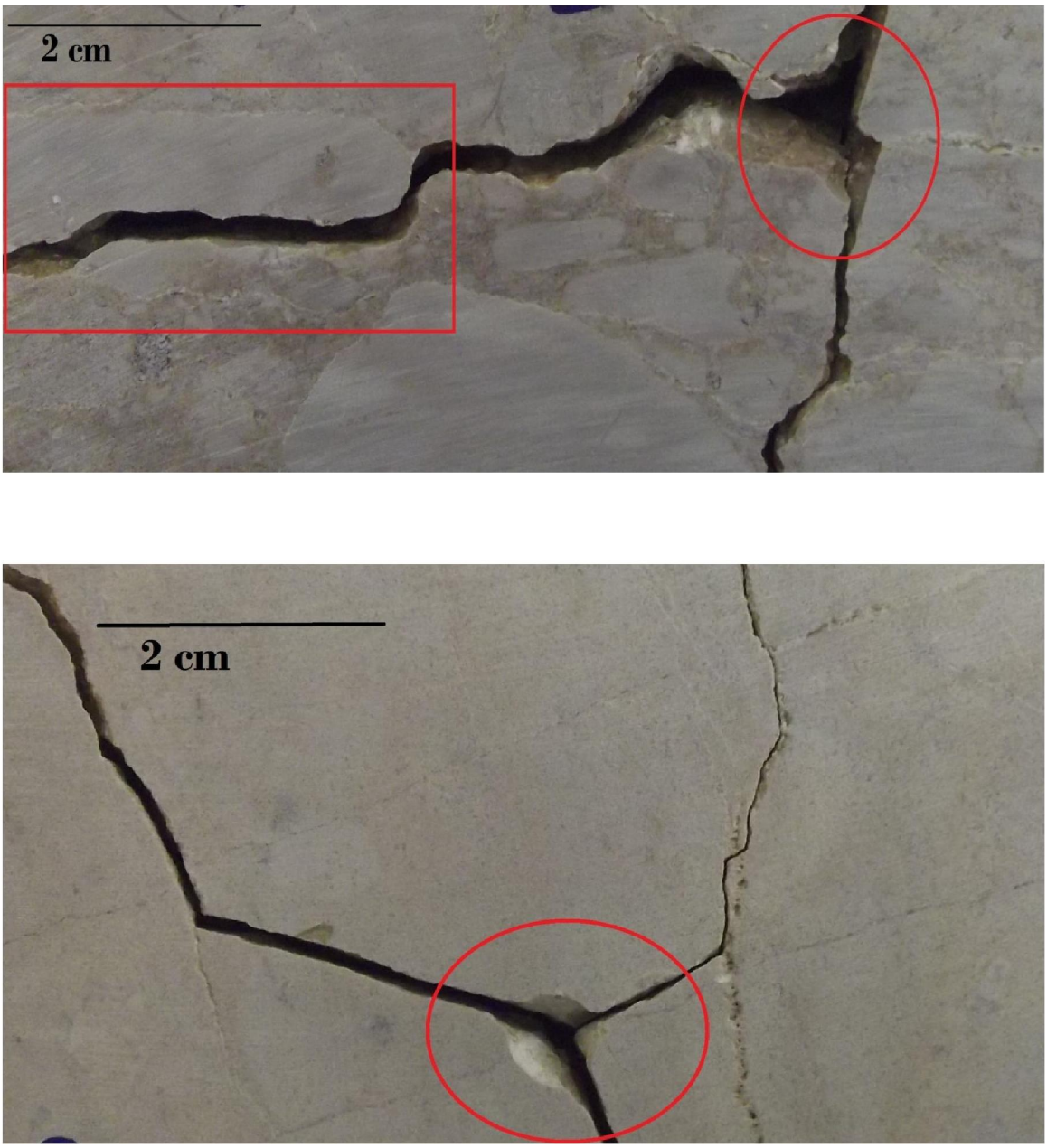

Figure 4.7 induced fractures within breccia and laminated mudstone along weakness zones

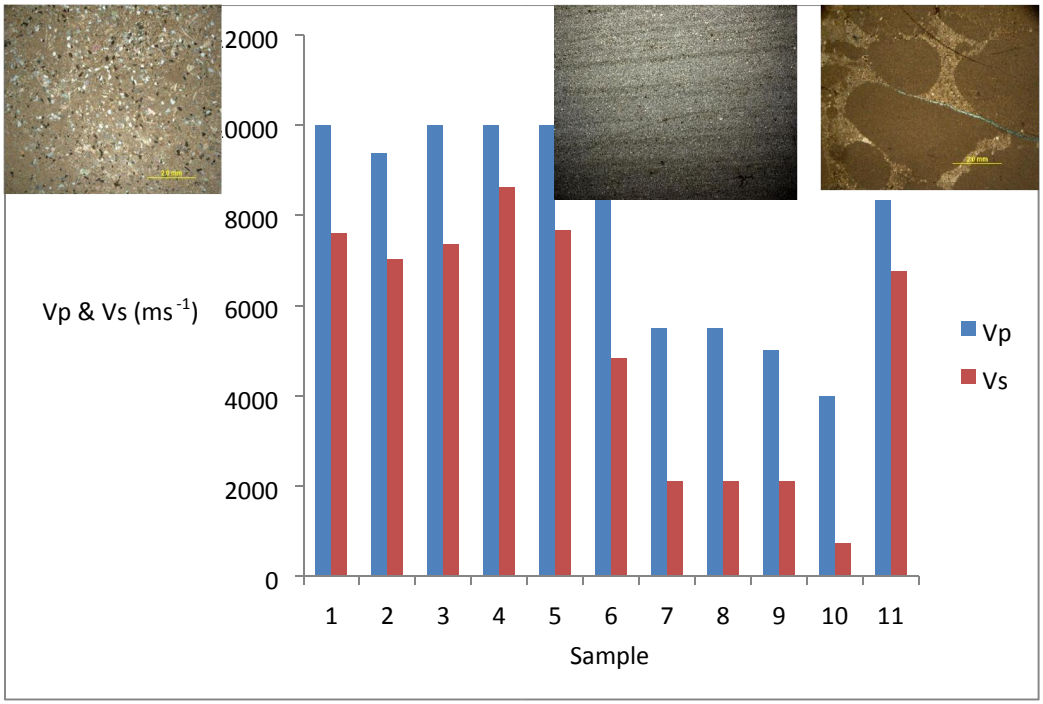

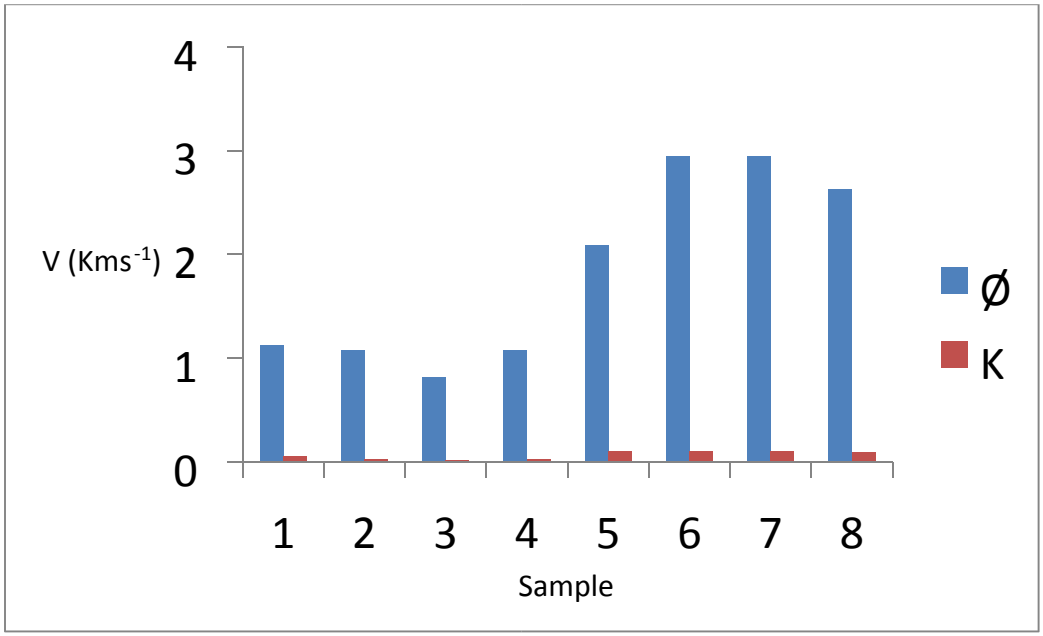

Figure 4.8 Histogram for P-&S-waves, porosity and permeability for tidal flat lithofacies association

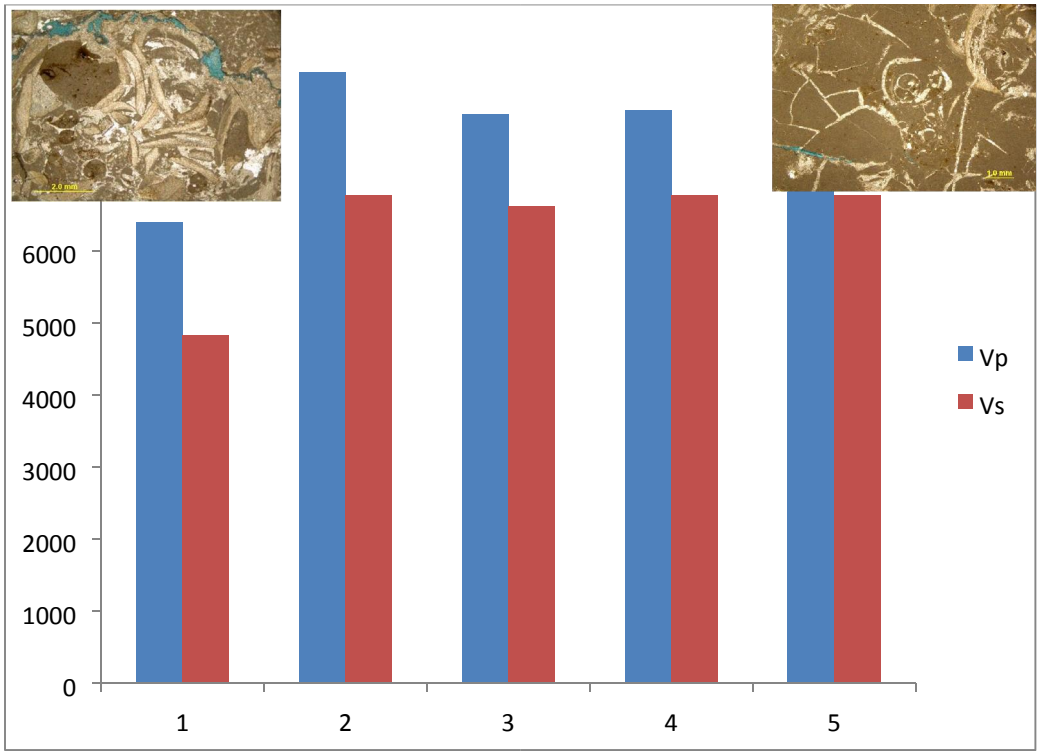

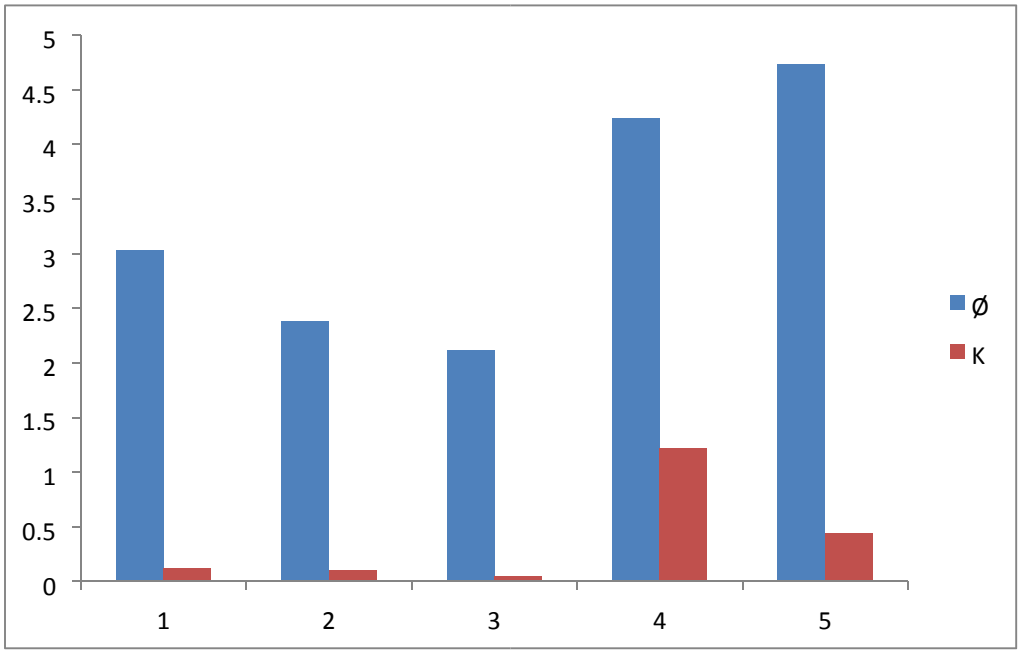

Figure 4.9 Histograms of Vp, Vs, porosity, and permeability of skeletal bank association

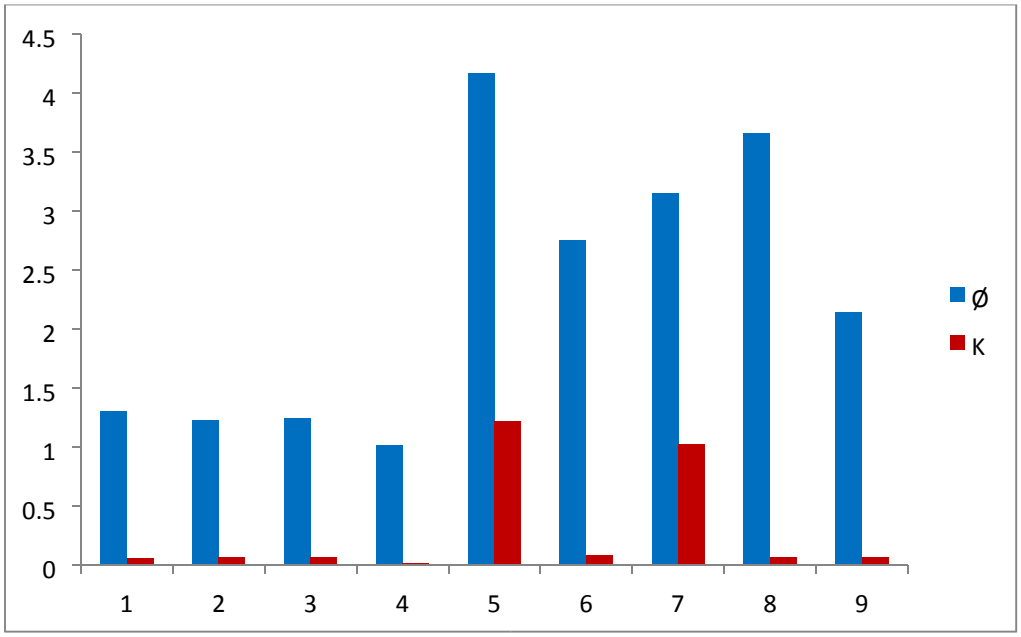

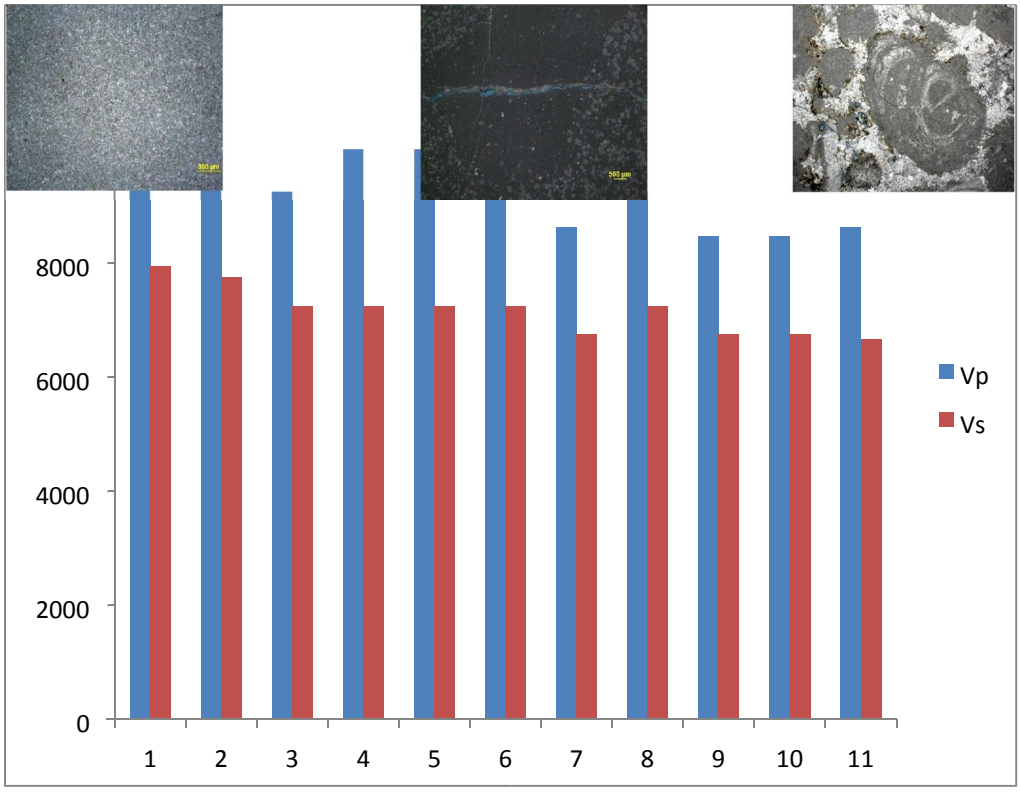

Figure 4.10 Histogram for Vp, Vs, porosity and permeability for Stromatoporoid lithofacies

4.2.3. Schmidt Hammer Rebound Number versus Point Load index:

Table (4) summarizes porosity, permeability, average Schmidt hammer hardness (RN), point load index (IS (50)) values for both Arab-D and Upper Jubaila lithofacies. Maximum RN value is 55 for the peloidal fossiliferous grainstone lithofacies and wavy rippled sandy grainstone facies, these lithofacies are lacking fractures in the outcrop and they are more massive than other lithofacies and thinly bedded. The mineral content has an effect on the strength of these lithofacies. This is noticed in wavy rippled grainstone where quartz grains are dominating in the petrographic section. The minimum value (15) is for laminated mudstone facies which is heavily fractured.

The maximum IS (50) value is 14 MPa for the wavy rippled sandy grainstone facies and the minimum reading is 1.5 Mpa for the laminated mudstone. These results agree with results of RN values and the same interpretation is applied here. The relationship between RN and IS (50) is characterized as non-linear and the coefficient of determination (R^2) is equal to 0.6 which shows moderate correlation (Figure 4.11).

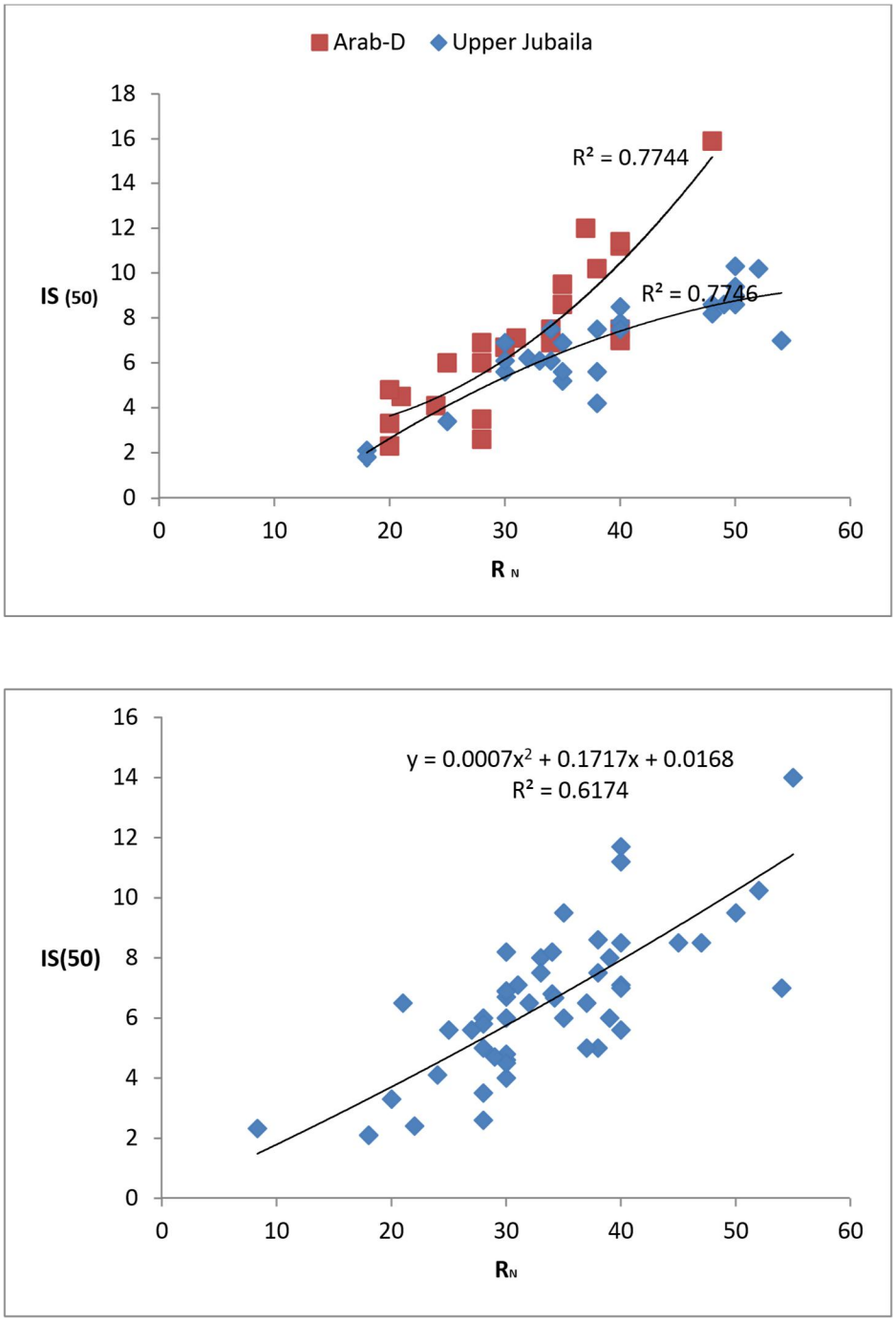

Figure 4.11 Point load index versus Schmidt Hammer Rebound number separately for both Arab-D and Upper Jubaila Member (up). Generalized for the whole section (down)

4.2.4. Schmidt Hammer\ point load index versus porosity and permeability:

Maximum porosity value is 5.4%, the minimum value is 0.82%, and the median is 2.1%. The maximum permeability reading is 1.26 md, the minimum is 0.01 md, and the average is 0.2 md. This indicates that the average porosity and permeability are low due to intensive diagenesis and cementation processes. (Figure 4.12) shows that RN is moderately correlated to porosity, inverse (negative) non-linear correlations are noticed. The same behavior is noticed in the IS (50) relationship with porosity (Figure 4.13).

RN is also weakly to moderately correlated with permeability, negative correlation is also noticed. (Figure 4.14), IS (50) shows the same behavior with permeability (Figure 4.15) and a clear power- function like correlation is observed here. Upper Jubaila samples are restricted within a narrow zone of low permeability and medium to high Schmidt Hammer Rebound Number and Point Load Index. This is because Upper Jubaila is weakly affected by fractures, which reduces the permeability. Meanwhile, Arab-D samples are scattered over the plot and contain both low to high permeability zones and mainly moderate permeability. Therefore, Arab-D member can be differentiated from Upper Jubaila Formation through their strength-permeability correlation more clearly than using strength-porosity correlation since both have the same trend for porosity.

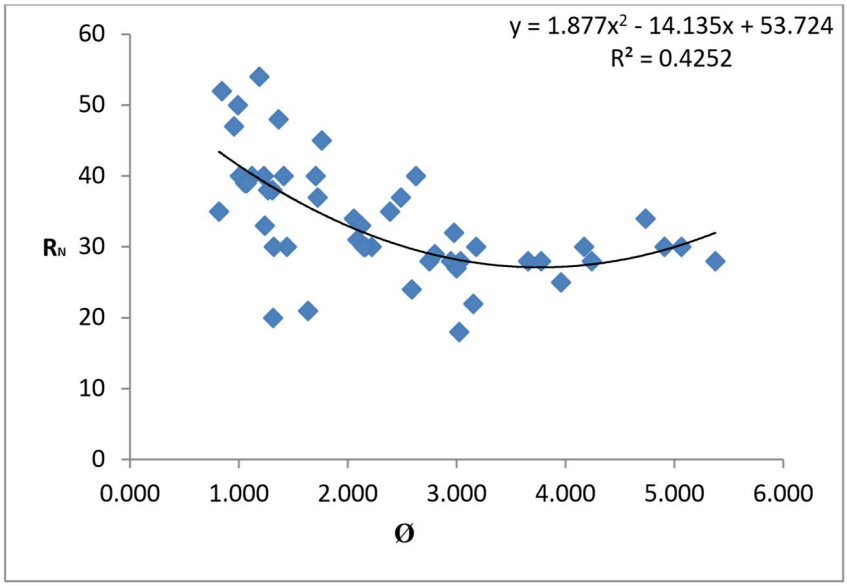

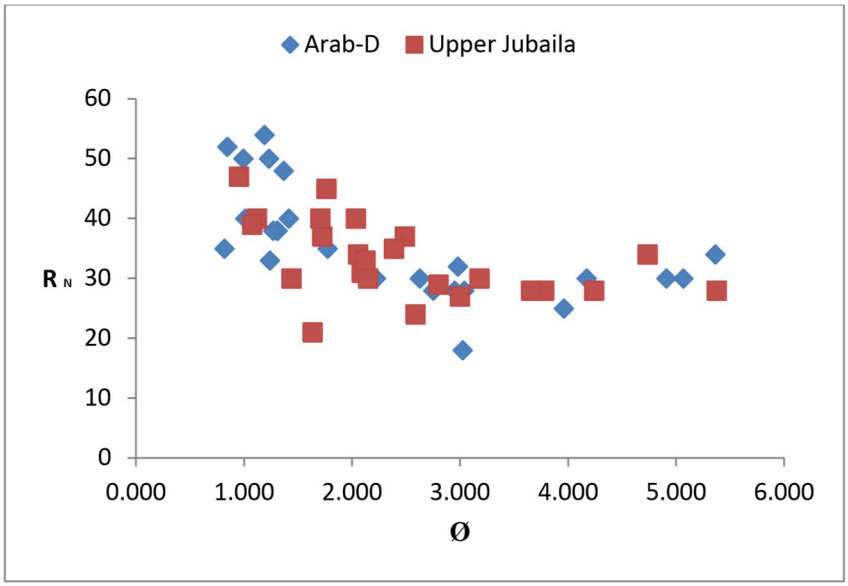

Figure 4.12 Generalized Schmidt Hammer Rebound Number versus porosity (up), seperately for both Arab-D and Upper Jubaila (down).

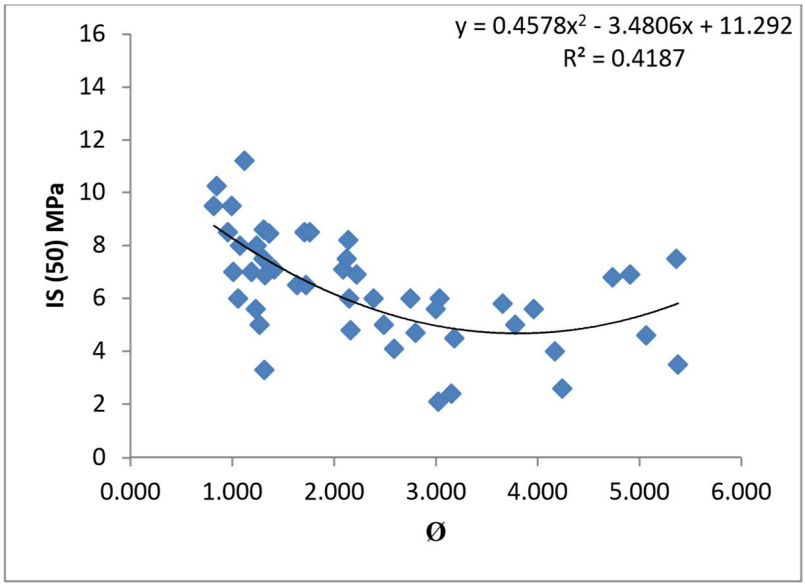

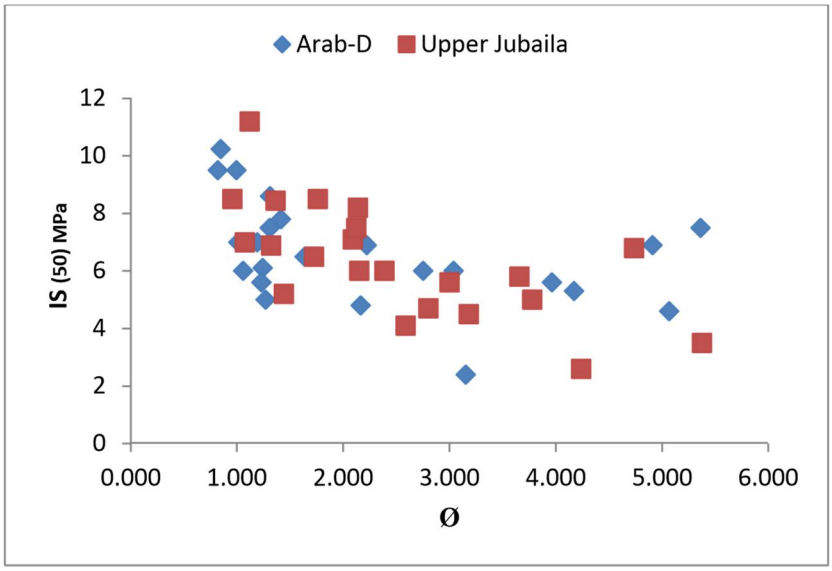

Figure 4.13 Generalized Point Load index versus porosity (up), seperately for Arab-D member and Upper Jubaila Formation (down)

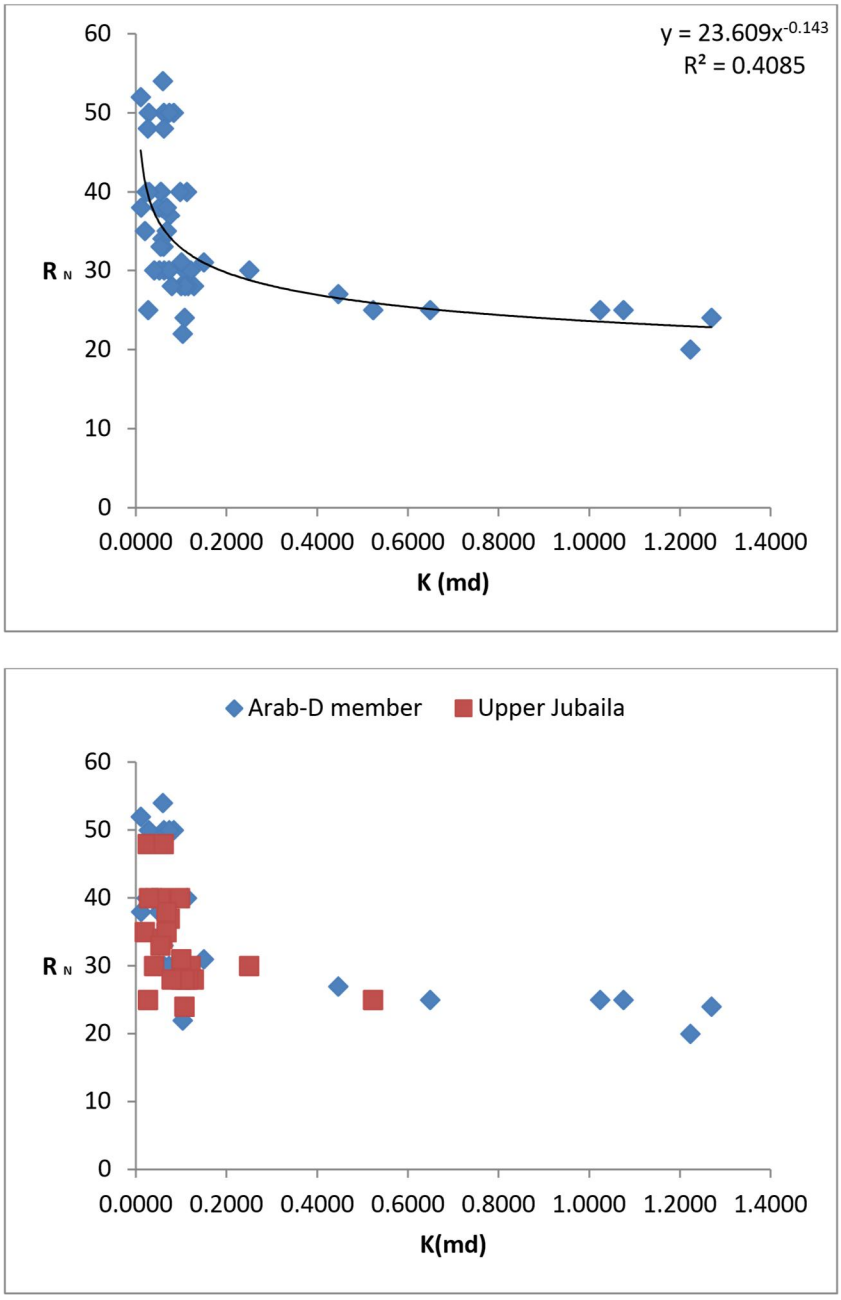

Figure 4.14 Generalized Schmidt Hammer Rebound Number versus permeability (up), seperately for both ArabD and Upper Jubaila (down).

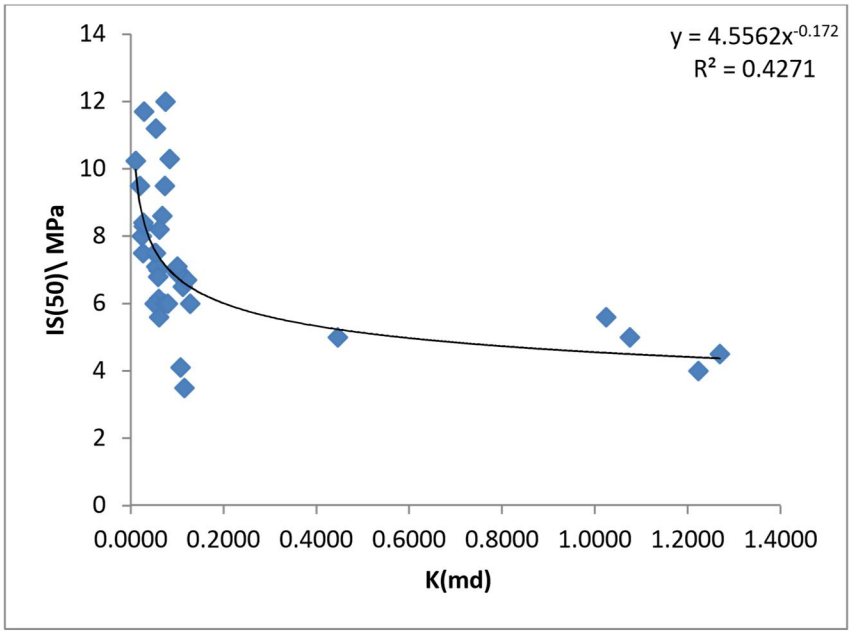

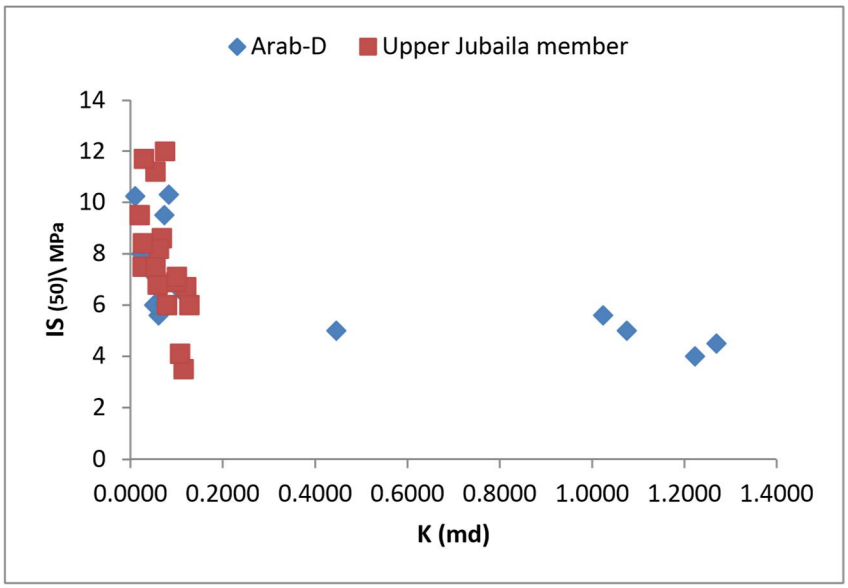

Figure 4.15 Generalized Point Load index versus permeability (up), separately for both Arab-D and Upper Jubaila (down).

4.2.4. Schmidt Hammer\ point load index versus wave velocity and dynamic elastic moduli:

Table (5) illustrates the results of ultrasonic wave velocity test. The maximum P-wave velocity is approximately 10000 ms^{-1}, the minimum velocity is 4000 ms^{-1}. The same range was recorded by (Ameen et al. 2009) for carbonate rocks in Ghawar oil field. High wave velocities are due to intensive and heavy diagenetic compaction and cementation processes which reduce porosity (Eberli et al. 2003). The maximum dynamic Poisson's ratio is 0.49 for laminated mudstone lithofacies and the minimum is 0.08 for Upper Jubaila facies such as stromatoporoid lithofacies, wave velocity is more affected by texture than other properties. High magnitudes of P-wave velocities and Poisson's ratio are due to dolomite and quartz minerals existence.

The maximum dynamic Young's modulus is 328 GPa for wavy rippled sandy lithofacies and the minimum is 36 GPa for laminated mudstone lithofacies. RN increases with increase in P-wave velocity (Vp) (Figure 4.16). The same relationship is found in point load index (Figure 4.17). This is mainly because the rock samples are strongly compacted and therefore wave can pass quickly through the rock specimen. Also, Poisson's ratio increases with decreasing of the strength represented by Schmidt hammer number and point load index. Dynamic Poisson's ratio is inversely proportional to RN (Figure 4.18) and IS (50) (Figure 4.19), polynomial and power-law correlations were found respectively. Dynamic Young's modulus increases with increasing of RN (Figure 4.20) and no clear relationship was found for the relationship between Ed and IS (50) (Figure 4.21).

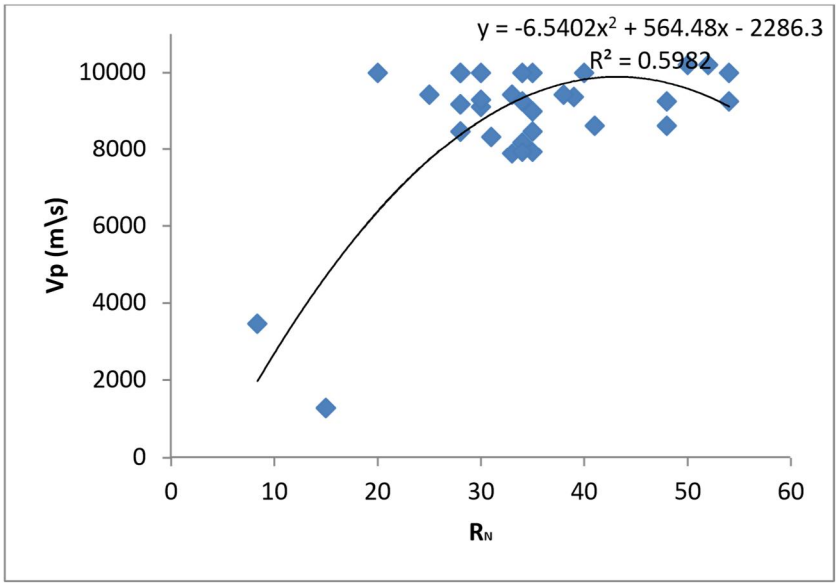

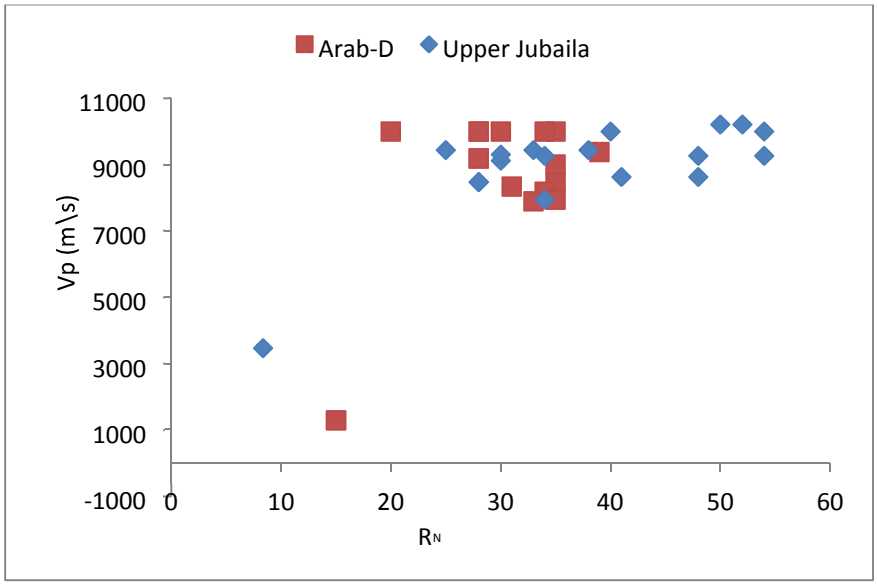

Figure 4.16 Generalized V p-versus Schmidt Hammer Rebound Number (up), seperately for both Arab-D and Upper Jubaila (down).

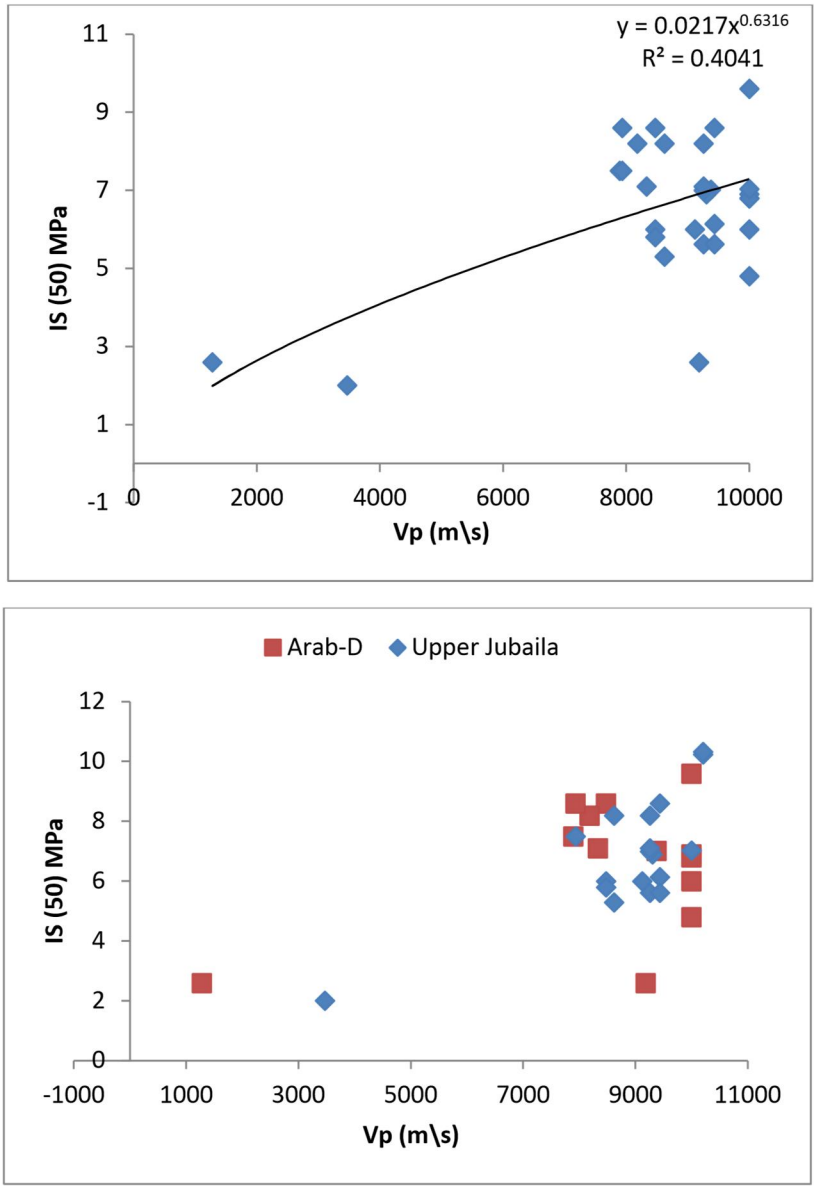

Figure 4.17 Generalized Point Load index versus V p (up), seperately for both Arab-D and Upper Jubaila (down).

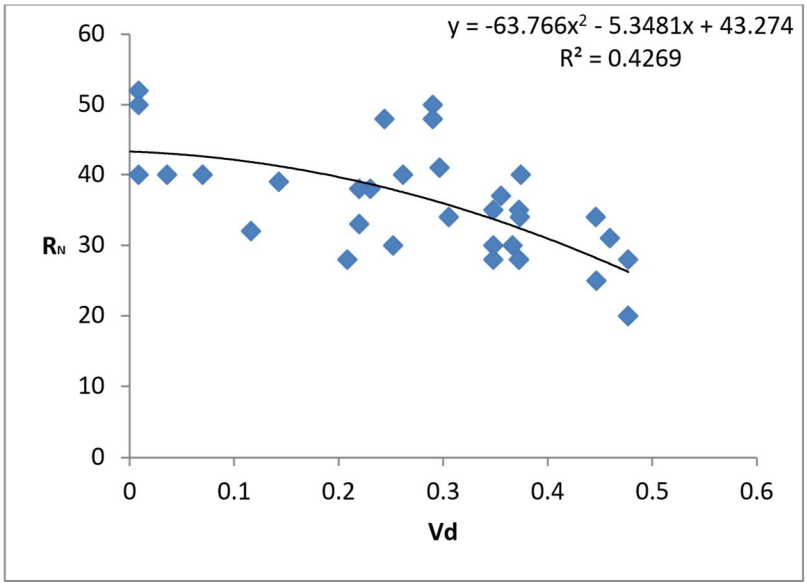

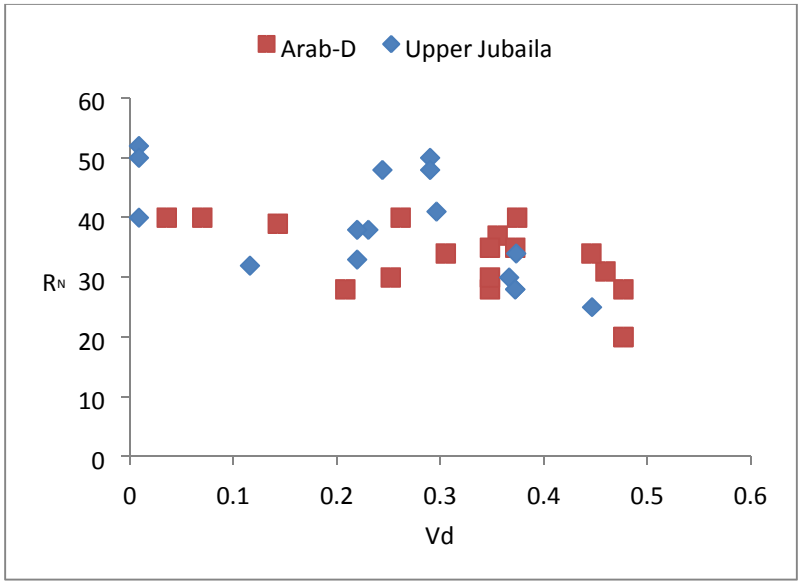

Figure 4.18 Generalized correlation of Schmidt Hammer versus dynamic Poisson's ratio (up), seperately for both Arab-D and Upper Jubaila (down).

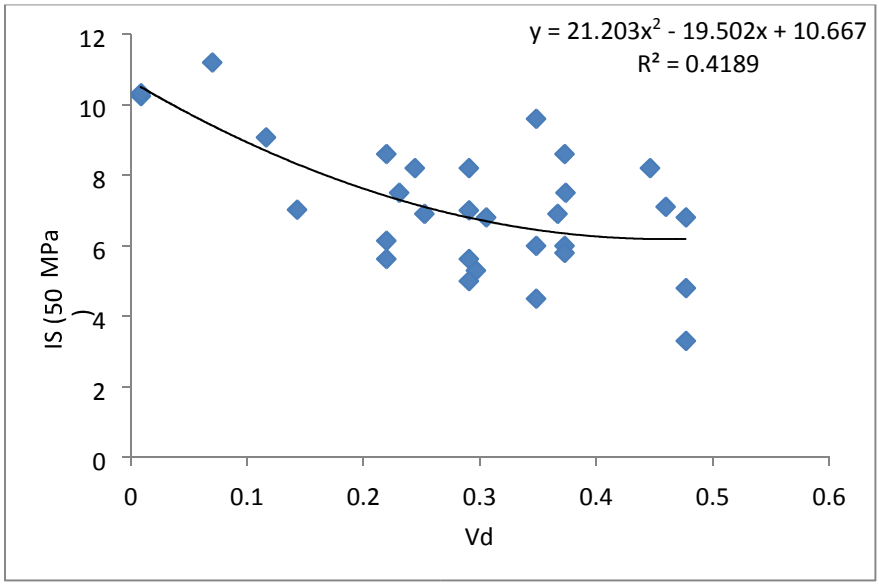

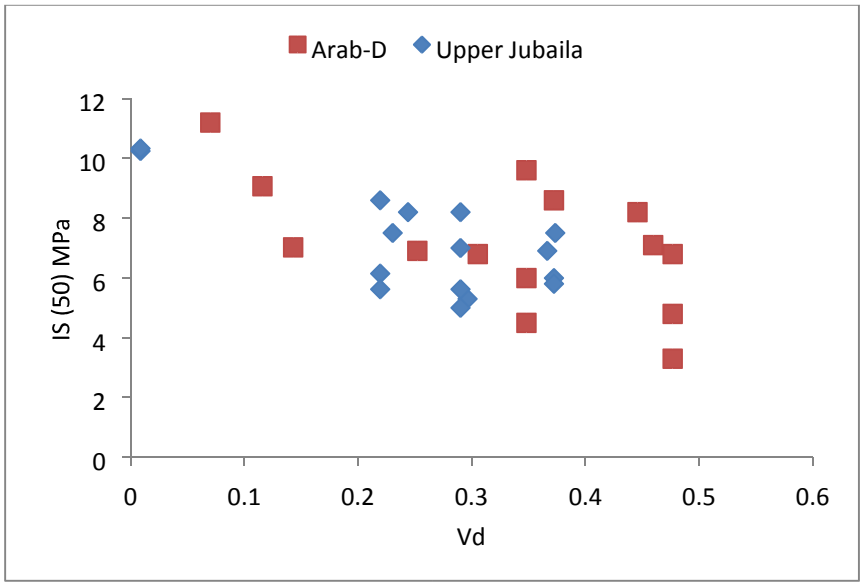

Figure 4.19 Generalized correlation of Point Load index versus dynamic Poisson's ratio (up), seperately for both Arab-D and Upper Jubaila (down).

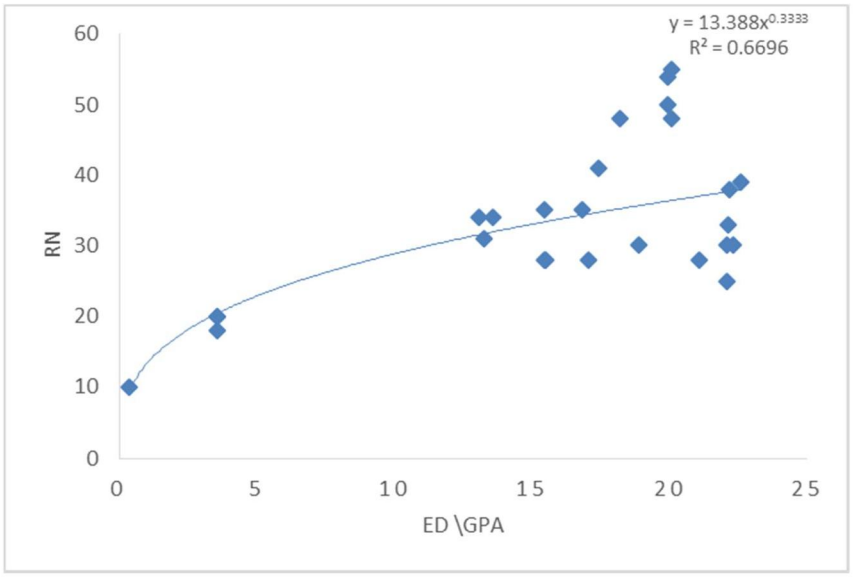

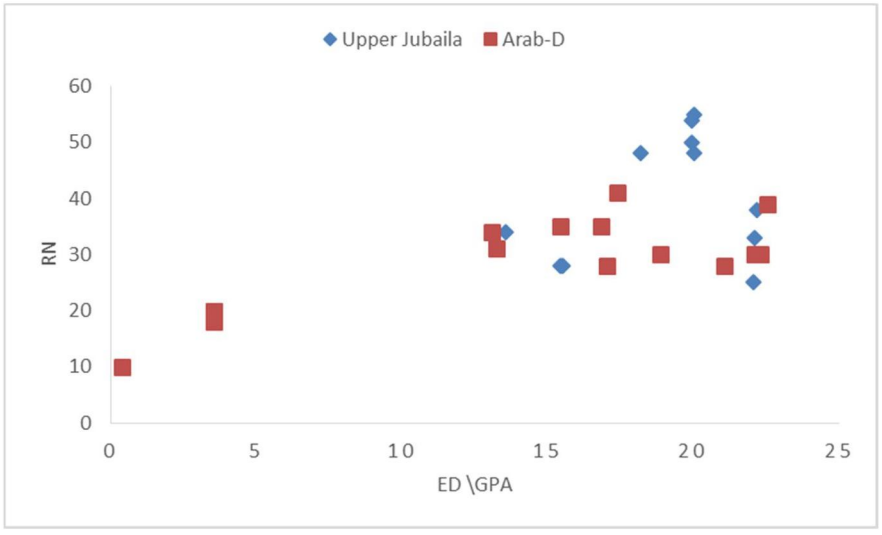

Figure 4.20 Generalized correlation of Schmidt Hammer versus dynamic Young's modulus (up), seperately for both Arab-D and Upper Jubaila (down).

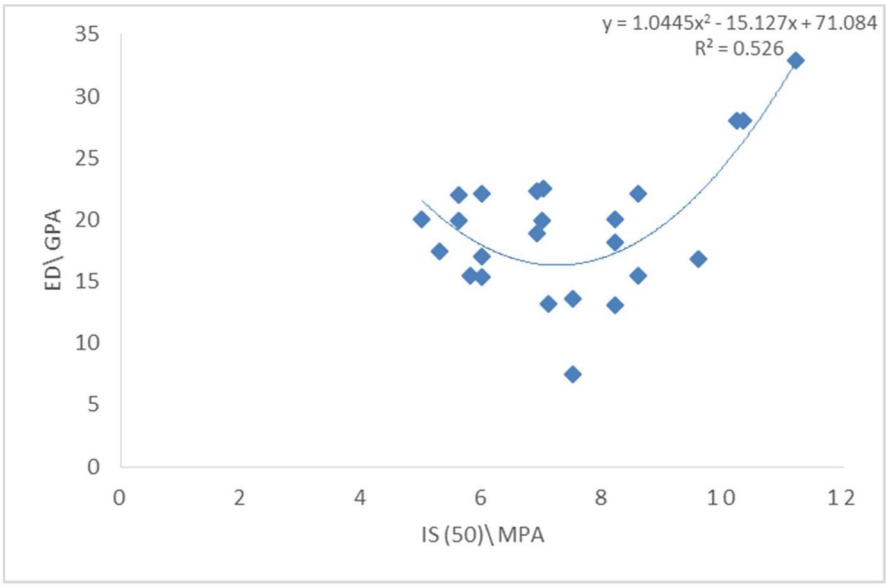

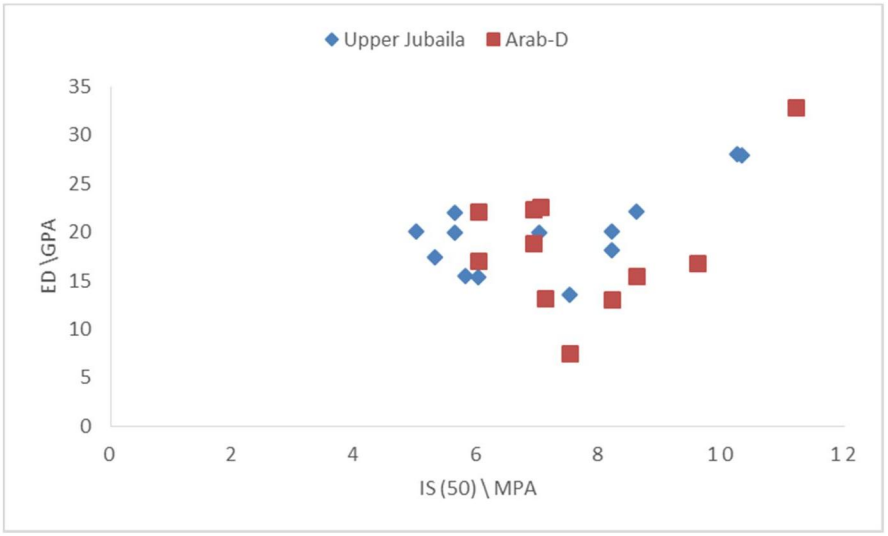

Figure 4.21 Generlaized correlation of dynamic Young's modulus versus Point Load index (up), seperately for both Arab-D and Upper Jubaila (down).

4.2.5. Wave velocity\ dynamic elastic moduli versus porosity and permeability:

S-wave velocity is inversely proportional to porosity; polynomial correlation was found (Fig. 4.22 a); inverse power correlation also was found between S-wave velocity and permeability (Fig. 4.22 b). P-wave velocity also decreases with increasing porosity (Fig. 4.22 c) and permeability (Fig. 4.22 d); polynomial correlation of the second order was found for Vp and porosity relation and power correlation for Vp-permeability.

These results were compared with the outcomes that have been found by Ameen et al. (2009) in which linear correlation characterized the Vp-porosity relation (Fig. 4.23), for the same porosity value in the subsurface; higher P-wave velocity is noticed. It is clear that the relationship is more complicated as a result of intensive diagenesis. Second-order polynomial and power correlations are characterizing the relation between dynamic Poison's ratio and porosity or permeability, respectively (Fig. 4.24).

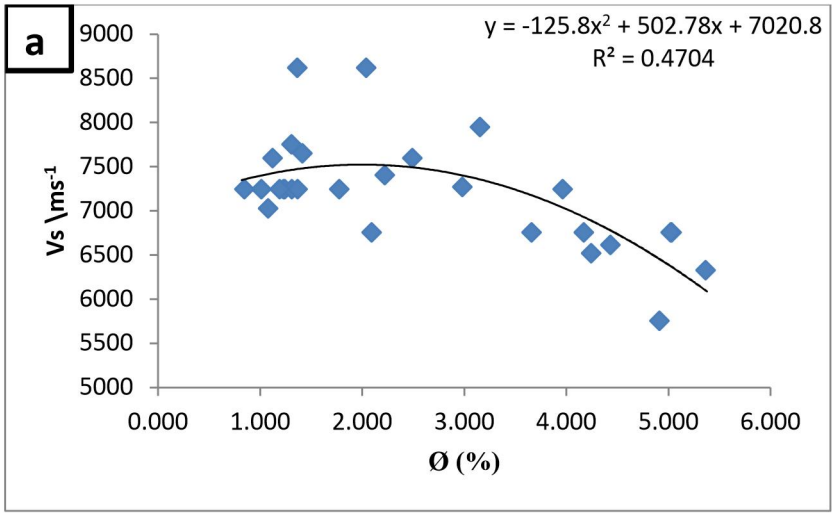
a
y = -125.8x² + 502.78x + 7020.8
R² = 0.4704
Vs \ms-1
9000
8500
8000
7500
7000
6500
6000
5500
5000
0.000
1.000
2.000
3.000
4.000
5.000
6.000
Ø (%)

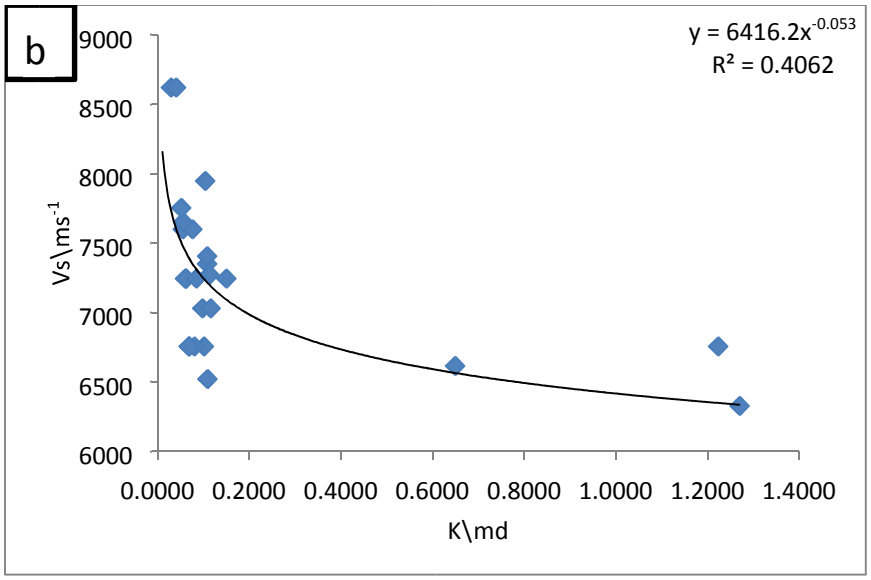
b
y = 6416.2x-0.053
R² = 0.4062
Vs\ms-1
9000
8500
8000
7500
7000
6500
6000
0.0000
0.2000
0.4000
0.6000
0.8000
1.0000
1.2000
1.4000
K\md

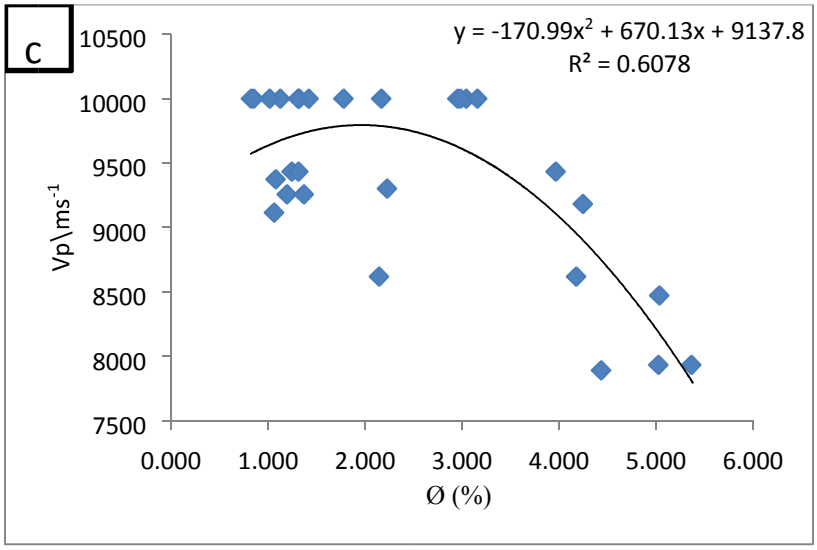

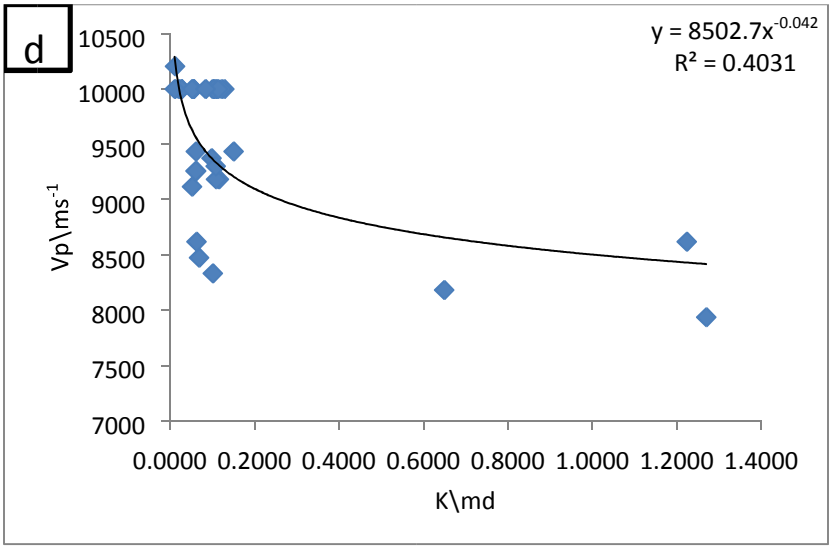

Figure 4.22 Correlation of (a) Vs versus porosity (b) Vs versus permeability (c) Vp versus porosity (d) Vp versus permeability

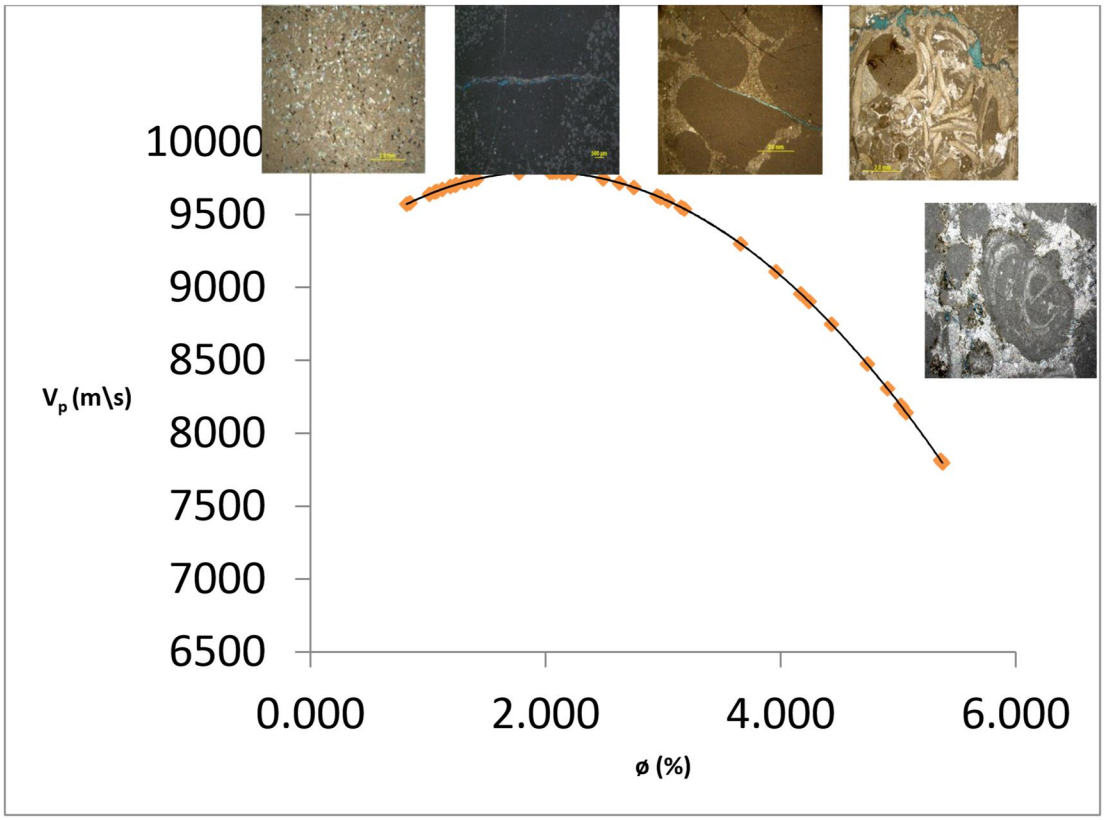

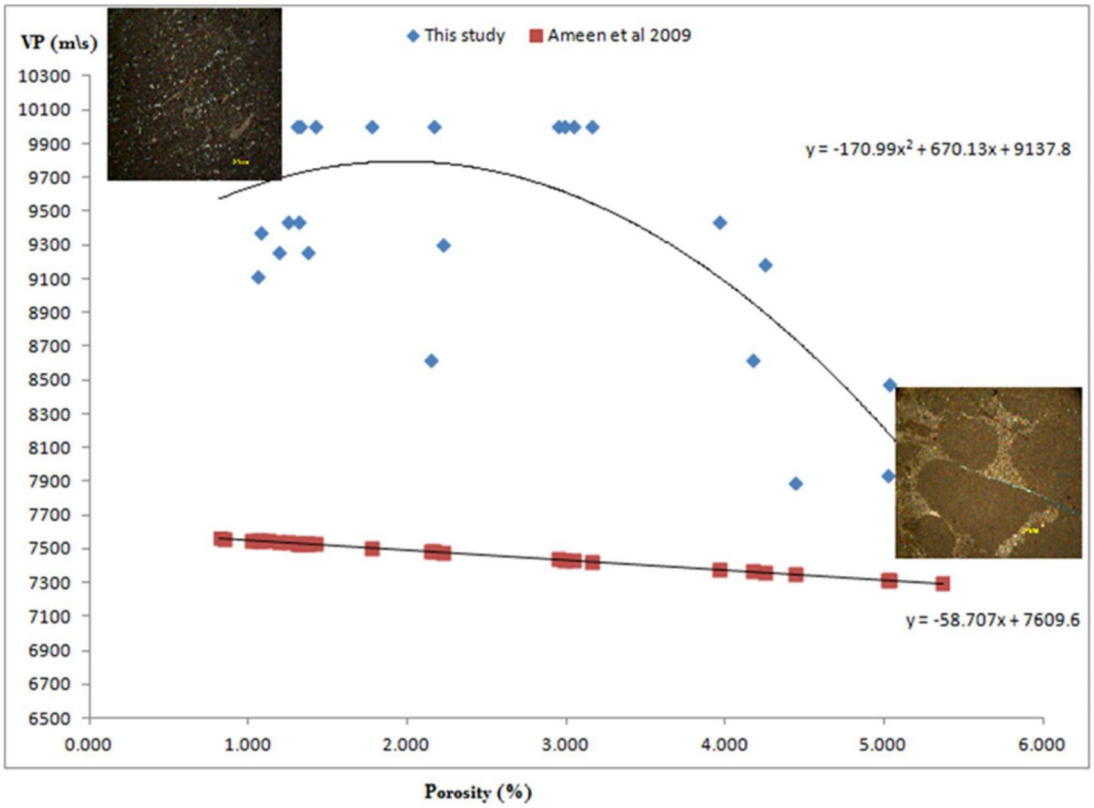

Figure 4.23 Correlation of P-wave velocity versus porosity for different lithofacies

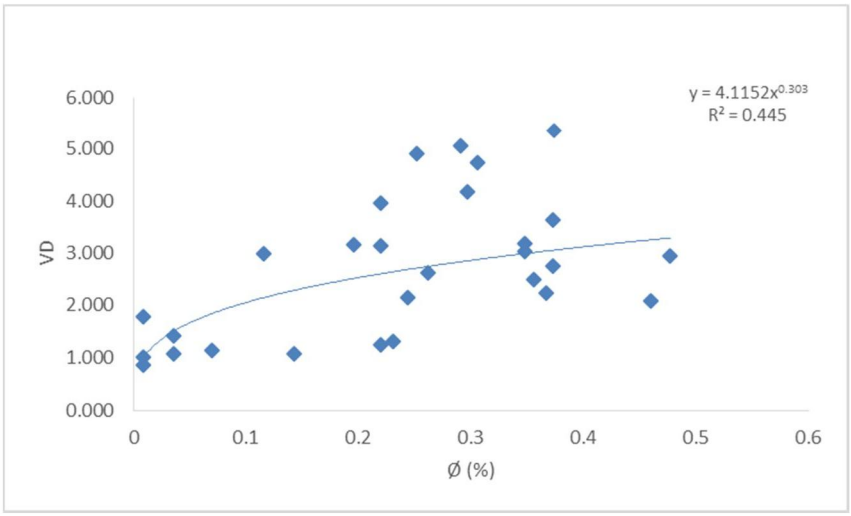

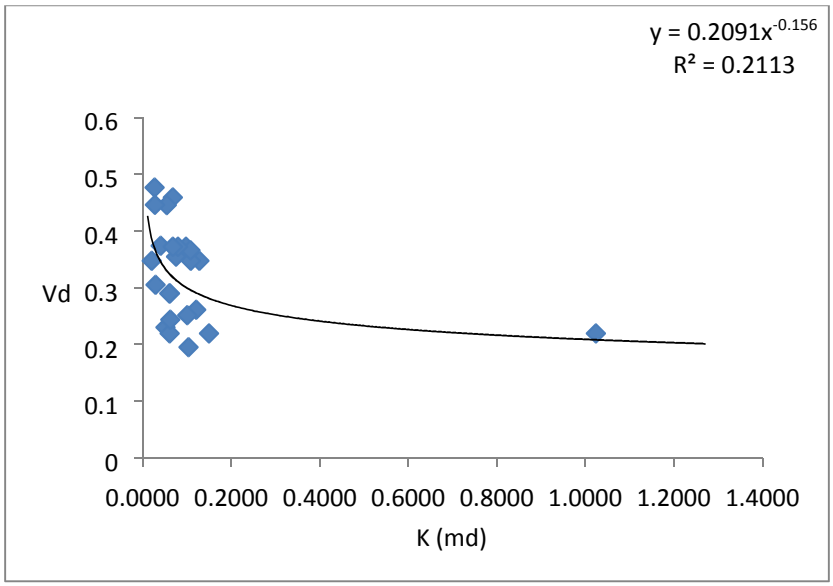

Figure 4.24 Dynamic Poisson's ratio versus porosity (up), and dynamic Poisson's ratio versus permeability (down)

Deere and Miller (1966) classification for intact rock strength was constructed based on dynamic Young's modulus and unconfined compressive strength (Fig. 4.25); Upper Jubaila samples fell in high to very high strength zones. Samples of Arab-D lithofacies are distributed along ranges which start fromlow strength (laminated mudstone lithofacies) to very high strength (wavy rippled sandy grainstone and peloidal fossiliferous grainstone). The results were interpreted in the sense

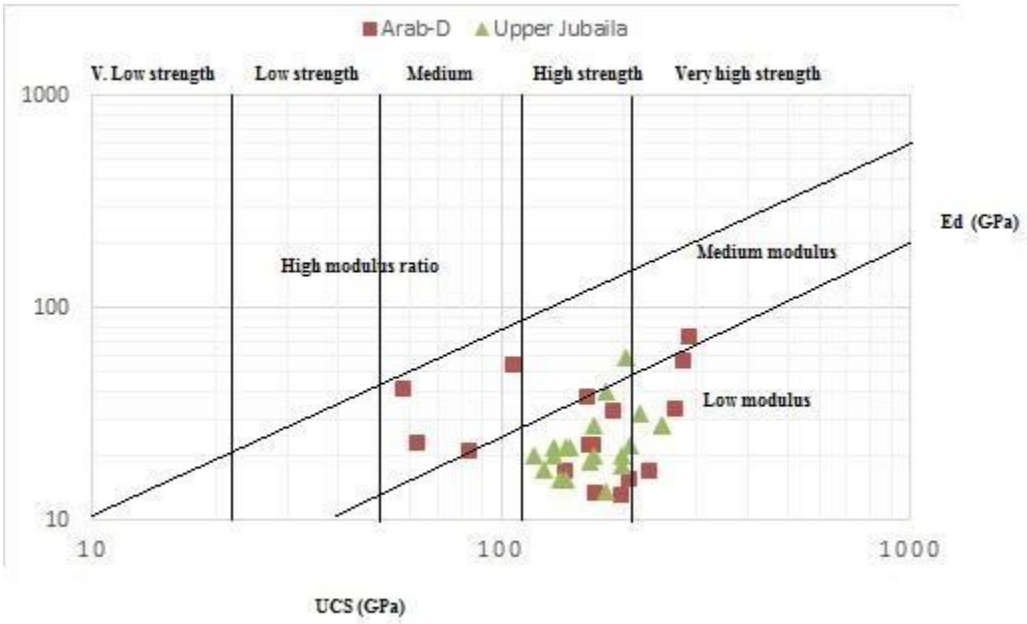

Figure 4.25 Intact rock classification for Upper Jubaila Formation and Arab-D member (adapted after Deere and Miller).

CHAPTER FIVE:

CONCLUSIONS AND RECOMMENDATION

5.1 Conclusions

1- Lithofacies within Upper Jubaila Formation was deposited under slope to ramp crest (stromatoporoid wackstone\ packstone and dolomitic mudstone\ wackstone). Meanwhile, Arab-D member deposited under shallow to deep lagoonal setting (laminated mudstone, skeletal grainstone, breccia, and sandy wavy rippled grainstone).

2- Most fractures affecting the Upper Jubaila Formation and Arab-D member are oriented NW and dipping in NE directions. This set is characterized by minor vertical displacement observed in both Upper Jubaila Formation and Arab-D member of Arab Formation.

3- This emphasizes an impact of Central Arabian Graben System (CAGS) on Wadi Nisah area and particularly within the exposure of Arab-D member and underlying Upper Jubaila Formation.

4- Depositional and diagenetic control on the fractures' behaviors and development was observed

5- Generally the lithofacies showed moderate correlation between geomechanical properties and porosity and permeability.

6- The Upper Jubaila is classified as strong to very strong intact rock, however, the Arab-D member ranged between low strength for tidal flat lithofacies and very high strength for wavy rippled sandy lithofacies.

7- Three geomechanical units were identified; Unit 1 corresponds to Arab-D member, Unit 2 is corresponding to the upper part of Upper Jubaila, and Unit 3 is equivalent to the lowermost part of Upper Jubaila Formation.
8- These geomechanical units reflect the effects of lithofacies, stratigraphy, superimposed weathering and post depositional diagenetic processes.

5.2 Recommendations

1- Expand this study to include all Jurassic rock units to understand the effects of Central Arabian Graben System on all formations
2- Integrate this data with subsurface data for better understanding the fractures development model in Arab-D Reservoir
3- Carry out more tests and focus on small scale targets such as lithofacies and lithofacies associations.
4- More elaboration of elemental and mineralogical effect on geomechanical properties through XRD and XRF.

Appendix

Table 4 Orientations and types of fractures cutting through Arab-D and Upper Jubail Members

Upper Jubaila Formation				
unit	Strike	dip	dip direction	type
Unit 1	110	7	Sw	H
	32	10	SE	H
	320	10	SW	H
	50	8	SE	H
	10	86	NW	V
	98	86	NW	V
Unit 2	15	9	SE	H
	90	10	S	H
	90	5	S	H
	100	12	SW	H
	95	70	SW	V
	15	82	NW	V
	145	84	SW	V
Unit 3	80	10	SE	H
	82	10	SE	H
	260	90	Non	H
	24	70	NW	V
	170	82	SW	V
Unit 4	90	0	Non	H
	25	14	SE	H
	20	12	NW	H
	158	85	NE	V
	35	90	Non	V
	90	70	N	V
Unit 5	75	9	SE	H
	64	10	SE	H
	16	6	SW	H
	170	90	Non	V
Unit 6	115	4	SW	H
	142	70	NE	V
	10	76	SE	V
	108	9	SW	H

Unit 7	60	14	NE	H
	105	4	SW	H
	20	90	SW	V
	140	80	NE	V
Unit 8	76	8	SE	H
	145	7	SW	H

	20	90	SW	V
	140	80	NE	V
Arab-D Member				
Unit 1	90	68	N	V
	160	70	SW	V
	25	62	SE	V
	45	10	SE	H
	14	10	SE	H
	100	5	SW	H
Unit 2	15	80	NW	V
	25	82	NW	V
	135	84	NE	V
	44	8	SE	H
	46	7	SE	H
Unit 3	128	16	SW	H
	40	14	SE	H
	135	8	SW	H
	0	75	W	V
	0	80	W	V
Unit 4	270	10	S	H
	65	18	SE	H
	150	75	NE	V
	40	8	NW	V
	160	85	SW	V
Unit 5	130	10	NW	H
	160	75	NE	V
Unit 6	80	16	SE	H
	160	75	NE	V

	20	64	NW	V
Unit 7	70	16	NE	H
	90	75	N	V
	10	90	Non	V
	80	18	SE	H

Unit	Strike	dip	dip direction
	160	70	SW
	40	90	Non
	90	70	SW
Unit 1	40	10	SE
	160	80	NE
	0	0	Non
Unit 2	100	60	SW
	40	90	Non
	350	90	Non
	90	82	S
Unit 3	0	10	E
	0	82	E
	100	78	SW
Unit 4	170	10	SW
	0	60	E
	40	78	SE
Unit 5	60	10	SE
	10	78	SE
	80	90	Non
Unit 6	130	12	SW
Unit 7	170	8	NE
	170	72	NE
	60	45	NW
	270	10	S
	90	90	Non
	60	75	NW
	35	14	SE
	170	78	NE
Unit 8	Arab-D Member		
	260	70	NW
	160	80	NE
Unit 1	65	10	NW
	260	70	NW
	160	80	NE
Unit 2	36	5	SE
	118	86	NE
	82	90	None
Unit 3	0	0	None

	58	82	SE
	48	64	SE
Unit 4	110	5	SW
	100	80	SW
	60	90	None
Unit 5	80	25	SE
	70 170	70	SE
	130	70 8	NE
Unit 6			SW
	0	80	E
	90	80	S
	130	80	NE
Unit 7	20	16	NW

Table 3 Results of porosity, permeability, Schmidt hammer number, and Point load index testing's.

	Sample	Ø (%)	RN	IS(50) (MPa)	K(md)	Description
Upper Jubaiala						
	S11- 1	1.305	38	7.5	0.0510	Dolomitic mudstone
	S11-2	-	-	8.3	0.0279	Dolomitic mudstone
	S11- 5	0.993	50	9.5	0.0731	Dolomitic wackstone
	S11- 9	2.221	30	6.9	0.1074	Dolomitic wackstone
	S11-11	2.978	32	6.5	0.1123	Stromatoporoid wackstone
	S11- 12	3.024	20	2.1	-	Stromatoporoid wackstone
	S11- 13	1.057	39	6	0.0511	Dolomitic mudstone
	S11- 15	3.152	22	2.4	-	Dolomitic wackstone
	S11- 14	1.413	40	7.1	0.0548	Stromatoporoid wackstone
	S13 -1	1.188	54	7	0.0594	Dolomitic mudstone
	S13 -2	1.240	33	8	0.0604	Dolomitic wackstone
	S13 -3	1.010	40	7	0.0111	Stromatoporoid wackstone
	S13 -4	1.365	48	-	-	Dolomitic wackstone
	S13 -5	-	35		0.0834	Stromatoporoid wackstone
	S13 -6	1.229	40	5.6	0.0612	Dolomitic mudstone
	S13 -7	0.845	52	10.24	0.0106	Dolomitic mudstone
	S13 -8	1.309	38	8.6	-	Stromatoporoid wackstone
	S13-9	-	30	8.2	0.0619	Dolomitic wackstone
	S13 -10	5.360	-	4.5	1.2690	Stromatoporoid wackstone
	S13 -11	3.960	25	5.6	1.0236	Stromatoporoid wackstone

	S13-14	4.170	30	4	1.2226	Stromatoporoid wackstone
	UJS1 - S7	1.268	38	5	0.4461	Dolomitic wackstone
	S13 -12	5.066	30	4.6	-	Stromatoporoid wackstone
	S14 -14	2.749	28	6	0.0793	Stromatoporoid wackstone
Arab-D member						
	S11- 19	4.908	30	6.7	0.1206	Laminated mudstone
	S11- 20	2.626	40	-	0.0971	Laminated mudstone
	S11- 21	2.948	28	1.5	0.0994	Laminated mudstone
	S11- 22	3.037	28	6	0.1276	Peloidal Fossileferous grainstone
	S11- 23	2.162	30	4.8	-	Laminated mudstone
	S11-24	1.315	15	3.3	-	Laminated mudstone
	S11- 25	0.818	35	9.5	0.0197	Laminated mudstone
	S11- 26	2.488	37	5	0.0750	Wavy rippled sandy grainstone
	S11- 27	1.636	21	6.5	-	Laminated mudstone
	S11- 28	1.120	40	11.2	0.0540	Wavy rippled sandy grainstone
	S11- 29	2.089	31	7.1	0.1002	Laminated mudstone
	S11- 30	2.588	24	4.1	0.1071	Laminated mudstone
	S13 -16	2.057	34	8.2	-	Laminated mudstone
	S13 -18	3.778	28	5	1.0750	Laminated mudstone
	S13 -20	1.075	39	8	0.0235	Wavy rippled sandy grainstone
	S14 -15	1.363	-	8.45	0.0268	Wavy rippled sandy grainstone
	S14 -16	2.139	-	8.2	0.0616	Stromatoporoid wackstone
	S14 -18	-	40	11.7	0.0288	Wavy rippled sandy grainstone
	S14 -20	4.240	28	2.6		Laminated mudstone
	S14 -22	2.124	33	7.5	0.0541	Peloidal Fossileferous grainstone
	S14 -24	2.387	35	6		Peloidal Fossileferous grainstone
	S14 -24b	3.657	28	5.8	0.0678	Laminated mudstone
	S 14-25	3.180	30	4.5		Laminated mudstone

S14 -28	5.376	28	3.5	0.1152	Laminated mudstone
S14 -30	4.735	34	6.8	0.0586	Peloidal Fossileferous grainstone
S 11-18	2.149	30	6	0.0726	Laminated mudstone
S1-18	1.441	30	-	-	Laminated mudstone
S1-18T	0.955	47	8.5	-	Laminated mudstone
S1-19	-	55	14	-	Wavy rippled sandy grainstone
S1-20T	2.800	29	4.7	-	Peloidal Fossileferous grainstone
S1-21	1.724	37	6.5	-	Peloidal Fossileferous grainstone
S1-23	1.707	40	8.5	-	Wavy rippled sandy grainstone
S1-26	1.762	45	8.5	-	Wavy rippled sandy grainstone
S1-27	2.999	27	5.6	-	Laminated mudstone
S1-30T	1.321	30	6.8	-	Laminated mudstone
Minimum	0.818	15	1.5	0.0106	
STD	1.2661	8.3030	2.328435	0.3411	
Maximum	5.376	55	14	1.2690	
Average	2.363	34.2	6.671765	0.1908	

Table 4 Results of ultrasonic wave velocity test which is represented by P-wave velocity, S-wave velocity , dynamic Poisson's ratio, and dynamic Young's modulus

sample	SV\ ms^{-1}		ρ(gm\cc)	RN	Is(50)(MPa)	vd	Ed(GP a)
	Vp	Vs					
Arab -D member							
S11-28	10000	7600	2.66	40	11.2	0.07	328
S11-26	-	-	2.69	37	12.1	0.36	-
S11-25	10000	4828	2.68	35	9.6	0.35	168
S11-24	10000	2105	2.71	-	-	0.48	35
S11-23	10000	2105	2.71	20	4.8	0.48	35
S11-22	10000	4827	2.71	28	6.0	0.35	170
S11-21	10000	2105	2.71	28	6.8	0.48	35
S11-21-2	-	-	-	9	2.1	-	-
S11-20	4000	727	2.70	15		0.26	360
S11-19	10000	5757	2.69	30	6.9	0.25	223
S11-29	8333	6756	2.68	31	7.1	0.46	132
S14-24	8474	6756	2.69	35	8.6	0.37	154
S13-20	9375	7031	2.66	39	7.0	0.14	225
S13-19	-	-	-	54	12.1	-	-
S13-16	8181	6617	2.69	34	8.2	0.45	130
S14-22	7894	6617	2.68	33	7.5	0.48	74
S14-28	9183	7031	2.69	28	-	0.21	210
S14-24	7936	6756	2.71	35	8.6	0.50	45
S14-30	10000	7352	2.70	34	6.8	0.31	380
S14-18	-	8620	2.71	40	11.7	0.37	-
S14-25	10000	8620	2.67	-	-	0.35	-
S14-20	9183	6521	2.69	28	2.6	0.01	226
S11-17	10000	7653	2.70	40	7.8	0.04	327
Upper							
Jubaila							
S11-15	10000	7948	2.72	34	7.1	0.20	-

S11-13	9117	6326	2.66	30	6.0	0.04	220
S11-11	10000	7272	2.68	32	9.1	0.12	316
S11-1	10000	7755	2.71	38	7.5	0.23	-
S11-9	9302	7407	2.71	30	6.9	0.37	188
S13-14	8620	6756	2.71	41	5.3	0.30	173
S13-12	9259	7246	2.69	-	8.2	0.29	200
S13-6	9259	7246	2.68	-	5.6	0.29	199
S13-3	10000	7246	2.68	40	7.0	0.01	278
S13-2	9433	7246	2.70	33	6.1	0.22	221
S14-14	8474	6756	2.69	28	6.0	0.37	154
S14-24	8474	6756	2.71	28	5.8	0.37	155
S13-11	9433	7246	2.69	25	5.6	0.22	220
S13-8	9433	7246	2.70	38	8.6	0.22	221
S13-7	10000	7246	2.69	52	10.2	0.01	280
S13-1	9259	7246	2.67	54	7.0	0.29	199
S14-16	8620	6666	2.71	48	8.2	0.24	181
S13-5	10000	7246	2.69	50	10.3	0.01	279
S13-10	7936	6329	2.70	34	7.5	0.37	135
S13-4	9259	7246	2.69	48	5.0	0.29	200
S14-15	-	8620	2.70	15	2.6	0.45	-
Maximum	10000	8620	2.72	54	12.1	0.50	380
minimum	4000	727	2.66	9	2.1	0.01	35
Average	9191	6470	2.69	34	7.5	0.27	196
STD	1106	1774	0.01	10	2.4	0.15	88

References

Ahr MW (2009) Geology of carbonate reservoirs, the identification, description, characterization of hydrocarbon reservoir in carbonate rocks. London: John Willey and sons.

Al-Fahmi, M., Cooke, M.L., Cole,J.C. (2014). Modeling of the Dammam outcrop fractures: Case study for fracture development in salt-cored structures. GeoArabia, 49-80.

Arman H, Hashem W, El Tokhi M, Abdelghany O, El Saiy A (2012) Petrographical and Geomechanical Properties of the Lower Oligocene Limestones from Al Ain City, United Arab Emirates. The Arabian Journal of Sciences and Engineering , DOI 10.1007/s13369013-0867-8.

Ameen MS, Brian GD, Somerville JM (2009) Predicting rock mechanical properties of carbonates from wireline logs (A case study: Arab-D reservoir, Ghawar field, Saudi Arabia). Marine and Petroleum Geology, v.26 , 430-444.

Aydin, A., Basu, A. (2005). The Schmidt hammer in rock material characterization. Engineering Geology, 1-14

Bai, T., Pollard. (2001). The unusual efficiency of fluid flow in fractures. Geophysical Research Letters, 65-68

Bertotti, G., Hardebol, N., Taal-van Koppen, J.K., Luthi, S.M.,. (2007). Toward a quantitative definition of mechanical units: New techniques and results from an outcropping deep-water turbidite succession (Tanqua-Karoo Basin, South Africa). American Association of Petroleum Geologists Bulletin, 1085–1098.

Broch EM, Franklin JA (1972) The point load strength test. International Journal of Rock Mecanichs and Minning Sci. Geomech. Abstract 9, 669–697.

Cantrell DL , Hagerty R (1999) Microporosity in Arab Formation carbonate, Saudi Arabia. GeoArabia, v.4, no.2 , 129-154.

Cantrell DL , Alkhammash A , Jenden PD (2007) Characterization and significance of dedolomite in Wadi Nisah. GeoArabia,v.12, no.3, 15-30.

Chang C, Zoback M, Khaksar A (2006) Empirical relations between rock strength and physical properties in sedimentary rocks. Journal of petroleum Sciences and Engineering, v. 51,223-237.

Das Gupta, U. (1978). A Study of Fractured Reservoir Rocks, with Special Reference to Mississippian Carbonate Rocks of Southwest Alberta. University of Toronto, PhD Dessertation.

Deere DU, Miller RP (1966) Engineering classification and index properties of rock, Tech. Report Air Force Weapons Lab., New Mexico, 65-116.

Dunham RJ (1962) Classification of carbonate rocks according to depositional sequences. American Association of Petroleum Geologists, PP.108-121, Memoir 1.

Eberli GP, Baechli GT, Anselmetti FS, Incze ML (2003) Factors controlling elastic properties in carbonate sediments and rocks. Society of Geophysical Exploration. 654-660.

Eltom H , Abdullatif O , Makkawi M , Abdulraziq A (2013) Microporosity in the upper Jurassic Arab-D carbonate Reservoir, Central Saudi Arabia: An outcrop analougue study. Journal of Petroleum Geology, v.36, no.3 , 281-297.

Eltom H, Abdullatif O, Makkawi M, Abdulraziq A (2014) Characterizing and modeling the Upper Jurassic Arab-D reservoir using outcrop data from Central Saudi Arabia. GeoArabia , v. 19, no. 2, p. 53-84.

Frost, E. L., and C. Kerans. (2010). Controls on syndepositional fracture patterns, Devonian reef complexes, Canning Basin, Western Australia. Journal of Structural Geology, 1231–1249.

Gale, J.F.W., Laubach, S.E., Marrett, R.A., Olson, J.E., Holder, J., Reed, R.M.,. (2004). Predicting and characterizing fractures in dolostone reservoirs: using the link. Geological Society of London, Special Publication, 177-192.

Goktan, R. M., Ayday, C. (1993). A suggested improvement to the Schmidt Rebound Hardness ISRM suggested method with particular reference to rock machineability. International Journal of Rock Mechanics and Mining Sciences abstract, 321-322.

Gudmundsson, A., Berg, S.S., Lyslo, K.B.,Skurtveit, E. (2001). Fracture networks and fluid transport in active fault zones. Journal of Structural Geology, 343-353.

Handin, J., Hager Jr., R.V., Friedman, M., Feather, J.N. (1963). Experimental deformation of sedimentary rocks under confining pressure; pore pressure tests. Bulletin of the American Association of Petroleum Geologists, 717-755.

Hariri, M. (2013). Fractures system within Dammam Dome and its relationship to the doming process, Eastern Saudi Arabia. Arabian Journal of Geosciences, 4943-4956.

Hughes GW (2004) Middle to Upper Jurassic Saudi Arabian carbonate petroleum reservoirs: biostratigraphy,micropalaeontology and palaeoenvironments, v.9, n.3, GeoArabia , 79-114.

ISRM (1981) Suggested methods for determining hardness and abrasiveness of rocks, Part 3. Commission on standardization of laboratory and field tests, abstract 18, 109.

Kahraman S (2001) Evaluation of simple methods for assessing the uniaxial compressive strength of rock.. International Journal of Rock Mechanics & Mining Sciences, v. 38 , 981-994.

Kahraman S, Yeken T (2008) Determination of physical properties of carbonate rocks from P-wave velocity, Bull Eng Geol Environ, v.67, 277–281.

Katz O, Reches Z, Roegiers JC (2000) Evaluation of mechanical rock properties using a Schmidt Hammer. Int. J. Rock Mech. Min. Sci. , v.37, 723–728.

Lamarche, J., Lavenu, A.P.C., B.D.M. Gauthier, Y. Guglielmi, O.Jayet. (2012). Relationships between fracture patterns, geodynamics and mechanical stratigraphy in Carbonates (South-East Basin, France). Tectonophysics, 231–245.

Lavenu, A.P.C., Lamarche, J., Gallois. A.,Gauthier, D.M. (2013). Tectonic versus diagenetic origin of fractures in a naturally fractured carbonate reservoir analog (Nerthe anticline, southeastern France). Bulliten of American Association of Petroleum Geologists, 2207–2232.

Larsen B, Gudmundsson A, Grunnaleite I, Sælen G (2010) Effects of sedimentary interfaces on fracture pattern, linkage, and cluster. Marine and Petroleum Geology, v.27 , 1531-1550.

Lonergan, L., Jolly, R.J.H., Rawnsley, K., Sanderson, D.J. (2007). Fractured Reservoirs. London: Geological Society of London.

Lucia FJ, Jennings JW, Rahnis M, Meyer FO (2001) Permeability and rock fabric from wireline logs, Arab-D reservior, Ghawar Field, Saudi Arabia. GeoArabia,v. 6,no. 4,619–646.

Nelson, R. A. (2001). Geological analysis of naturally fractured. Houston: Gulf Professionnal Publishing.

Okla SM (1987) Algal microfacies in Upper Tuwaiq mountain limestone (Upper Jurassic) near Riyadh, Saudi Arabia. Palaeogeography, Palaeoclimatology, Palaeoecology, v. 58, 55-61.

Ortega, O.J., J.F.W. Gale, R.Marrett. (2010). Quantifying diagenetic and stratigraphic controls on fracture intensity in platform carbonates: An example from the Sierra Madre Oriental, northeast Mexico. Journal of Structural Geology, 1943-1959.

Powers RW (1962). Arabian Upper Jurassic carbonate reservoir rocks. In: W. E. Ham (Ed.), Classification of Carbonate Rocks: A Symposium. AAPG Memoir 1, 122-192.

Powers RW , Ramirez LF, Redmond CD , Elberg LE (1966) Geology of the Arabian Peninsula. Sedimentary Geology of Saudi Arabia. USGS , 560-D.150p.

Powers RW (1968) International stratigraphic lexicon;volume 3, Asia, part 10b (1). Saudi Arabia Lexique stratigraphique international; v.3, Asie, fascicule , 177.

Read JR, Thornten PN, Regan WM (1980) A rational approach to the point load test. In: Proceedings Aust-N.Z. Geomechanics, v. 2,. p. 35–9.

Shalabi FI, Cording EJ, Al-Hattamleb OH (2007) Estimation of rock engineering properties using hardness tests. Eng. Geol., v. 90, 138– 147.

Steineke M, Bramkamp RA , Sander NJ (1958) Stratigraphic relations of Arabian Jurassic oil. American Association of Petroleum Geologists Symposium , 1294–1329.

Tuğrul A, Zarif IH (2000) Engineering aspects of limestone weathering in Istanbul, Turkey. Bulletin of Engineering Geology Environ. ,v.58,no. 3, 191–206.

Vaslet D, Manivit J, Linindre YM (1989) Proposal for new reference sections of the Early Triassic Sudair Shale, Kingdom of Saudi Arabia. Professional Papers – Kingdom of Saudi Arabia, Ministry of Petroleum and Mineral Resources, PP3, 45-59.

Yasar E, Erdogan Y (2004) Estimation of rock physiomechanical properties using hardness methods. Eng. Geol.v. 71, 281– 288.

Ziegler, M. A. (2001). Late Permian to Holocene Paleofacies Evolution of the Arabian Plate and its Hydrocarbon Occurrences. GeoArabia, 445-504.

VITAE

Name: Ammar Juma Abdlmutalib Mohammed

Nationality: Sudanese

Date of Birth: 2/27/1988

Email: mr_ammarjumma@hotmail.com

Address: Sudan-Khartoum

Academic Background:

Bachelor degree from geology department, faculty of sciences, University of Khartoum

Master degree from Earth Sciences Department, King Fahd University of Petroleum and Minerals

 Journal publications:

Abdulmutalib A, Abdullatif O, Korvin G, Abdulraheem A (2015), The relationship between lithological and geomechanical properties of tight carbonate rocks from Upper Jubaila and Arab-D Member outcrop analog, Central Saudi Arabia. Arabian Journal of Geosciences, DOI 10.1007/s12517-015-1957-6 (Published)

Abdulmutalib A, Abdullatif O, Korvin G, Abdulraheem A , Multi-scale Fracture characterization of tight carbonates of Arab-D Member and Upper Jubaial Formation, Central Saudi Arabia (under prep. For submission to bulletin of engineering geology and the environment)

 Conference papers:

Abdlmutalib A, Abdullatif O (2015) Fractures Patterns of Tight Carbonates of Upper Jurassic Arab-D Member and Upper Jubaila Formation Outcrops, Central Saudi Arabia, EGU General assembly, Vol. 17, EGU2015-6602, 2015 Vienna, Austria.